



The Journal of Gemmology

Volume 35 / No. 3 / 2016





Gem-A

THE GEMMOLOGICAL ASSOCIATION
OF GREAT BRITAIN

Book now for the Gem-A Conference 2016

Saturday 5 and Sunday 6 November



Boasting an incredible line-up of speakers, the Gem-A Conference is not to be missed. Further your knowledge by attending talks from renowned gem experts, network with some of the world's top gemmologists and attend exclusive seminars and trips, including the Mineral Gallery at the Natural History Museum and the Crown Jewels at the Tower of London. Hurry, booking closes on 21 October 2016.

SATURDAY PROGRAMME

Ian Harebottle

The critical role of colour and design in ensuring the future of the jewellery sector

Jim Clanin

The fundamentals of mining for coloured gemstones and mineral specimens

David Fisher

Progress in the detection of diamond treatments

John Dyer

The science and the art of gem cutting

Robert Weldon

In Peter Rainier's footsteps: journey to the Chivor emerald mine

SUNDAY PROGRAMME

Helen Molesworth

The history of gemstones

Dr Michael Wise

Hiddenite emerald deposits of North Carolina

Danny Sanchez

Photomicrography of inclusions

Pat Daly

Identification techniques

Bill Larson

Gemstones and gem mining in San Diego County, California

To book for the Conference please visit:

www.eventbrite.com/e/gem-a-conference-2016-tickets-25865073130

Members have been sent a special booking code for the Conference via email. If you haven't received this please contact events@gem-a.com.

Creating gemmologists since 1908

Join us.



COLUMNS

181 What's New

FourPro Photo Studio | Gemax Pro digital microscope | GemoLog Color Stone Gem Tester | PhosView | Diamond literature compilations | Gem Testing Laboratory *Lab Information Circular* | GRS Alert on manufactured phosphorescent pebbles | ICGL *Newsletter*

184 Gem Notes

Almandine from Israel | Anatase from Pakistan | Cat's-eye apatite from Madagascar | Aquamarine from Pakistan | Chrome chalcidony from Tanzania | Yellow dravite from Tanzania | New garnets from East Africa | Quartz cubes from Ukraine | Star sapphire showing a variable number of rays | 'Zebra Star' sapphire from Tanzania | Scapolite from Tanzania with magnetite inclusions | Gastropod shell as the core of a natural pearl | Yttrium alumino-silicate glass imitating peridot | HPHT-treated blue sapphires | Myanmar Gems Emporium



Cover Photo:

New technologies, such as laser ablation inductively coupled plasma time-of-flight mass spectrometry (see article on pp. 212–223), are helping gem labs make more accurate geographic origin determinations on high-end stones such as these Kashmir sapphires (~7.3 and 8.5 ct). Photo by Julien Xaysongkham/SSEF.

p. 192



p. 253



ARTICLES

Feature Articles

212 Simultaneous High Sensitivity Trace-Element and Isotopic Analysis of Gemstones Using Laser Ablation Inductively Coupled Plasma Time-of-Flight Mass Spectrometry

By Hao A. O. Wang, Michael S. Krzemnicki, Jean-Pierre Chalain, Pierre Lefèvre, Wei Zhou and Laurent Cartier

224 Synthetic Emeralds Grown by IG Farben: Historical Development and Properties Related to Growth Technology

By Karl Schmetzer, H. Albert Gilg and Elisabeth Vaupel

Gemmological Brief

248 A Diamond with a Transient 2804 cm^{-1} Absorption Peak

By Jianjun Li, Chengxing Fan, Shuxiang Chen and Guibua Li

253 Conferences

Arizona Geological Society | International Geological Congress

256 Letters

257 Gem-A Notices

262 Learning Opportunities

265 New Media

268 Literature of Interest

The Journal is published by Gem-A in collaboration with SSEF and with the support of AGL and GIT.



Editor-in-Chief

Brendan M. Laurs
brendan.laurs@gem-a.com

Production Editor

Mary A. Burland
mary.burland@gem-a.com

Marketing Consultant

Ya'akov Almor
bizdev@gem-a.com

Editorial Assistant

Carol M. Stockton

Editor Emeritus

Roger R. Harding

Executive Editor

Alan D. Hart

Associate Editors

Edward Boehm, *RareSource, Chattanooga, Tennessee, USA*; Alan T. Collins, *King's College London*; John L. Emmett, *Crystal Chemistry, Brush Prairie, Washington, USA*; Emmanuel Fritsch, *University of Nantes, France*; Rui Galopim de Carvalho, *Portugal Gemas, Lisbon, Portugal*; Lee A. Groat, *University of British Columbia, Vancouver, Canada*; Thomas Hainschwang, *GGTL Laboratories, Balzers, Liechtenstein*; Henry A. Hänni, *GemExpert, Basel, Switzerland*; Jeff W. Harris, *University of Glasgow*; Alan D. Hart, *Gem-A, London*; Ulrich Henn, *German Gemmological Association, Idar-Oberstein*; Jaroslav Hyršl, *Prague, Czech Republic*; Brian Jackson, *National Museums Scotland, Edinburgh*; Stefanos Karpampelas, *GRS Gemresearch Swisslab, Meggen, Switzerland*; Lore Kiefert, *Gübelin Gem Lab Ltd., Lucerne, Switzerland*; Hiroshi Kitawaki, *Central Gem Laboratory, Tokyo, Japan*; Michael S. Krzemnicki, *Swiss Gemmological Institute SSEF, Basel*; Shane F. McClure, *Gemmological Institute of America, Carlsbad, California*; Jack M. Ogden, *Striptwist Ltd., London*; Federico Pezzotta, *Natural History Museum of Milan, Italy*; Jeffrey E. Post, *Smithsonian Institution, Washington DC, USA*; Andrew H. Rankin, *Kingston University, Surrey*; George R. Rossman, *California Institute of Technology, Pasadena, USA*; Karl Schmetzer, *Petershausen, Germany*; Dietmar Schwarz, *AIGS Lab Co. Ltd., Bangkok, Thailand*; Menahem Sevdemish, *GemeWizard Ltd., Ramat Gan, Israel*; Guanghai Shi, *China University of Geosciences, Beijing*; James E. Shigley, *Gemmological Institute of America, Carlsbad, California*; Christopher P. Smith, *American Gemmological Laboratories Inc., New York, New York*; Evelyne Stern, *London*; Elisabeth Strack, *Gemmologisches Institut Hamburg, Germany*; Tay Thy Sun, *Far East Gemmological Laboratory, Singapore*; Pornsawat Wathanakul, *Gem and Jewelry Institute of Thailand, Bangkok*; Chris M. Welbourn, *Reading, Berkshire*; Joanna Whalley, *Victoria and Albert Museum, London*; Bert Willems, *Leica Microsystems, Wetzlar, Germany*; Bear Williams, *Stone Group Laboratories LLC, Jefferson City, Missouri, USA*; J.C. (Hanco) Zwaan, *National Museum of Natural History 'Naturalis', Leiden, The Netherlands*.

Content Submission

The Editor-in-Chief is glad to consider original articles, news items, conference/excursion reports, announcements and calendar entries on subjects of gemmological interest for publication in *The Journal of Gemmology*. A guide to the various sections and the preparation of manuscripts is given at www.gem-a.com/index.php/news-publications/publications/journal-of-gemmology/submissions, or contact the Production Editor.

Subscriptions

Gem-A members receive *The Journal* as part of their membership package, full details of which are given at www.gem-a.com/membership. Laboratories, libraries, museums and similar institutions may become Direct Subscribers to *The Journal*.

Advertising

Enquiries about advertising in *The Journal* should be directed to the Marketing Consultant. For more information, see www.gem-a.com/index.php/news-publications/publications/journal-of-gemmology/advertising.

Database Coverage

The Journal of Gemmology is covered by the following abstracting and indexing services: Australian Research Council academic journal list, British Library Document Supply Service, Chemical Abstracts (CA Plus), Copyright Clearance Center's RightFind application, CrossRef, EBSCO (Academic Search International, Discovery Service and TOC Premier), Gale/Cengage Learning Academic OneFile, GeoRef, Mineralogical Abstracts, ProQuest, Scopus and the Thomson Reuters' Emerging Sources Citation Index (in the Web of Science).

Copyright and Reprint Permission

For full details of copyright and reprint permission contact the Editor.

The Journal of Gemmology is published quarterly by Gem-A, The Gemmological Association of Great Britain. Any opinions expressed in *The Journal* are understood to be the views of the contributors and not necessarily of the publisher.

Printed by DG3 (Europe) Ltd.

© 2016 The Gemmological Association of Great Britain

ISSN: 1355-4565



Gem-A
THE GEMMOLOGICAL ASSOCIATION
OF GREAT BRITAIN

21 Ely Place
London EC1N 6TD
UK

t: +44 (0)20 7404 3334
f: +44 (0)20 7404 8843
e: information@gem-a.com
w: www.gem-a.com

Registered Charity No. 1109555
Registered office: Palladium House,
1-4 Argyll Street, London W1F 7LD

President

Maggie Campbell Pedersen

Vice Presidents

David J. Callaghan, Alan T. Collins,
Noel W. Deeks, E. Alan Jobbins,
Andrew H. Rankin

Honorary Fellows

Gaetano Cavalieri, Terrence
S. Coldham, Emmanuel Fritsch

Honorary Diamond Member

Martin Rapaport

Chief Executive Officer

Alan D. Hart

Council

Justine L. Carmody – Chair
Kathryn L. Bonanno, Paul F. Greer,
Kerry H. Gregory, J. Alan W.
Hodgkinson, Nigel B. Israel, Jack
M. Ogden, Richard M. Slater,
Christopher P. Smith

Branch Chairmen

Midlands – Georgina E. Kettle
North East – Mark W. Houghton
South East – Veronica Wetten
South West – Richard M. Slater

Understanding Gems™

What's New

INSTRUMENTS AND TECHNIQUES

FourPro Photo Studio

Announced in late 2015, this Italian-made modular photography system helps with taking professional-quality photos of jewellery without shadows and unwanted reflections. The components are sold separately and can be purchased in almost any configuration: light box (with or without light fixtures), holder with rotating arm and camera/lens adapter, remote-controllable Canon Reflex EOS camera, robotic kit for 3D animation, and various software for use with a computer or tablet (Android or iPad). The system will accommodate the user's own camera. For more information, visit www.fourpro.com.



CMS

GemoLog Color Stone Gem Tester

Released in June 2016 from U.S.-based Tri Electronics Inc., this testing unit includes an optical pen connected to a handheld controller with a digital readout. It reportedly can be used on loose or mounted faceted samples to separate natural ruby, sapphire, emerald, garnet, alexandrite and spinel from synthetics and imitations. Although no information is available on the manufacturer's website (<http://trielectronics.com>), a limited description can be found at www.kassoy.com/prodcat/gemstone-testers.asp.



CMS

Gemax Pro Digital Microscope

Introduced in 2015, this portable high-definition digital microscope includes an approximately 9 cm LCD screen with 3.5 megapixel image-capture capability, a diffused LED lighting system and 20×–220× optical magnification. The unit comes with its own software, in 12 languages, and is both PC- and Mac-compatible. Weighing just 1,250 g and measuring 23.2 cm high, 14.9 cm long and 10.6 cm wide, the microscope is truly portable. For additional information, visit www.amazon.com/Gemax-Pro-Digital-Microscope/dp/B01FN08OPY, but note that the microscope is available from numerous retail sources worldwide.



CMS

PhosView

During the September 2016 Hong Kong Jewellery & Gem Fair, the International Institute of Diamond Grading & Research (part of The De Beers Group of Companies, London) released PhosView for screening parcels of polished colourless or near-colourless diamonds for potential HPHT-grown synthetics. The compact device can accept loose stones weighing 0.3 points to 1 ct, as well as some jewellery items. The user can manually separate potential HPHT synthetics for further testing using built-in manipulator arms. PhosView cannot identify CVD synthetics, diamond simulants or treated natural diamonds. For more information, visit www.iidgr.com/instruments/Phos_View.

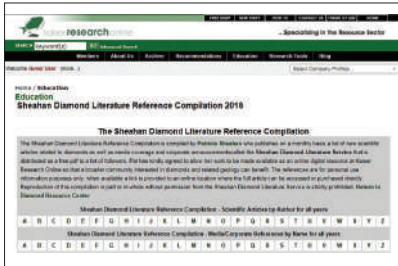


BML

NEWS AND PUBLICATIONS

Diamond Literature Compilations

Since September 2015, reference compilations of scientific diamond literature prepared by Patricia Sheahan (honorary research associate at the University of British Columbia, Canada) have been posted in the education section of Kaiser Research Online at <https://secure.kaiserresearch.com/s2/Education.asp>. Annual listings are available from 2005 to the present and include the following fields: author, title, source, region and keywords. In addition, Sheahan's diamond reference compilations are listed by author or media/corporate name for all years. It is also possible to directly receive free monthly diamond literature reference compilations by emailing Patricia Sheahan at konsult@compuserve.com and indicating the subscription request in the subject line. **BML**



Annual listings are available from 2005 to the present and include the following fields: author, title, source, region and keywords. In addition, Sheahan's diamond reference compilations are listed by author or media/corporate name for all years. It is also possible to directly receive free monthly diamond literature reference compilations by emailing Patricia Sheahan at konsult@compuserve.com and indicating the subscription request in the subject line. **BML**

Gem Testing Laboratory Lab Information Circular

The July 2016 issue of the Gem Testing Laboratory (Jaipur, India) *Lab Information Circular* includes reports on polymer-treated hessonite; yellow-green translucent opal; a large 'coppery'-coloured star sapphire; unusual fluorescence in mounted, light greyish brown CVD synthetic diamonds; dyed, stabilized alunite sold as gaspeite; a brightly coloured, banded assembled material made with dyed, powdered limestone in polymer and sold as 'rainbow calsilica'; and a plastic bead showing the flame-like structure seen in conch pearls. Download the newsletter from http://gtljaipur.info/ProjectUpload/labDownload/LIC_Vol73_July2016_Eng.pdf. **CMS**

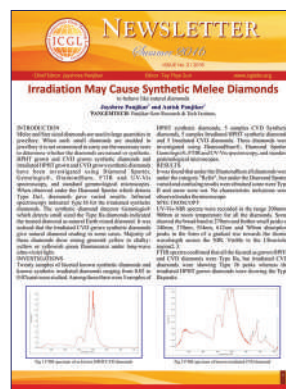


GRS Alert: Phosphorescent Pebbles are Synthetic Aggregates

In April 2016, Gemresearch Swisslab AG (Lucerne, Switzerland) warned the gem trade about a number of manufactured fluorescent pebbles that have been sold for high prices and submitted to their laboratories since 2014. Marketed as natural rounded pebbles, but also seen as carved specimens, the material fluoresces green under strong light and patchy blue-to-green to long-wave UV radiation, with strong green phosphorescence to both. The material proved to be a synthesized aggregate of Sr-Al oxides with traces of Dy and other rare-earth elements. The online report (<http://gemresearch.ch/phosphorescent-synthetic-aggregate>) includes an informative video. **CMS**



ICGL Summer 2016 Newsletter



The 2016 No. 2 issue of the International Consortium Gem-Testing Laboratories' *Newsletter* contains four reports on synthetic and treated diamonds: irradiated melee-sized CVD synthetics that might test as natural with a Gemlogis instrument, the detection of fracture-filled diamonds, characteristics and identification of nano-coated 'Ice Pink' diamonds from Lotus Colors Inc., and a brief description of a mounted 'pink' diamond showing a partially worn pavilion coating responsible for its pink appearance. Download the *Newsletter* from <http://icglabs.org>. **CMS**

What's New provides announcements of new instruments/technology, publications, online resources and more. Inclusion in **What's New** does not imply recommendation or endorsement by Gem-A. Entries were prepared by Carol M. Stockton (CMS) or Brendan M. Laurs (BML), unless otherwise noted.

SSEF+

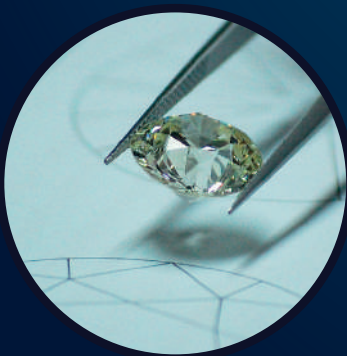
SCHWEIZERISCHES GEMMOLOGISCHES INSTITUT
SWISS GEMMOLOGICAL INSTITUTE
INSTITUT SUISSE DE GEMMOLOGIE



ORIGIN DETERMINATION · TREATMENT DETECTION

DIAMOND GRADING · PEARL TESTING

EDUCATION · RESEARCH



THE SCIENCE OF GEMSTONE TESTING

Gem Notes

COLOURED STONES

Almandine from Negev, Israel

In 2013, some dark red crystals were found in the southern mountains of the Negev Desert region near Eilat, Israel. This area is known to be rich in granite- and quartz-bearing rocks. Around 500 g of samples were collected during a two-month period, and a few were fashioned as cabochons, the biggest weighing 1.54 ct.

Gemmological testing was performed on seven rough samples and on one partially polished piece. They ranged from 0.38 to 0.67 g, averaging slightly over 0.4 g and measuring 4.3–7.8 mm in maximum dimension. All of the crystals exhibited a slightly flattened dodecahedral crystal form with shallow surface striations. They displayed a very dark, highly saturated, red colour with a distinct brownish tint, typical of some garnet (Figure 1). The samples were highly included, and microscopic examination revealed dark irregular-shaped crystals and an abundance of fluid inclusions with some fissures. The RI of the partially polished piece was above the limit of a standard gemmological refractometer (1.80). Most of the samples had hydrostatic SG values from 4.13 to 4.15, with a maximum value of 4.17 and the minimum of 4.10. These properties are consistent with almandine with some spessartine component.

Energy-dispersive X-ray fluorescence (EDXRF) chemical analysis with an Amptek X123-SDD spectrometer confirmed the anticipated high Fe content and a minor Mn component. A very minor amount of Ca also was detected. Absorption spectra recorded with a Unicam UV540 spectrophotometer revealed a classic almandine spectrum (peaks at 507 and 526 nm and a doublet at 573/578 nm) with weak spessartine features (409, 417, 421, 426 and 431 nm). Raman analysis with an Enwave 789 spectrometer yielded a consistent Raman shift of 915 cm^{-1} , and a comparison to the RRUFF database confirmed the garnet to be predominantly almandine.



Figure 1: These dark brownish red crystals and cabochons (0.60–1.54 ct) of almandine originate from the Negev Desert of Israel. Photo by G. Borenstein.

Due to their small size and the abundance of inclusions, these garnets are unlikely to be of commercial interest. However, based on their geographic origin, they may be related to the ancient Nofekh gem that is mentioned in the breastplate of the high priest of the Israelites. Commentaries by Philo Judaeus (Yonge, 1855) and Flavius Josephus (Court, 1770), and a passage in the *Targum Pseudo-Jonathan* (McNamara and Maher, 1994), have all pointed toward a precious stone resembling a burning coal in this breastplate, which might have been garnet.

Guy Borenstein FGA (guy@gemewizard.com)
Gemewizard Ltd., Ramat Gan, Israel

Cara Williams FGA
Stone Group Laboratories
Jefferson City, Missouri, USA

References

- Court J., 1770. *Josephus, Antiquities of the Jews*, Vol. 3. Christopher Earl, Birmingham, 885 pp.
- McNamara M. and Maher M., 1994. *The Aramaic Bible: Targum Neofiti 1: Exodus, Targum Pseudo-Jonathan: Exodus*. Michael Glazier, Wilmington, Delaware, USA, 334 pp.
- Yonge C.D., 1855. *The Works of Philo Judaeus: The Contemporary of Josephus*. H.G. Bohn, London, 509 pp.

GIT 2016

“The Fullmoon of GEMUnity”

The 5th GIT International Gem and Jewelry Conference

Pattaya, Thailand

November 14 - 15, 2016

with Pre- and Post- Conference Excursions

Conference Dates:



November 14 - 15, 2016

Technical Session

Oral and Poster Presentations
The Zign Hotel, Pattaya, Thailand



November 9 - 13, 2016

Pre-Conference Excursion*

Mandalay & Mogok, Myanmar
(Please see our website for the
recommended flights and visa
information)
Documents Submission by
October 13, 2016



November 16 - 18, 2016

Post-Conference Excursion*

Chanthaburi & Trat, Thailand

* Limited seats available on first come first serve basis

Some Interesting Topics:

- “Gem Corundum Deposits with Regards to Their Geological Origin”
Gaston Giuliani
- “HPHT - Treated Sapphire: Before and After”
Hyunmin Choi
- “Purple Garnet from a New Deposit in Mozambique”
Thanong Leelawatanasuk
- “Manufacturing & Cutting Edge Technology”
Victor Tuzlukov
- “Trends Forecasting: Design Directions 2017 - 18”
Paola De Luca

Registration Fees:

Normal	On-Site	Remarks
USD 150	USD 350	Student
USD 300		Participant
USD 1700**	Pre-Conference Excursion	
USD 350	Post-Conference Excursion	

** Excluding air tickets

Accommodation:

The Zign Hotel, Pattaya, Thailand

Hotel Booking for GIT2016: git2016@thezignhotel.com

Contact Secretariat:

Email: git2016@git or th

Tel: +66 2634 4999 ext.453



www.git2016.com

Faceted Anatase from Pakistan

Anatase (TiO₂) is polymorphous with rutile and brookite. Faceted anatase is rarely encountered, although gemmy material has been reported from Switzerland, Russia and Brazil (O'Donoghue, 2006). Recently, gem dealer Dudley Blauwet (Dudley Blauwet Gems, Louisville, Colorado, USA) obtained faceted anatase from another locality: Kharan, Baluchistan, Pakistan. He first encountered this anatase while on a buying trip to Peshawar, Pakistan, in approximately 2000. Almost all of the initial pro-



Figure 2: These faceted anatase gemstones (0.10–0.17 ct) are from Baluchistan, Pakistan. Photo by Bilal Mahmood and Kelly Kramer.

duction consisted of opaque crystals on matrix, as well as some loose pieces that had fallen off matrix. More recently, in October 2014, Blauwet obtained ~30 g of crystals that measured up to 2 cm and contained small areas that were transparent enough to facet. In May 2016 he received eight gems from his cutting factory that weighed 0.10–1.56 ct. The smaller stones contained fewer inclusions, and he loaned three of them to American Gemological Laboratories for examination.

The samples weighed 0.10–0.17 ct and were brownish orange to yellowish brown (Figure 2). They were confirmed as anatase with Raman spectroscopy using a 514 nm laser. Refractive indices were over the limit of a standard refractometer, and when viewed in the polariscope all the samples 'blinked' upon rotation, consistent with the uniaxial nature of anatase. Hydrostatic SG values ranged from 3.83 to 3.87. Qualitative chemical analysis using EDXRF spectroscopy showed major amounts of Ti and no

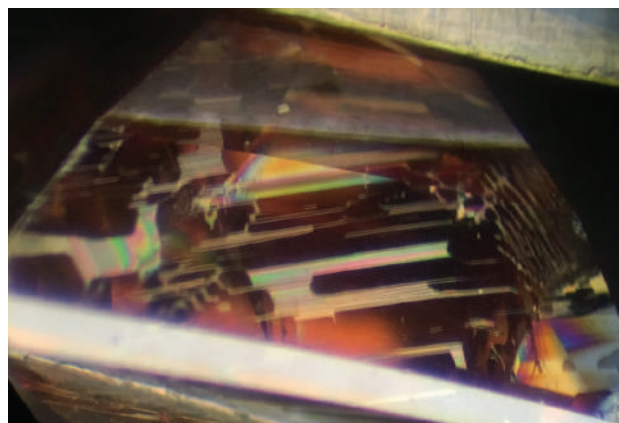


Figure 3: Iridescent thin films are seen along cleavage planes in this 0.16 ct anatase. Photomicrograph by B. Clark.

trace elements. A multi-channel ultraviolet-visible-near infrared (UV-Vis-NIR) spectrometer recorded no absorption features. Microscopic examination revealed a series of iridescent thin films along cleavage planes in each sample (e.g. Figure 3). Additionally, short, fine tubules and fine particles were visible.

Anatase may appear visually similar to rutile, but the latter mineral is easily differentiated by its higher SG value (4.23 vs. 3.82–3.95; O'Donoghue, 2006).

Bryan Clark (bclark@aglgemlab.com)
American Gemological Laboratories
New York, New York, USA

Reference

O'Donoghue M., Ed., 2006. *Gems*, 6th edn. Butterworth-Heinemann, Oxford, 380.

Large Cat's-eye Apatite from Madagascar

For many years, Madagascar has been a source of small quantities of gem-quality apatite that is notable for its bright blue coloration, similar

to Paraíba-type tourmaline. Rarely, this material shows chatoyancy (Kammerling et al., 1995). Recently, gem dealer Dudley Blauwet brought to



Figure 4: This cat's-eye apatite from Madagascar weighs 584.22 ct, and is shown here in incandescent light. Photo by J. Rakovan.

our attention a cat's-eye apatite from Madagascar of a different colour that was notable for its large size (Figures 4 and 5). He obtained the 584.22 ct cabochon in April 2016 while on a buying trip to Ratnapura, Sri Lanka. The merchant who sold him the stone specialized in acquiring rough sphene (titanite) from the Darren mine located near Ambilobé in the Vohemar District of northern Madagascar. This supplier stated that the rough apatite used to cut this stone also was found at the Darren mine. This is generally consistent with a report by Pezzotta (1999), who documented apatite crystals up to 7 cm long associated with sphene, quartz and other minerals in alpine clefts of the Vohemar-Ambilobé region.

The apatite cabochon was examined by one of the authors (JR) for this report. It measured



Figure 5: Elongate planar veils traverse the length of the 584.22 ct apatite, as shown here in transmitted daylight-equivalent illumination. The c-axis is oriented perpendicular to these veils. Photo by J. Rakovan.

4.9 × 3.85 × 3.2 cm, and exhibited a colour shift from reddish brown in incandescent light to greenish yellow-brown in daylight-equivalent illumination (again, see Figures 4 and 5). A well-defined chatoyant 'eye' ran the length of the stone when it was viewed with reflected pinpoint illumination. Transmitted lighting revealed elongate planar veils of fluid inclusions that also traversed the length of the stone (Figure 5). Examination of the stone with a polariscope showed that these veils were generally oriented perpendicular to the c-axis. Microscopic examination revealed abundant growth channels parallel to the c-axis that were responsible for the chatoyancy (Figure 6a). At higher magnification, some of these growth tubes were seen to be partially filled with black or red solid phases (Figure 6b).

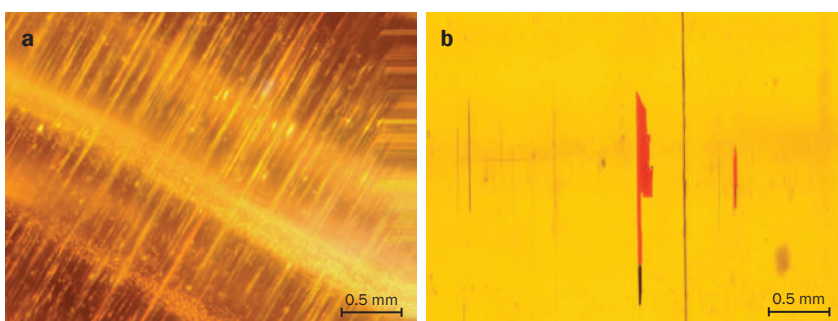


Figure 6: (a) Oblique transmitted lighting shows abundant growth tubes oriented parallel to the c-axis that are responsible for the apatite's chatoyancy. Perpendicular to these are thick planar veils of fluid inclusions (here, viewed edge-on). (b) Higher magnification reveals that some of the growth tubes are filled with black or red solid phases. Photomicrographs by J. Rakovan.

Confocal Raman spectroscopy using a 785 nm laser with a Renishaw InVia Raman microscope confirmed that the host gem was fluorapatite, but the solid phases in the inclusions could not be identified due to a high fluorescence background in the 500–200 cm^{-1} region and especially above 1000 cm^{-1} . Confocal Raman analysis with a 633 nm laser also produced strong fluorescence. Based on the inclusions' coloration and geological environment of formation, the red phase is probably hematite or lepidocrocite and the black material is likely a manganese oxide mineral.

The alpine clefts of northern Madagascar are known for producing large and fine specimens of

sphene and quartz, and these are now joined by chatoyant apatite.

*Dr John Rakovan (rakovajf@muohio.edu)
Miami University, Oxford, Ohio, USA*

Brendan M. Laurs

References

- Kammerling R.C., Koivula J.I., Johnson M.L. and Fritsch E., 1995. Gem News: Cat's-eye apatites from Madagascar. *Gems & Gemology*, **31**(3), 205–206.
- Pezzotta F., 1999. *Madagascar—A Mineral and Gemstone Paradise*. M.D. Jarnot, G.A. Neumeier, W.B. Simmons and G.A. Staebler, Eds., extraLapis English No. 1, Lapis International LLC. East Hampton, Connecticut, USA (see pp. 76–79).

Unusual Aquamarine from Pakistan

For decades, Pakistan has been an important producer of aquamarine and other pegmatitic minerals. In June 2015, gem dealer Dudley Blauwet obtained an unusual broken crystal of aquamarine while on a buying trip to northern Pakistan. His supplier stated that it came from Shah Nassir peak, near the village of Nyet in the Braldu Valley. The crystal locally contained conspicuous aggregates of green inclusions and also showed some chatoyant areas. In May 2016, four cabochons were cut from the 86.1 g crystal: The two largest (101.39 and 97.43 ct; e.g. Figure 7) were pale bluish green and had areas of weak chatoyancy along with patches of the green inclusions, while the two smaller gems (24.64 and 20.00 ct; e.g. Figure 8)

were greenish blue and displayed a sharp cat's-eye but contained no green inclusions.

Blauwet loaned the 97.43 ct cabochon to the American Gemological Laboratories for examination. The stone had RIs of 1.573–1.581 (birefringence 0.008) and a hydrostatic SG of 2.71, consistent with beryl. Confirmation of its identity was obtained by Raman analysis using a 514 nm laser. EDXRF chemical analysis of the sample showed the expected major amounts of Si and Al for beryl,

Figure 7: This 97.43 ct aquamarine cabochon from Pakistan contains conspicuous aggregates of green inclusions. Photo by Kelly Kramer and Bilal Mahmood.



Figure 8: This cat's-eye aquamarine (24.64 ct) was cut from the same piece of rough as the stone in Figure 7. Photo by Orasa Weldon.





Figure 9: An ocean-like scene of monazite-Ce inclusions is present within the aquamarine cabochon shown in Figure 7. Photomicrograph by Christopher P. Smith; magnified 30 \times .

as well as traces of Fe, Na and Mn. UV-Vis-NIR spectra collected with a multi-channel spectrometer showed typical aquamarine absorption features at 370 and 427 nm.

The cabochon revealed an extremely faint 'eye' when viewed with a concentrated fibre-

optic light source in certain directions. More interesting were the dense zones of yellowish green inclusions that created an ocean-like atmosphere (Figure 9); these were identified using Raman microspectroscopy (by comparison with the RRUFF database) as monazite-Ce. Gübelin and Koivula (2005) also documented yellowish green monazite inclusions in a beryl from Pakistan, but those in the present stone had a much finer texture. Additionally, the 97.43 ct cabochon contained small aggregates of greyish green and black zircon, as well as 'fingerprints' and very fine particles.

Blauwet reported that he has occasionally encountered similar specimens of aquamarine (only as one or two pieces at a time) since the early 2000s during various visits to northern Pakistan.

Bryan Clark

Reference

Gübelin E.J. and Koivula J.I., 2005. *Photoatlas of Inclusions in Gemstones*, Vol. 2. Opinio Publishers, Basel, Switzerland, 331.

Chrome Chalcedony from Tanzania

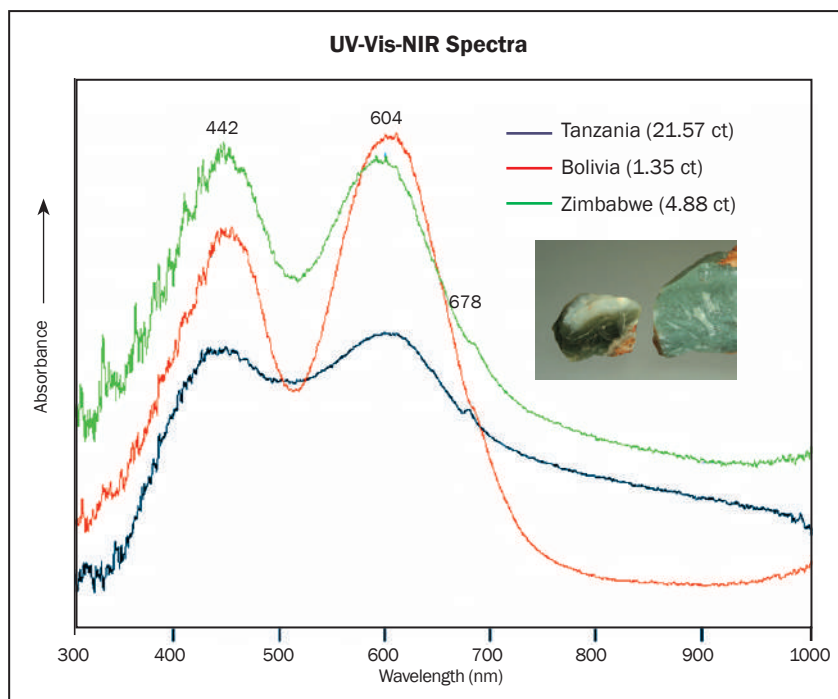
Chrome chalcedony is a rare variety of chalcedony that is typically dark green or 'olive' green, and is known from just a few localities worldwide: Zimbabwe ('mtorolite'), Bolivia, Turkey and Australia (Hyršl, 1999; Willing, 2003). It can be mistaken for similar-appearing chrysoprase, which is coloured by nickel. Like chrysoprase, chrome chalcedony occurs only in weathered ultramafic rocks.

Figure 10: Chrome chalcedony from Tanzania (left, 42 mm long) has a similar colour appearance to gem silica from the Lily mine in Peru (right). Photo by J. Hyršl.



A new material sold as 'gem silica' (Figure 10) appeared in 2016 from an unknown locality in Tanzania. While visiting Idar-Oberstein, Germany, this author saw approximately 20 polished cabochons that were up to about 5 cm in maximum dimension. Gem silica, also known as chrysocolla chalcedony (Frazier and Frazier, 1999), is another rare variety of chalcedony, which is coloured by microscopic inclusions of copper silicates. The colour of the new material showed obvious inhomogeneities consisting of 'turquoise' blue and near-colourless areas. The coloured portions were very similar to gem silica from Arizona, Peru or Namibia (see, e.g., Figure 10). The RI of the material was 1.537, and it remained bright upon rotation in a polariscope (i.e. aggregate reaction). When exposed to short-wave UV radiation, the colourless areas displayed strong yellow-green fluorescence and the blue parts luminesced light yellow-green, while in long-wave UV both areas fluoresced milky white. Viewed with a Chelsea filter, the blue areas appeared pink. UV-Vis-NIR

Figure 11: UV-Vis-NIR spectra for chrome chalcedony from Tanzania, Bolivia and Zimbabwe show chromium-related absorption features at 442, 604 and 678 nm. The inset shows the tested samples from Bolivia (left, 26 mm long) and from Zimbabwe (right); photo by J. Hyršl.



spectroscopy of the blue areas revealed chromium as the chromophore (Figure 11; see also Henn et al., 2016), so the correct description of this material is chrome chalcedony.

Dr Jaroslav Hyršl (hyrsl@hotmail.com)
Prague, Czech Republic

References

Frazier S. and Frazier A., 1999. The chrysocolchalcidony connection. *Lapidary Journal*, **52**(11), 34–40.

Henn U., Schültz-Guttler R. and Stephan T., 2016. Grüne undurchsichtige Quarze. *Gemmologie: Zeitschrift der Deutschen Gemmologischen Gesellschaft*, **65**(1/2), 9–22.

Hyršl J., 1999. Chrome chalcedony—a review. *Journal of Gemmology*, **26**(6), 364–370, <http://dx.doi.org/10.15506/JoG.1999.26.6.364>.

Willing M.J., 2003. A new chrome chalcedony occurrence from Western Australia. *Journal of Gemmology*, **28**(5), 265–279, <http://dx.doi.org/10.15506/JoG.2003.28.5.265>.

Yellow Dravite from Tanzania

During the 2016 Tucson gem shows, Todd Wacks (Tucson Todd’s Gems, Tucson, Arizona, USA) showed author BML a yellow 11.13 ct tourmaline that he faceted from a piece of rough recently obtained on a buying trip to Tanzania by Sir-Faraz Ahmad (Farooq) Hashmi (Intimate Gems, Glen Cove, New York, USA). The rough material was reportedly found in October–November 2015 in the Landanai region of north-eastern Tanzania, in an area that is known for producing green ‘chrome’ tourmaline. The rough consisted of a round ‘nodule’ that showed a few crystal faces (Figure 12, left). In faceting the gemstone, Wacks cut a small table and a deep pavilion to maximize the colour appearance (Figure 12, right).

Landanai is located in the same region of East Africa that produces ‘golden’ yellow tourmaline, particularly in the Taita-Taveta District of southern Kenya (see Simonet, 2000, and references therein). The tourmaline from this area is commonly dravite with a minor uvite component. Since the slightly orangey yellow coloration of the present tourmaline was somewhat different from the typical ‘golden’ tourmaline, we decided to examine the stone in more detail.

Refractive indices measured by author BML were typical for tourmaline: 1.620–1.639 (birefringence 0.019). Microscopic examination revealed a few minor ‘fingerprints’ and a single colourless mineral inclusion. Additional testing



Figure 12: The tourmaline gem nodule from Tanzania on the left was faceted into the 11.13 ct stone on the right. Photos by Todd Wacks (left) and Orasa Weldon (right).

was performed by author GRR at the California Institute of Technology. The composition of the sample was determined by energy-dispersive X-ray analysis using a Zeiss 1550 VP field-emission scanning electron microscope (SEM) with an Oxford Instruments X-MaxN SDD energy-dispersive spectroscopy (EDS) analysis system. A square-shaped area (155 μm wide) on the table of the stone was analysed. Because the sample was not carbon coated to conduct away electrons from the SEM beam, the analysis was run in variable-pressure mode. The X-ray spectrum (Figure 13) indicated that the stone was dominantly a Na,Mg-aluminosilicate. Minor amounts of Ca, Fe and Ti (but no Mn) also were detected. Detailed analysis

of the X-ray spectrum with Oxford Instruments AZtec software showed that a significant amount of boron was present in addition to the other elements mentioned above. The data confirmed that the tourmaline was dravite, with Fe and Ti most likely responsible for its colour.

The slightly orangey yellow colour of the dravite showed moderate dichroism such that the E \perp c direction had the more intense colour. Compared to many dravites of similar size, which are commonly brown, this sample showed a low intensity of colour and a high degree of transparency. To confirm the cause of colour, Vis-NIR spectroscopy was performed. Absorption spectra (Figure 14) were obtained through the girdle of

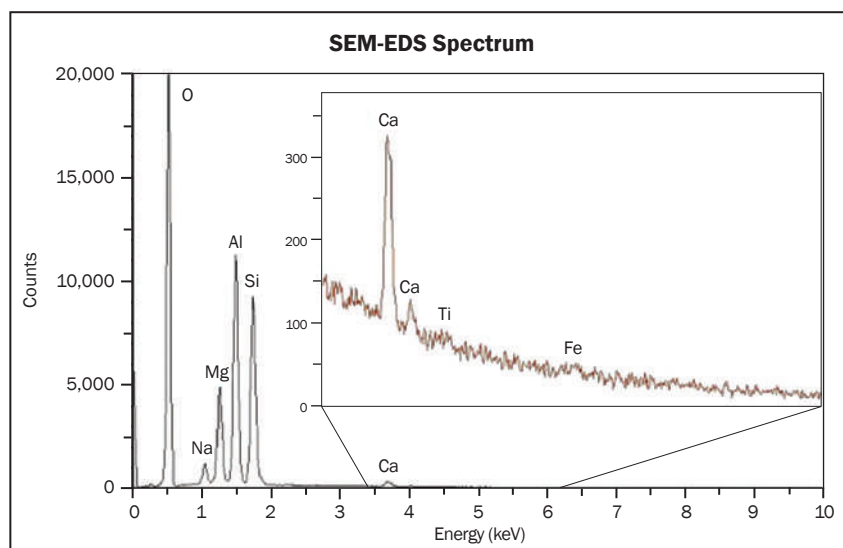


Figure 13: SEM-EDS chemical analysis shows that the tourmaline in Figure 12 is Mg-rich with some Na and minor Ca, corresponding to a dravite composition. Also present are traces of Fe and Ti.

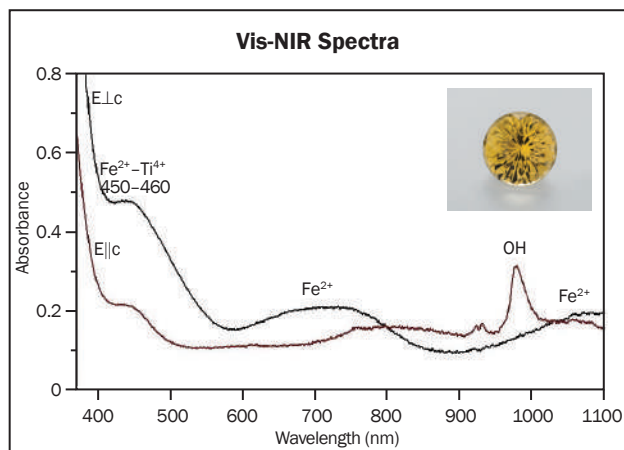


Figure 14: Polarized Vis-NIR absorption spectra of the yellow dravite show a dominant feature in the 450–460 nm region that is caused by Fe^{2+} – Ti^{4+} intervalence charge transfer. The spectrum is plotted for a 10.0 mm sample thickness.

the stone with the beam polarized both parallel and perpendicular to the girdle direction, corresponding to the $E_{\perp c}$ direction and approximately to $E_{\parallel c}$, respectively. A prominent absorption feature was recorded in the 450–460 nm region, and this is also an important characteristic of brown dravite such as the material from Yin-*nietharra*, Australia. It arises from Fe^{2+} – Ti^{4+} intervalence charge transfer (Mattson and Rossman,

1988), and is the dominant cause of colour in this dravite. Fe^{2+} -related features occurred near 700 and 1100 nm, and narrower peaks in the 900–1000 nm region were overtones of OH absorptions in the infrared.

This attractive yellow dravite is much lighter coloured than typical brown dravite because of its low Fe and Ti contents. Its spectrum is similar to that of the golden dravite from Kenya (cf. Simonet, 2000), except that the broad absorption band in that material was centred at 435 nm rather than in the 450–460 nm region.

Dr George Rossman (grr@gps.caltech.edu)

and Chi Ma

California Institute of Technology

Pasadena, California, USA

Brendan M. Laurs

References

- Mattson S.M. and Rossman G.R., 1988. Fe^{2+} – Ti^{4+} charge transfer in stoichiometric Fe^{2+} , Ti^{4+} -minerals. *Physics and Chemistry of Minerals*, **16**, 78–82, <http://dx.doi.org/10.1007/bf00201333>.
- Simonet C., 2000. Geology of the Yellow mine (Taita-Taveta District, Kenya) and other yellow tourmaline deposits in East Africa. *Journal of Gemmology*, **27**(1), 11–29, <http://dx.doi.org/10.15506/jog.2000.27.1.11>.

New Garnets from East Africa

During a buying trip to Arusha, Tanzania, from late May to early June 2016, rough stone dealer Farooq Hashmi encountered some new garnet rough that was reported to be from north-eastern Tanzania or south-eastern Kenya. Several kilograms were available as pebbles and fractured pieces ranging up to ~10 g. The garnet was sold by local dealers as rhodolite. The colour of the material showed some variation, and Hashmi purchased only the lighter material (with a more purple colour in daylight), which he has marketed as 'Rhodolaya'.

Hashmi loaned three faceted stones (e.g. Figure 15) and 18 rough samples to authors CW and BW for examination. The cut stones weighed 3.24, 3.36 and 3.89 ct, and measured up to $9.4 \times 8.2 \times$

Figure 15: These two specimens (3.24 and 3.89 ct) are representative of some of the new garnet production from East Africa. The stones were faceted by Marvin M. Wambua, Safigemscutters Ltd., Nairobi, Kenya; photo by B. Williams.



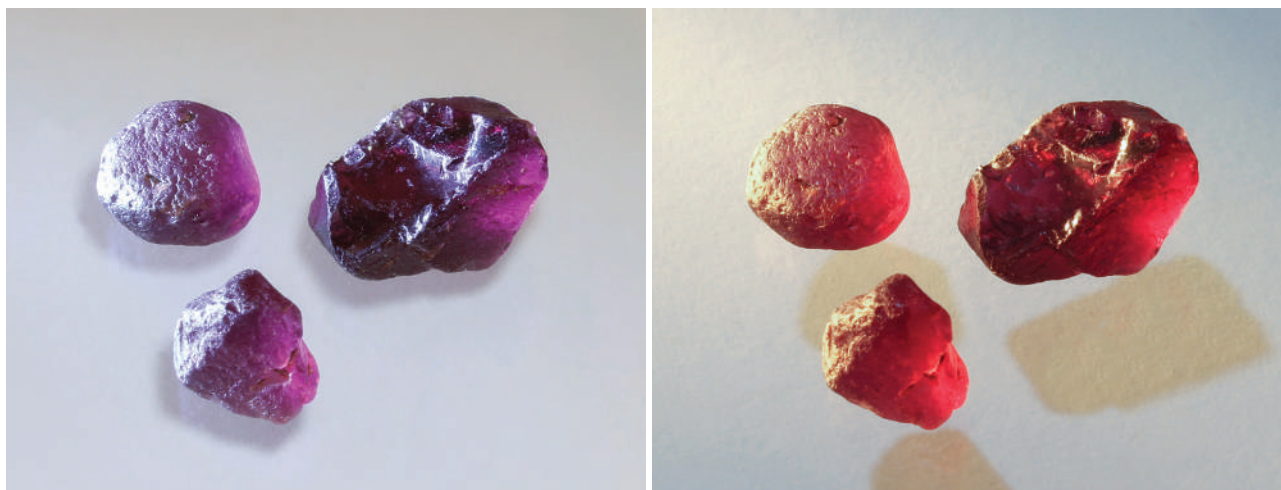


Figure 16: These rough garnets (2.1–5.4 g) appear strongly bluish purple in daylight (left) and slightly orangey red in incandescent light (right). Photos by B. Williams.

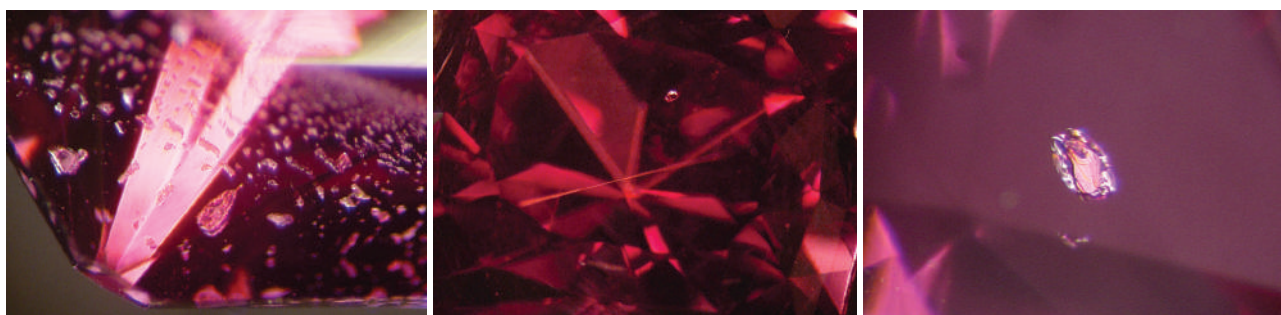
6.2 mm. The rough material weighed a total of 50.1 g and the piece with the longest dimension measured 21.3 mm. The faceted stones appeared moderate purplish red (typical of rhodolite) under daylight-type illumination, and changed to a slightly orangey red (as commonly seen in malaya garnet) in incandescent light. However, in these authors' opinion, there was not enough of a shift to label it colour-change garnet. The rough stones appeared slightly orangey red in incandescent light and displayed a strong bluish purple in transmitted daylight (Figure 16), but the latter colour was not evident in the faceted stones, possibly due to dichromatism as a result of their smaller size and therefore shorter path length of light.

Refractive indices varied slightly from 1.743 to 1.749, and the hydrostatic SG value of all three cut stones was 3.82; these data are consistent with pyralspite garnet. The faceted samples exhibited various appearances between crossed polarizers, with one showing no strain and re-

maining dark during rotation, one behaving like an anisotropic stone and blinking four times during a complete rotation, and one showing patchy anomalous birefringence. Some of the rough material also displayed patchy birefringence. All of the faceted stones were eye-clean, but the microscope revealed a 'fingerprint', a fine colourless needle and a dark reflective crystalline inclusion surrounded by tension fractures (Figure 17). UV-Vis spectroscopy showed mainly almandine-related absorptions at 505, 527 and 575 nm. Raman analysis yielded a pattern expected for pyralspite garnets, and the samples showed moderate magnetic susceptibility.

Chemical data for the three faceted stones was obtained by author AUF via standard-based SEM-EDS analysis using a Jeol JSM-6400 instrument with the Iridium Ultra software package by IXRF Systems Inc. The data showed a similar composition for all three samples (Table I), consisting mainly of the pyrope component (58.9–62.2 mol%) with ma-

Figure 17: The faceted garnet samples were found to contain a 'fingerprint' (left), a colourless needle (centre) and a crystalline inclusion (centre and right). Photomicrographs by C. Williams; magnified 40× (left and right) and ~15× (centre).



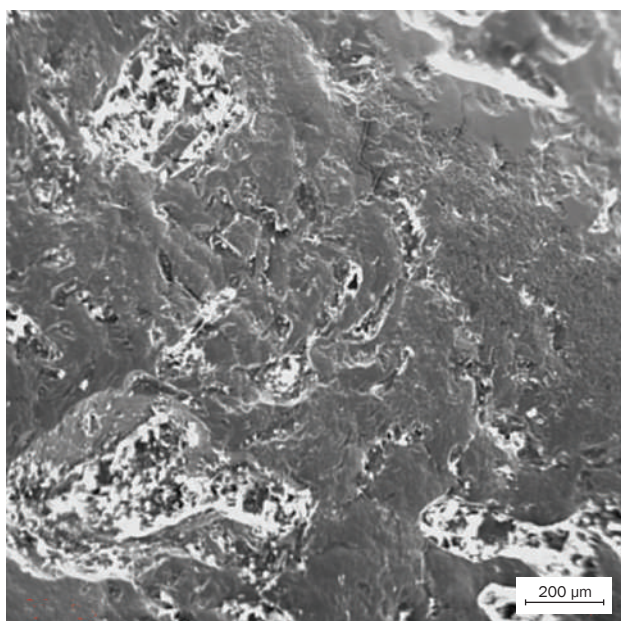
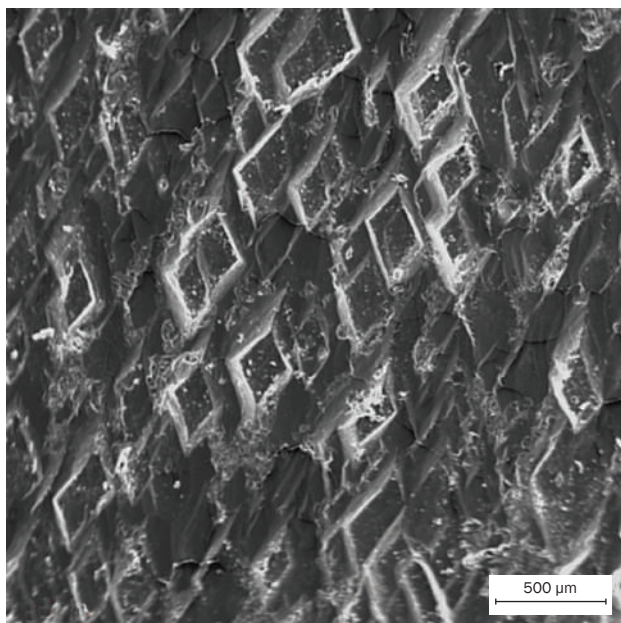


Figure 18: These SEM images of the surface features of two garnet pebbles show evidence of chemical etching (top) and the effects of mechanical abrasion from alluvial transport (bottom). Images by A. U. Falster.

for almandine (24.0–28.5 mol%), and much lower spessartine (6.9–9.8 mol%) and grossular (5.2–5.9 mol%) components. Minor amounts of V, Cr and Ti also were present in all samples. This combination is commonly seen in garnets of the rhodolite

Table I: Representative SEM-EDS analyses of three new garnets from East Africa. *

Composition	Trilliant	Round	Cushion
Oxide (wt.%)			
SiO ₂	40.89	41.03	41.01
TiO ₂	0.15	0.17	0.11
Al ₂ O ₃	23.04	23.02	22.98
Cr ₂ O ₃	0.15	0.15	0.20
V ₂ O ₃	0.26	0.24	0.05
FeO	12.41	11.89	13.98
MnO	4.71	4.20	3.35
MgO	16.15	17.30	16.32
CaO	2.24	2.00	2.00
Total	100.00	100.00	100.00
Ions based on 12 oxygens			
Si	2.990	2.985	2.999
Ti	0.008	0.009	0.006
Al	1.986	1.975	1.981
Cr ³⁺	0.009	0.009	0.012
Bi ³⁺	0.000	0.000	0.000
V ³⁺	0.015	0.014	0.003
Fe ²⁺	0.759	0.724	0.855
Mn	0.292	0.259	0.207
Mg	1.761	1.876	1.778
Ca	0.175	0.156	0.157
Mol% end members			
Pyrope	58.9	62.2	59.4
Almandine	25.4	24.0	28.5
Spessartine	9.8	8.6	6.9
Grossular	5.9	5.2	5.2

* Data are auto-normalized by the software, and therefore the sum of the oxides is 100 wt.%.

and malaya varieties. Interestingly, SEM images of the surface of the rough samples showed evidence of both chemical etching and mechanical abrasion from alluvial transport (Figure 18).

East Africa continues to be an important source of gem-quality pyrospite garnets, as shown by this attractive new material.

*Cara Williams FGA and Bear Williams FGA
(info@stonegrouplabs.com)
Stone Group Laboratories
Jefferson City, Missouri, USA*

*Alexander U. Falster and William ‘Skip’ B. Simmons
Maine Mineral and Gem Museum, MP2 Group
Bethel, Maine, USA*

Quartz Cubes from Volodarsk-Volynski, Ukraine

The Volynian granitic pegmatite deposits in western Ukraine are historic sources of superb gem-

quality beryl, topaz and smoky quartz (Lyckberg et al., 2009). Quartz was the main target for min-

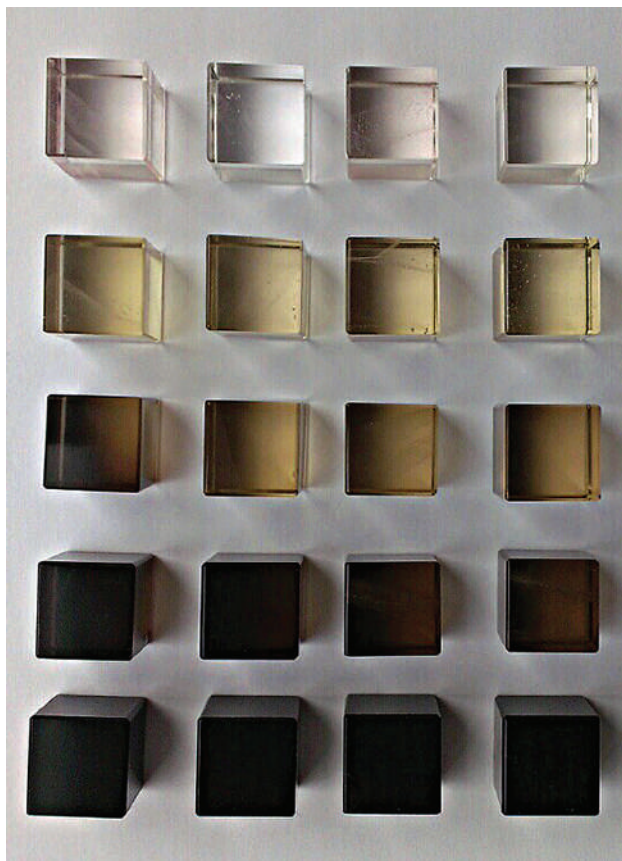


Figure 19: These polished quartz cubes from Volodarsk-Volynski, Ukraine, show various amounts of smoky coloration, ranging from black (untreated) to near-colourless (heated to 340–350 °C). Each cube measures 2 cm wide. Photo by Dr Rostyslav Kyrii, mine manager.

ing back in the Soviet era due to its piezoelectric properties. Since approximately 2012, the three major mines in the area have been under the control of PJSC Kwartssamotvit (Volodarsk-Volynski, Zhitomir Oblast, Ukraine), with this author being a consultant since March 2016. The company mines only one deposit at a time due to ongoing flooding by groundwater that requires pumping on a 24-hour basis. The two main levels of the mines are at approximately 60 and 120 m depth. Large quartz crystals have been found in all of the mines and at all levels. Due to the large size of the gem-bearing ‘pockets’ or cavities—typically several metres in dimension, making them some of the largest in the world—only one pocket at a time is mined by the current full-time operation.

Due to natural radiation within the pegmatite, most of the quartz is so smoky that it appears black (morion). The radiation damage can be re-

versed by heating the quartz to temperatures up to 350°C. The fading of the smoky colour is carefully controlled according to the heating temperature, yielding a full range from dark smoky to near-colourless. The temperature range needed to produce a given colour is not always consistent; because the various pockets have different radiation histories, the quartz from each behaves slightly differently.

The heating process is done by placing the quartz (rough pieces or entire crystals) within sand in an oven. The sand helps provide even heating and reduces fracturing due to thermal expansion and contraction. Approximately 40 minutes to one hour is taken to bring the quartz up to the chosen temperature, and it is held there for one hour. The temperature is then slowly reduced over a period of about 12 hours. Starting with morion, the temperatures used to produce the various colours are as follows: dark brown—270–290°C, light brown—290–300°C, pale smoky to citrine—310–320°C, and near-colourless—340–350°C.

After heat treatment, the quartz is processed into sets of polished cubes (e.g. Figure 19) at the company’s cutting centre in Volodarsk-Volynski for use in modern jewellery designs. Each colour set consists of five cubes that measure 2 cm wide. In addition, some smaller cube sets are being created for earrings (4 and 6 mm) and pendants (8 mm), and beads also are being cut. These quartz products are presently being produced from six cutting lines (three automated). Several dozen prototype cube sets have been manufactured, and the company is currently starting full production.

The cubes typically contain veils and feathers that add interest to the quartz by forming various three-dimensional inclusion patterns. The sets also provide an educational example of the effect of annealing a naturally irradiated gem material.

*Dr Maury Morgenstein (memgmi@gmail.com)
Geosciences Management International Inc.
Waldport, Oregon, USA*

Reference

Lyckberg P., Chornousenko V. and Wilson W.E., 2009. Famous mineral localities: Volodarsk-Volynski, Zhitomir Oblast, Ukraine. *Mineralogical Record*, **40**(6), 473–506.

An innovator in gemstone reporting

- Identification of colored gemstones • Country of origin determination • Full quality and color grading analysis



AMERICAN GEMOLOGICAL LABORATORIES



580 5th Ave • Suite 706 • New York, NY 10036, USA
www.agilgemlab.com • +1 (212) 704 - 0727

Star Sapphire Showing a Variable Number of Rays

This article documents an unusual nine-rayed star sapphire that weighs 8.47 ct ($11.89 \times 10.16 \times 6.06$ mm) and originated in Myanmar according to its owner. The stone is accompanied by a report from GRS GemResearch Swisslab that is dated 2007. A nine-rayed star is observed when the cabochon is illuminated at its centre with a pinpoint light (Figure 20a). The asterism consists of a complete six-rayed star of white-coloured rays that is bisected on its right side by a three-rayed star of

a higher density of inclusions (corresponding to the area showing the 12-rayed star). The latter bands were quite similar to those seen in 'Gold Sheen' sapphires from Kenya (Bui et al., 2015). Observed with transmitted light (Figure 21, right), the whitish and brownish bands appeared darker, while the blue bands were lighter. This highlights the presence of mechanical coloration by inclusions constituting the whitish and brownish bands of the blue sapphire.

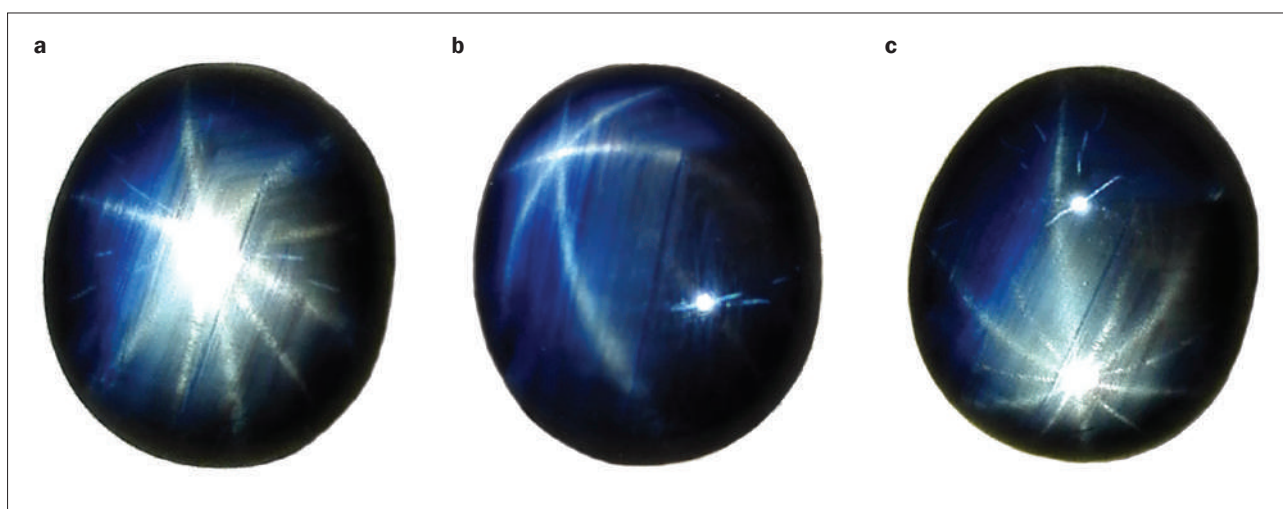


Figure 20: Depending on how this 8.47 ct sapphire cabochon is illuminated, it displays (a) a nine-rayed star, (b) a six-rayed star or (c) a 12-rayed star. The pinpoint light source is positioned over the centre, bottom right and top-centre of the stone, respectively. Photos by T. N. Bui.

pale brown colour. However, when moving the light source along the stone, the number of rays does not stay constant: a white six-rayed star is observed on one end of the cabochon (Figure 20b) and a 12-rayed star composed of both pale brown and white rays is seen on the opposite end (Figure 20c). This suggests an inhomogeneity of the inclusions that produce the asterism in the host sapphire, thus motivating further investigations.

The body colour of the sapphire was blue and its overall diaphaneity ranged from transparent to slightly translucent. Growth zoning was observable as banding along the crystallographic directions of the corundum host. Two different areas of the cabochon could be distinguished (Figure 21, left): a transparent area with narrow whitish and blue growth zoning (corresponding to the area showing the six-rayed star) and a translucent-to-opaque portion with broad brownish bands and

The white six-rayed star in Figure 20 has branches that are oriented perpendicular to or at $\pm 30^\circ$ from the growth zoning bands. A pale brown six-rayed star, partly visible within the nine-rayed star of Figure 20a and complete in the 12-rayed star of Figure 20c, is perpendicular to the former so its branches are parallel to or at $\pm 60^\circ$ from the growth zoning bands. These observations suggest that the white six-rayed star is formed by rutile-type inclusions and the pale brown one by hematite/ilmenite-type inclusions (cf. Hughes, 1997, p. 446).

Close inspection of the inclusions at high magnification revealed some details about the microstructure of the whitish and brownish bands. On the end of the cabochon showing the six-rayed star, the density of the acicular inclusions on the surface was weak. Networks of needles, in three different orientations and intersecting

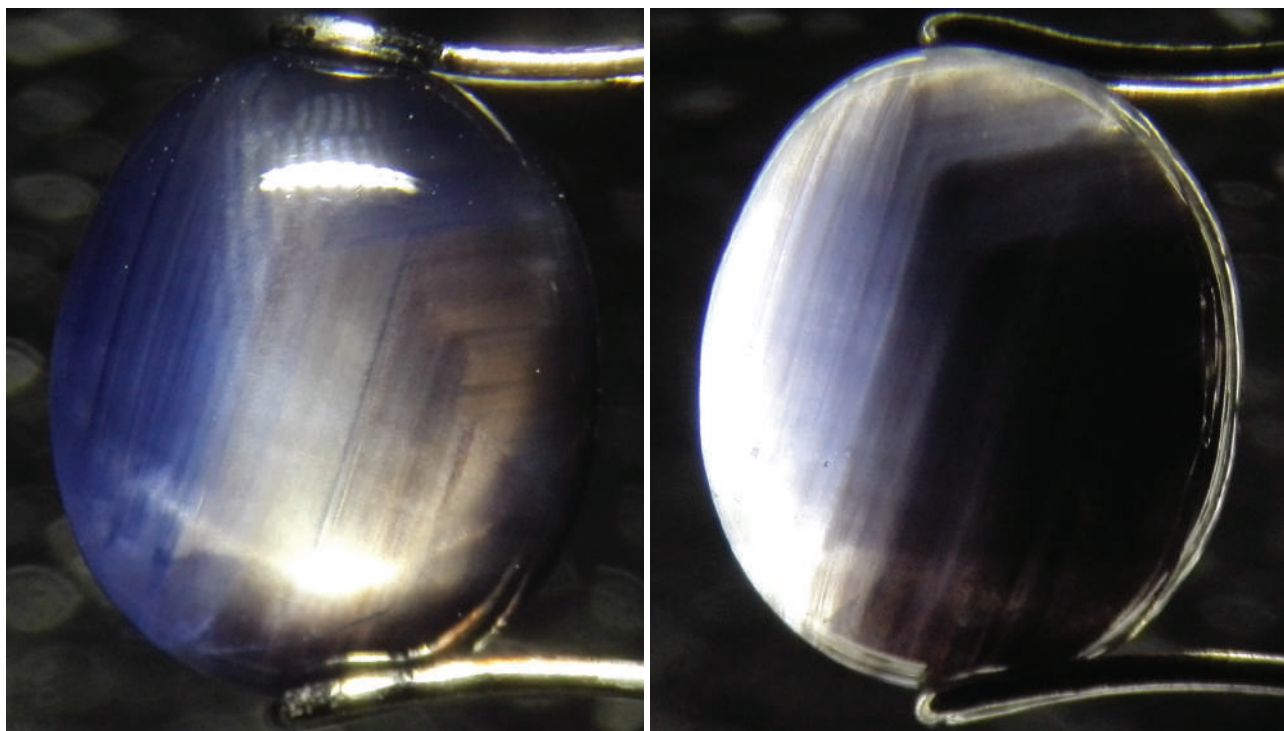


Figure 21: As seen in the left photo in brightfield illumination, colour and growth zoning in the 8.47 ct star sapphire are characterized by white (left portion) and brown-bronze (right portion) bands along the crystallographic directions of the corundum host. Transmitted light (right photo) reveals the mechanical coloration by the inclusions constituting the growth bands. Photomicrographs by T. N. Bui.

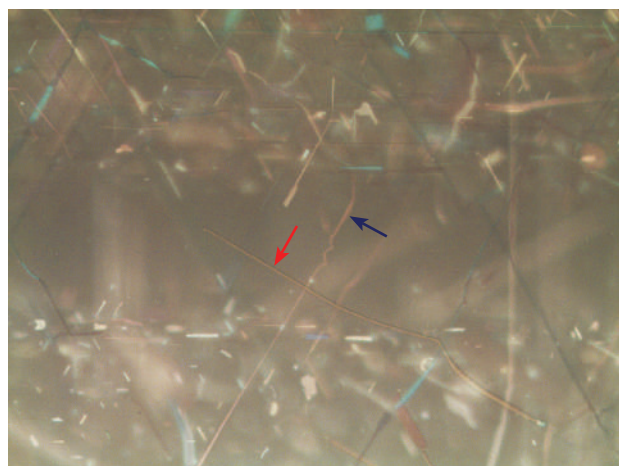
at 120° typical of the three-fold rotational symmetry, were present within the basal pinacoid. These needles were oriented parallel to the corundum growth bands. Two similar networks of needles and platelets were present on the other end of the stone showing the 12-rayed star. The needles were parallel to the growth bands, while the platelets were perpendicular to it. The density of the inclusions in the latter network was quite high. Both networks appeared to overlap, but in fact they grew in alternating layers along the *c*-axis (Figure 22).

Raman spectra of the inclusions (Figure 23) gave results that were quite similar to previous studies (e.g. Palanza et al., 2008; Bui et al., 2015). The needles on the end of the cabochon showing the six-rayed star were identified as rutile, while both rutile and ilmenite were present on the other end, producing the 12-rayed star.

By analysing the pattern of the growth zoning in this Burmese sapphire, we deduce that crystal growth began from the bottom side of the brownish area. The initial input of fluids rich in Ti and Fe resulted in abundant exsolved phases of epigenetic inclusions in the host sapphire. Sharp

changes in the concentrations of Ti and Fe at each growth step produced the oscillating broad brownish bands along the crystallographic directions in the basal pinacoid.

Figure 22: Networks of oriented inclusions consisting of needles and/or platelets lie within the basal pinacoid of the sapphire, where they form alternating layers. Both rutile (blue arrow) and ilmenite (red arrow) inclusions were identified in the brownish growth bands of the cabochon. Photomicrograph by T. N. Bui, brightfield illumination; field of view $330 \times 250 \mu\text{m}$.



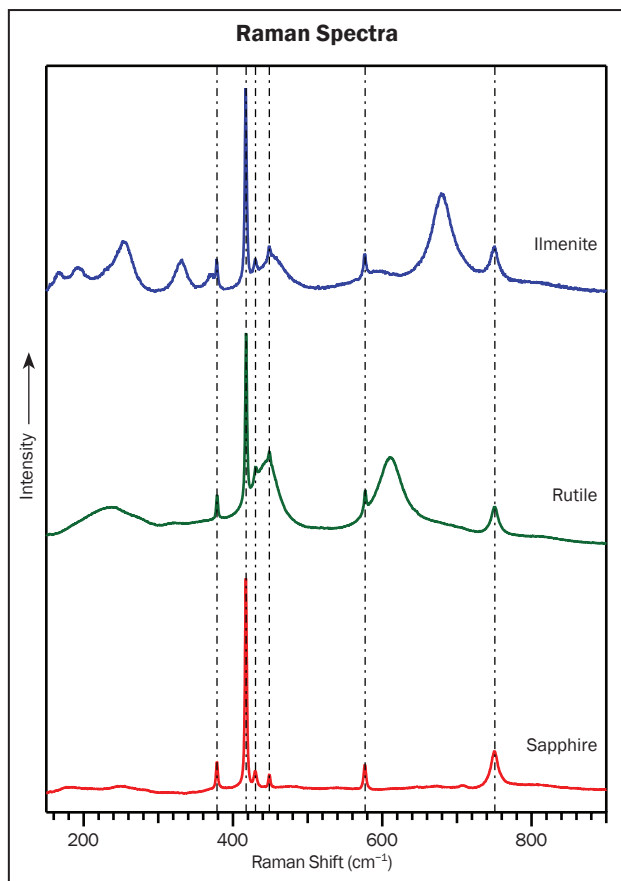


Figure 23: Raman spectra are shown for the host sapphire and for the inclusions responsible for the whitish and the brownish growth zoning, respectively—identified as rutile and both rutile and ilmenite needles and/or platelets. The vertical dashed lines indicate the Raman peaks of corundum superimposed on those of the analysed inclusions.

Microscopic observation of the inclusions in the brownish area at different positions along the c-axis (not shown here) revealed that inclusions of the same type were co-planar. This suggests that a fluctuation of Ti- and especially Fe-rich fluids occurred during crystal growth along the c-axis. Assuming a constant Ti input, Fe-poor fluids lead to rutile and Fe-rich to ilmenite. Subsequently, the input of Fe-rich fluids drastically

decreased, generating only exsolution of rutile during further growth of the crystal in the basal plane. This explains the six- and 12-rayed stars that were produced, respectively, by exsolution of rutile and both rutile and ilmenite.

Nature's decision to vary the seasoning of Fe-rich fluids during the formation of the corundum crystal—combined with a controlled or fortuitous cutting orientation of the rough so that the border between the two regions was located at the centre of the cabochon—are simultaneously responsible for the unusual nine-rayed asterism visible only when the stone is illuminated at its centre.

Acknowledgements: This work was partially funded by Almini Beijing Trading Co. Ltd. (阿尔米尼北京贸易有限公司), China. We are grateful to Tanzim Khan Malik for supplying the sample. Our gratitude goes to Yiannis Karvelis for proof-reading the English text.

Thanh Nhan Bui (tnhan93@gmail.com)
 Université catholique de Louvain
 Louvain-la-Neuve, Belgium

Katerina Delioussi and Dr Katrien De Corte
 HRD Antwerp, Belgium

Jean-Pierre Gauthier
 Centre de Recherches Gemmologiques
 Nantes, France

References

- Bui T.N., Delioussi K., Malik T.K. and De Corte K., 2015. From exsolution to 'gold sheen': A new variety of corundum. *Journal of Gemmology*, **34**(8), 678–691, <http://dx.doi.org/10.15506/JoG.2015.34.8.678>.
- Hughes R.W., 1997. *Ruby & Sapphire*. RWH Publishing, Boulder, Colorado, USA, 512 pp.
- Palanza V., Di Martino D., Paleari A., Spinolo G. and Prospero L., 2008. Micro-Raman spectroscopy applied to the study of inclusions within sapphire. *Journal of Raman Spectroscopy*, **39**(8), 1007–1011, <http://dx.doi.org/10.1002/jrs.1939>.

Unusual Star Sapphire from Tanzania

In this study, we document an interesting Tanzanian star sapphire that is set in a gold ring. Called 'Zebra Star', the stone resides in author PE's collection. Rather than displaying uniform

blue coloration, the background consists of a series of striated parallel bands of various widths that range from white to dark blue (Figure 24). Such a thick-banded zonal structure is unusual



Figure 24: The asteriated Tanzanian sapphire (~13 × 9 mm) in this ring displays large and distinct colour bands that are oriented perpendicular to the vertical branch of the star. Photo by J.-P. Gauthier.

in sapphire, although it was reported by Fritsch and Lulzac (2004) in the case of a slightly asteriated stone, without any reference to the country of origin.

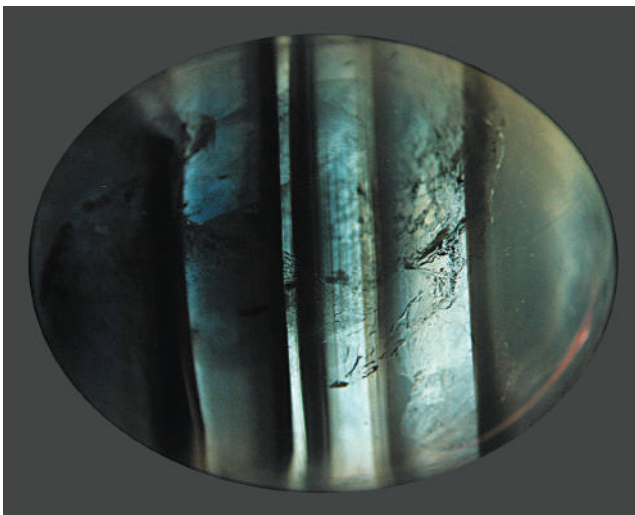
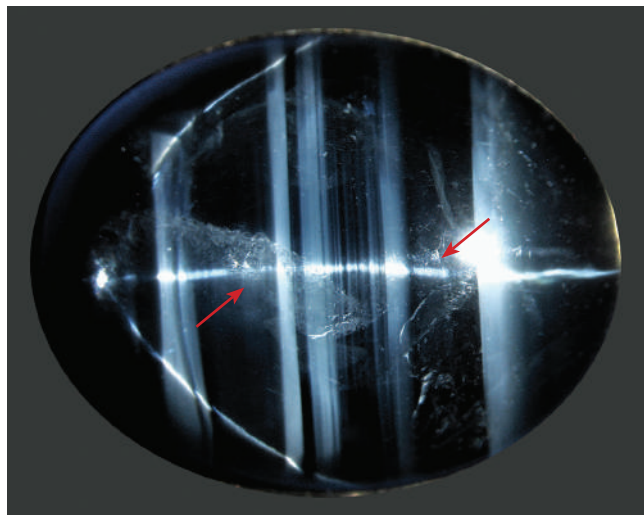
The cabochon measured approximately 13 × 9 × 6 mm. It was first observed with a Leica S8 APO binocular microscope (up to 80×), and then with a Leica DM4000 B for higher magnification (up to 400×). To avoid removing the stone from the ring, we examined it by lighting the front side

with a regular desk lamp and the back with a special illuminator. Reflected light (Figure 25, left) showed broad and narrow bands of alternating dark and light hues. The opacity of the stone prevented focusing the microscope inside the white bands. Transmitted light (Figure 25, right) produced an inversion of the band hues, while confirming the opacity of the white bands and conversely demonstrating the transparency of the dark bands.

On the vertical branch of the star oriented perpendicular to the colour bands, it was possible to detect the presence of thin white acicular inclusions (Figure 26, top). These inclusions, oriented parallel to the colour banding, accounted for the chatoyancy of the corresponding branch of the star. Their relative orientation with respect to the bands, their aspect ratio and their colour suggested they are rutile needles (cf. Sahama, 1982; Hughes, 1997, pp. 94 and 446). The high density of these inclusions ‘mechanically’ colours the white zones (cf. Hughes, 1997, p. 447), whereas the depleted zones showed significant transparency and therefore appeared dark.

Viewing the same area of the stone with the star branch at 60° from the colour banding showed another set of reflective needles that was oriented perpendicular to that branch (Figure 26, bottom). A similar observation was made for the third branch of the star at 120°. In each case, the

Figure 25: The ~13 × 9 mm star sapphire is shown here in reflected light (left) and in transmitted illumination (right). The banding displays a reversal of shades between the two images. Also visible in the left image are ‘fingerprint’ inclusions (red arrows). Since it was challenging to produce homogeneous transmitted lighting, the reversal of band hues is less evident on the left side of the stone in that photo. Both images have been edited to show the stone without the surrounding mounting. Photos by J.-P. Gauthier.



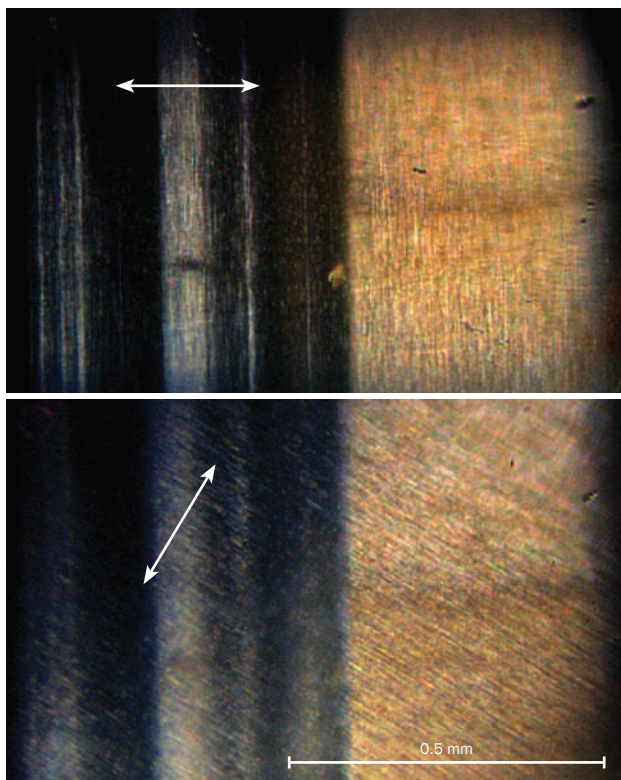


Figure 26: These two images, taken at the same position of the star sapphire, show the orientation of needle inclusions according to the direction of the particular star branch (indicated by arrows) that is illuminated. The top photo shows the main branch of the star, perpendicular to the colour banding, while the bottom image illuminates the star branch at 60° from the previous one. The visible needles are, in each case, those oriented perpendicular to the corresponding star branch. Photomicrographs by J.-P. Gauthier.

density of needles was higher in the white zones and lower in the darker ones. At high magnification, the rutile needles were seen to have widths in the micron range (Figure 27).

The sharp change in rutile-needle concentration among the thick bands oriented in a single direction gives this sapphire its unusual and appealing striped appearance. By contrast, in most asteriated gem corundum, considered as ‘homo-geneous’, each of the three needle systems is distributed uniformly without any preferential localization, resulting in a star that is seen over a uniform body colour. It is also common to see growth zoning defined by concentric hexagonal patterns that are generally formed by narrow zones (e.g. Gübelin and Koivula, 2008, pp. 222–223, 226), which are quite different from the banded effect described here.

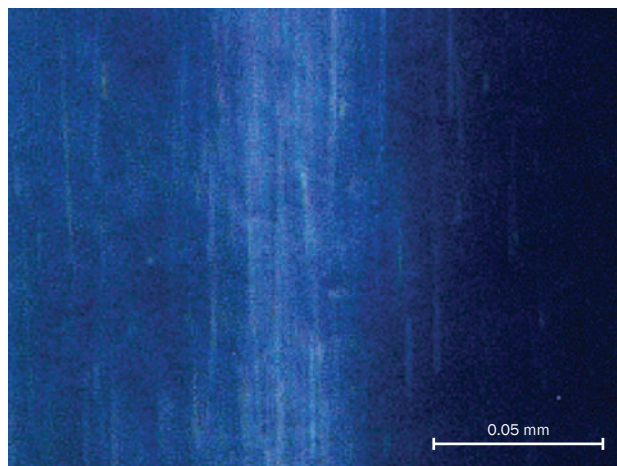


Figure 27: At high magnification, the needles in the star sapphire (oriented vertically in this image) exhibit widths in the micron range. Photomicrograph by J.-P. Gauthier.

The banded zoning in this sapphire is apparently due to fluctuating inputs, during crystallization, of fluids rich and poor in minor elements (i.e. Ti for rutile), followed by exsolution of rutile inclusions in amounts corresponding to the sharp changes in impurity concentration within each growth step. Thus, the formation of this Tanzanian star sapphire was controlled by particular circumstances, specifically during fluid inputs, which created highly contrasting broad bands that are rich or poor in acicular inclusions. The single direction of the striations in the sapphire may be explained by the cutter’s decision to use just one segment of the hexagonal growth pattern that was present in the original rough stone.

Pascal Entremont and Jean-Pierre Gauthier
(jpk.gauthier@gmail.com)

Centre de Recherches Gemmologiques
Nantes, France

Thanh Nhan Bui

References

- Fritsch E. and Lulzac Y., 2004. Gem News International: Unusual star and “cat’s-eye” sapphire. *Gems & Gemology*, **40**(4), 345–346.
- Gübelin E.J. and Koivula J.I., 2008. *Photoatlas of Inclusions in Gemstones*, Vol. 3. Opinio Publishers, Basel, Switzerland, 672 pp.
- Hughes R.W., 1997. *Ruby & Sapphire*. RWH Publishing, Boulder, Colorado, USA, 512 pp.
- Sahama T.G., 1982. Asterism in Sri Lankan corundum. *Schweizerische Mineralogische und Petrographische Mitteilungen*, **62**(1), 15–20.

Scapolite from Tanzania with Magnetite Inclusions

During the February 2016 Tucson gem shows, gem dealer Dudley Blauwet bought a 48.06 g scapolite crystal that contained numerous black inclusions. It appeared light yellow when viewed down the c-axis and greyish tan down the a- and b-axes. His East African supplier indicated that the stone came from an unspecified deposit in Tanzania, but not from the previously known scapolite mines in the Dodoma area. The crystal was faceted into two stones (weighing a total of ~87 carats), rather than one, to avoid a fracture in the centre and also to show the best colour by cutting the table perpendicular to the c-axis.

Blauwet loaned one of the stones, a 31.44 ct light brown cushion cut (Figure 28), to American Gemological Laboratories for examination. Standard gemmological testing was consistent with scapolite, and the RIs of 1.542–1.560 (birefringence 0.018) indicated an intermediate composition between the Na-rich end-member marialite and the Ca-rich end-member meionite, though somewhat closer to marialite (cf. Deer et al., 1963). The hydrostatic SG was 2.66. The stone fluoresced moderate purplish pink to long-wave UV radiation and moderate orangey red to short-wave UV. The black platelet inclusions were con-

spicuous to the unaided eye. Microscopic examination showed the platelets were both discoid and irregular in shape (Figure 29), and were randomly oriented throughout the stone. The inclusions were identified as magnetite with Raman spectroscopy using a 514 nm laser.

Magnetite inclusions have been documented previously in brown cat's-eye meionite from the Dodoma area (Mayerson et al., 2003). However, their distribution and appearance—oriented fine needles, elongated platelets and flat dendrites—were much different than the magnetite inclusions in the present sample.

Monruedee Chaipaksa (mchaipaksa@aglgemlab.com)
American Gemological Laboratories
New York, New York, USA

Brendan M. Laurs

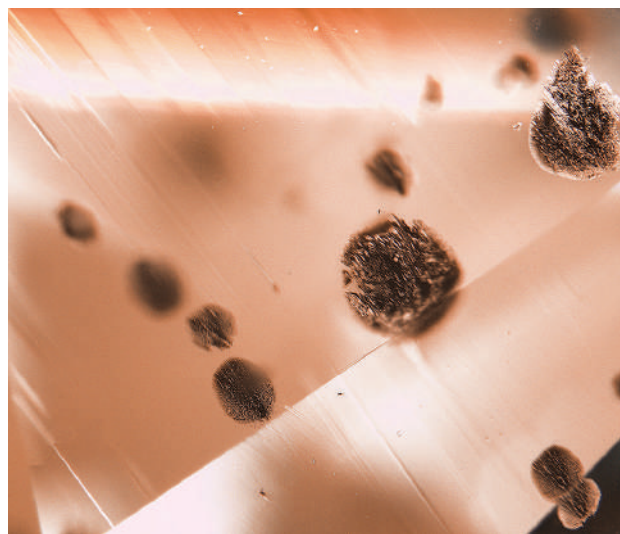
References

- Deer W.A., Howie R.A. and Zussman J., 1963. *Rock-forming Minerals, Vol. 4—Framework Silicates*. Longman, London, 321–337.
- Mayerson W.M., Elen S. and Owens P., 2003. Gem News International: Cat's-eye scapolite from Tanzania. *Gems & Gemology*, **39**(2), 158–159.

Figure 28: This 31.44 ct scapolite from Tanzania contains many black inclusions that are visible to the unaided eye. Photo by Alex Mercado and Kelly Kramer.



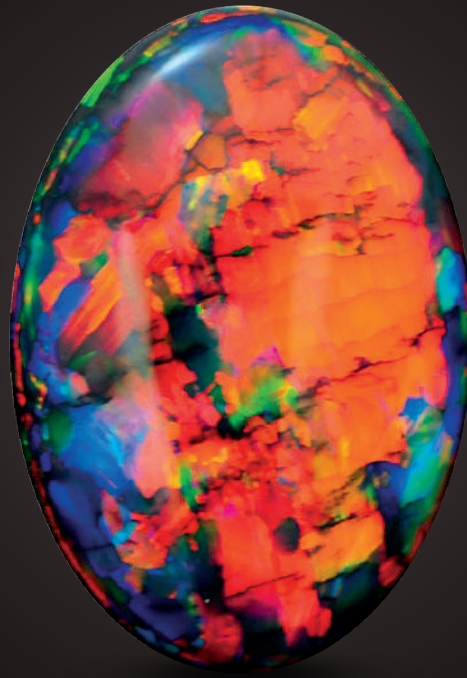
Figure 29: The inclusions in the scapolite consist of discoid and irregular-shaped black platelets that were identified as magnetite. Photomicrograph by Christopher P. Smith; magnified 32x.



The Fire Within

“For in them you shall see the living fire of the ruby, the glorious purple of the amethyst, the sea-green of the emerald, all glittering together in an incredible mixture of light.”

- Roman Elder Pliny, 1st Century AD



BLACK OPAL 15.7 CARATS

Suppliers of Australia's finest opals to the world's gem trade.

CODY  OPAL

LEVEL 1 - 119 SWANSTON STREET MELBOURNE AUSTRALIA

T. +61 3 9654 5533 E. INFO@CODYOPAL.COM

WWW.CODYOPAL.COM


INTERNATIONAL
COLORED GEMSTONE
ASSOCIATION
MEMBER

PEARLS

A Gastropod Shell as the Core of a Natural Pearl

As a pearl-testing laboratory, the LFG (French Gemmological Laboratory, in Paris) examines numerous natural pearls every day. Therefore we are accustomed to seeing the typical structures of natural pearls, such as calcitic cores surrounded by aragonitic growth rings. But once in a lifetime, we have the opportunity to discover a pearl such as the one we describe here.

A half-drilled brown nacreous pearl weighing 9.84 grains (2.46 ct) and measuring 6.86–6.96 × 7.31 mm (Figure 30) was recently submitted for examination. The usual procedure to identify the natural or cultured origin of a pearl relies on X-

ray radiography to visualize its inner structure. For example, the presence of a bead or graft residue in the centre reveals a cultured origin. X-radiography (Figure 31) of the present sample was performed with an RX Solutions DeskTom 130 micro-tomography system, and further examination with UV-Vis and Raman spectrometry and chemical analysis indicated that it was of saltwater origin and that the colour was natural. round structures. Because a radiograph is a two-dimensional projection of a three-dimensional structure, analysing such a pattern can be quite difficult. In this case, we were able to perform X-ray tomography with the same device, allowing us to visualize digitally reconstructed slices of the pearl to reveal its internal structure in more detail (Figure 32). This clearly showed a gastropod seashell as the origin of the pearl's growth. Seashell cores in pearls are described extremely rarely, and to our knowledge, only one such X-radiograph has been published (Bari and Lam, 2009). The concentric fissures seen around the

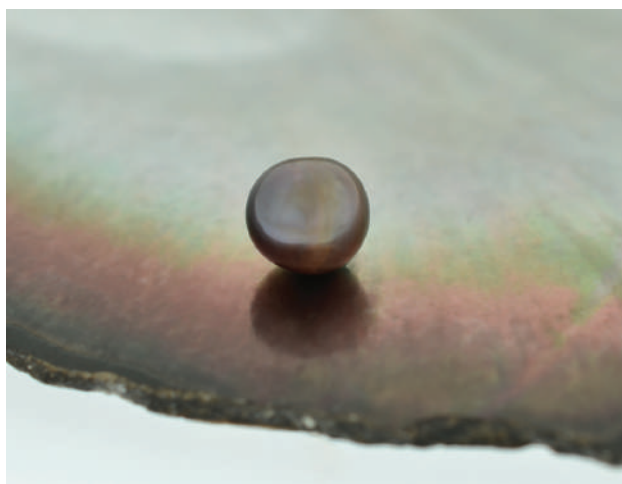


Figure 30: This natural brown pearl (9.84 grains; 6.86–6.96 × 7.31 mm) proved to contain a very unusual shell core. Photo by O. Segura.

radiography to visualize its inner structure. For example, the presence of a bead or graft residue in the centre reveals a cultured origin. X-radiography (Figure 31) of the present sample was performed with an RX Solutions DeskTom 130 micro-tomography system, and further examination with UV-Vis and Raman spectrometry and chemical analysis indicated that it was of saltwater origin and that the colour was natural.

When reviewing the X-radiograph, we noticed what appeared to be an unusual void in the centre of the pearl that showed some strange



Figure 31: X-radiography of the pearl shows an unusual structure (approximately 1.3 mm long) in the centre, close to the end of the drill hole. Image by O. Segura.

seashell are typical of natural pearls, and have been described as growth patterns.

With the help of reconstruction software (thanks to Solène Valton and the RX Solutions team), it was possible to digitally 'extract' the seashell from the pearl (Figure 33). The shell measured only 1.28 × 0.78 mm wide, and a slab could be seen in its opening that may be a remnant of the mollusc's operculum. The three-dimensional

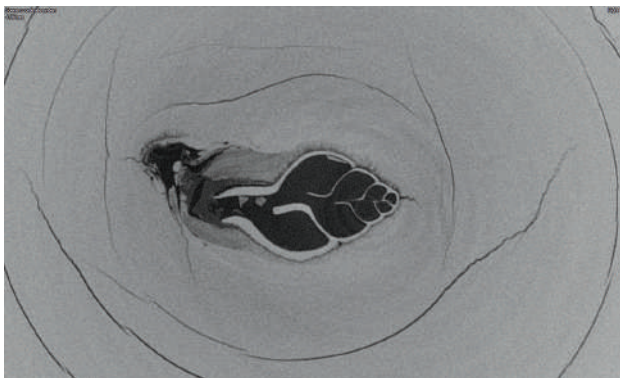


Figure 32: This X-ray tomography reconstruction clearly reveals the tiny shell (approximately 1.3 mm long) responsible for the pearl's growth. Image by O. Segura.

image and corresponding slices showed a small depression in the shell's largest whorl due to the drilling process. Although the drill hole did not actually reach the inner seashell core, this slight damage evidently occurred when the surrounding layers of the pearl were compressed by the drill bit. Fortunately the pearl was only half drilled, preserving this unique evidence of its formation.

All the structures of the seashell were visible, enabling us to distinguish the first four smooth spirals determining the protoconch. The anatomy of this shell—including the shoulders on the body whorl, the central axis (columella) and the siphonal canal structures—are interesting details that permit us to identify this marine mollusc (Gastropoda class, Neogastropoda, Buccinoidea, Fasciolaridae).

The improvement of analytical methods such as X-radiography and X-ray tomography,

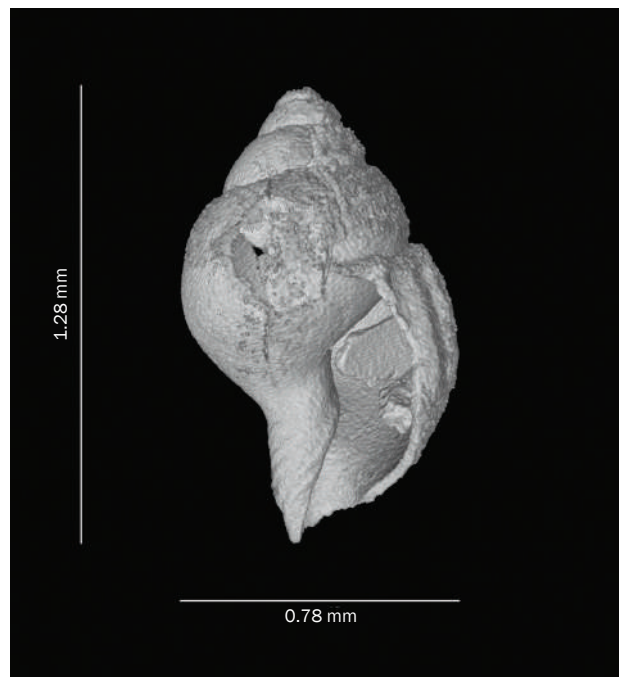


Figure 33: Image processing was used to create this three-dimensional reconstruction of the shell in the pearl's core. Image by O. Segura.

and the high quality and precision of the resulting images, provide the specialist with a great quantity of structural information. As shown here, this new imagery may allow the user to establish a thorough—and at times remarkable—conclusion.

Olivier Segura (o.segura@bjop.fr) and Sophie Leblan
Laboratoire Français de Gemmologie
Paris, France

Reference

Bari H. and Lam D., 2009. *Pearls*. Skira, Milan, 336 pp.

SYNTHETICS AND SIMULANTS

A New Peridot Imitation—Yttrium Aluminosilicate Glass

Peridot has become increasingly popular in the Chinese market. Within China, there are two famous peridot deposits: Jiaohe in Jilin Province and Zhangjiakou in Hebei Province. Various materials have been used to imitate peridot, such as barium-zirconium glass or lead-oxide silica glass (McClure and Reinitz, 1999; Hain-schwang, 2009).

Recently, the National Gemstone Testing Center Laboratory in Beijing received a green oval modified brilliant for identification (Figure 34). The client purchased the sample as Chinese peridot; it weighed 6.08 ct and measured 13 × 11 × 6 mm. Visually it resembled peridot, except for a lack of doubling of the facet junctions, and it was free of inclusions under 40× magnification.



Figure 34: This faceted 6.08 ct sample was identified as a new imitation of peridot: yttrium aluminosilicate glass. Photo by W. Han.

Its hydrostatic SG value was 3.37, and the refractometer showed a single RI of 1.661, which ruled out peridot. It exhibited a 'Maltese cross' pattern in the polariscope, and was inert to both long- and short-wave UV radiation.

Infrared reflectance spectroscopy revealed two bands at 962 and 476 cm^{-1} (Figure 35), which do not correspond to the spectrum of ordinary silica glass. Semi-quantitative EDXRF chemical analysis revealed mainly Y, Si, Pr and Al, along with minor Mg and traces of Fe, S, Mn, Cr, K, Ca, Cu and Zn. UV-Vis spectroscopy showed main absorption bands at 440 and 590 nm (Figure 36), which are caused by internal f-f transitions of Pr^{3+} (Zhang et al., 2009), resulting in the attractive green colour of the sample.

We identified this peridot imitation as a Pr^{3+} -coloured yttrium aluminosilicate glass. Glass has been used to imitate gemstones for centuries. However, this is the first instance we have encountered of yttrium aluminosilicate glass being used to imitate Chinese peridot. Customers should be aware of this imitation when buying peridot in the marketplace.

*Dr Wen Han (181177297@qq.com),
Dr Taijin Lu and Qian Deng
National Gems & Jewelry Technology
Administrative Center, Beijing, China*

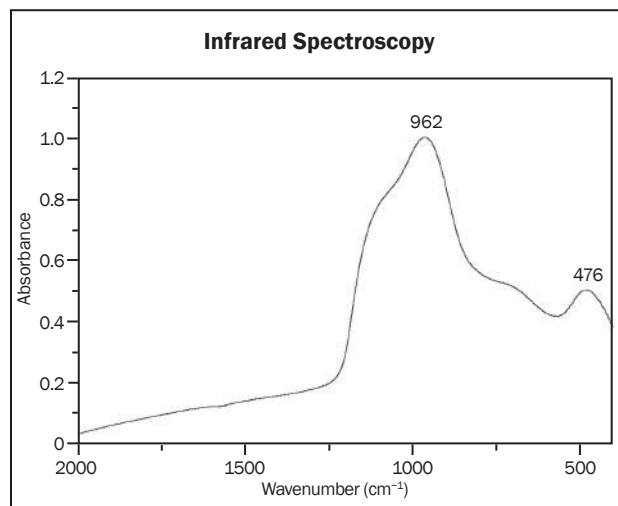


Figure 35: Infrared reflectance spectroscopy of the peridot imitation reveals bands at 962 and 476 cm^{-1} that are not typical of ordinary silica glass.

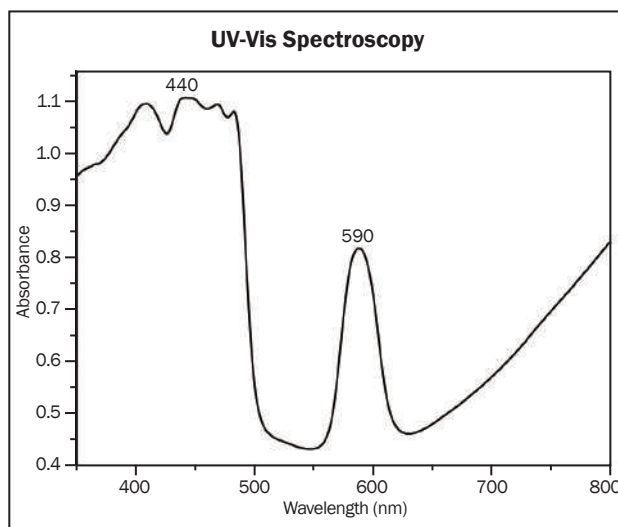


Figure 36: UV-Vis spectroscopy of the peridot imitation shows absorptions at 440 and 590 nm that are attributed to Pr^{3+} .

References

- Hainschwang T., 2009. Gem News International: High-RI barium-zirconium glass imitation of peridot and other gems. *Gems & Gemology*, **45**(4), 307–308.
- McClure S.F. and Reinitz I., 1999. Gem Trade Lab Notes: Glass imitation of peridot. *Gems & Gemology*, **35**(1), 44.
- Zhang X., Li M., Liu Z., Hu Y. and Wu J., 2009. Research progress on rare earth colored [sic] and UV absorption in glass. *Bulletin of the Chinese Ceramic Society*, **28**(6), 1208–1212.

A. Kleiman & Co.



Simply...
Pure...
Quality

Natural and Untreated

+1-415-982-3500

Tucson AGTA GemFair

Hong Kong March Gem Show at the Asia World Expo

BASELWORLD

Las Vegas AGTA GemFair

Hong Kong September Gem Fair at the Asia World Expo

TREATMENTS

HPHT-Treated Blue Sapphire: An Update

Since 2014, reports have circulated about blue sapphires being treated by a Korean company using a high-pressure, high-temperature (HPHT) technique (see Choi et al., 2014a,b; Song et al., 2015; e.g. Figure 37). According to the treater, the starting material consists of pale blue sapphire from Sri Lanka, and there is no addition of any chemical component except for a small quantity of water during the treatment process. The main advantage in applying HPHT treatment is that the technique may help avoid fracturing due to differential thermal expansion of solid or fluid inclusions, as well as help minimize thermal decomposition of some mineral inclusions. HPHT-treated blue sapphires have entered the gem market during the past few years, but to the authors' knowledge the treatment has not yet been applied to other colour varieties of corundum.

Initial research on samples before and after treatment showed that Fourier-transform infrared (FTIR) spectroscopy is useful for distinguishing the HPHT-processed samples from standard heat-treated sapphire; the presence of a strong absorption band centred at 3047 cm^{-1} with a shoulder at 2627 cm^{-1} was evident in the stones after HPHT treatment (Choi et al., 2014a,b). Surprisingly, however, a subsequent study by another

group of researchers who HPHT-treated their own samples did not find any strong absorption features in the $3050\text{--}3040\text{ cm}^{-1}$ region after treatment (Song et al., 2015).

The present study provides an update on HPHT-treated blue sapphires that have been seen at The Gem and Jewelry Institute of Thailand's (GIT) laboratory, and reports some of the gemmological properties of these sapphires for the first time. Since 2013, more than 40 blue sapphires suspected of being HPHT treated were submitted by various clients. The stones weighed 1.91–15.21 ct, and all showed the strong diagnostic absorption band in the $3050\text{--}3040\text{ cm}^{-1}$ region of the FTIR spectra. Basic properties were measured by standard gemmological instruments, and spectroscopic data were collected at GIT using an Eagle III micro-EDXRF unit, a PerkinElmer Lambda 950 UV-Vis-NIR spectrophotometer and a Thermo Nicolet 6700 FTIR spectrometer.

The sapphires were a moderate to intense blue, and had RIs of 1.759–1.770 (birefringence 0.008–0.010) and hydrostatic SG values of 3.97–4.00. Stones tested with the polariscope showed a doubly refractive, uniaxial, single-crystal reaction. Fluorescence ranged from inert to moderate red in long-wave UV radiation and inert to weak red in short-wave UV. These properties are consistent

Figure 37: This 1.19 ct sapphire is shown before (left) and after (right) HPHT treatment. Photomicrographs by Youngsoo Chung; magnified 10 \times .



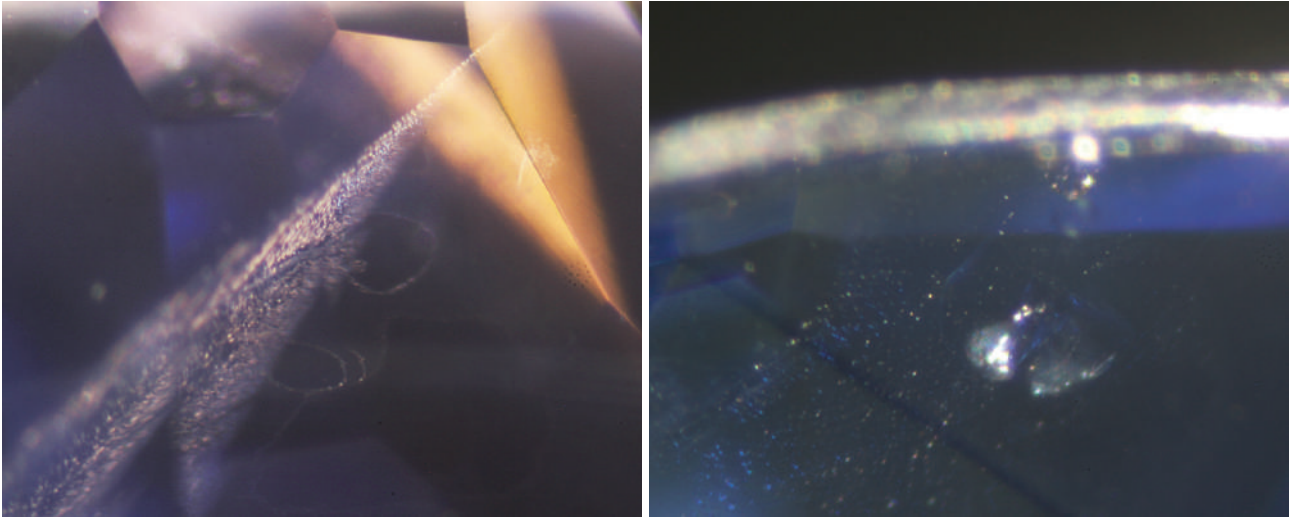


Figure 38: Inclusion scenes in HPHT-treated sapphires may consist of 'fingerprint' inclusions accompanied by slightly healed thin-film tension cracks (left), or clusters of thermally altered 'snowball' inclusions with fuzzy tension halos, as well as trails of pinpoint inclusions and clouds of minute particles (right). Photomicrographs by N. Atsawatanapirom (left) and J. Jakkawanvibul (right); magnified 40 \times .

with those of gem corundum. Observation with the gemmological microscope revealed various internal features, including 'fingerprints' that were often accompanied by peculiar thin-film tension cracks (Figure 38, left) and clusters of altered mineral inclusions ('snowballs') with fuzzy tension halos (Figure 38, right). Trails of pinpoint inclusions and clouds of minute particles also were seen. Most of the inclusion features are similar to those of conventionally heated sapphires, except for the healed tension fractures that looked hazy rather than forming the tiny droplets that are typically seen in normally heated stones.

As expected, EDXRF chemical analysis of the blue sapphires (Table II) showed relatively low-to-moderate Fe contents (0.05–0.23 wt.% Fe_2O_3) and traces of Ga (0.01–0.02 wt.% Ga_2O_3). Visible spectra (e.g. Figure 39) showed a typical dominant absorption band due to Fe^{2+} – Ti^{4+} intervalence charge transfer (IVCT) that is responsible for their

Table II: Trace-element contents of HPHT-treated sapphires by EDXRF spectroscopy.*

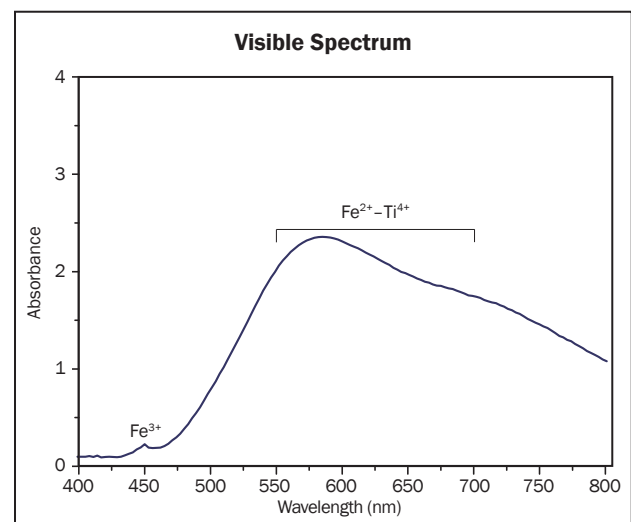
Oxide	Range (wt.%)
TiO_2	0.01–0.04
V_2O_5	0.003–0.02
Cr_2O_3	0.003–0.01
Fe_2O_3	0.05–0.23
Ga_2O_3	0.01–0.02

* Data from the analysis of 11 selected samples.

blue coloration. The mid-IR spectra recorded a strong absorption band centred at 3047 cm^{-1} with a shoulder at 2627 cm^{-1} ; by comparison, untreated blue sapphires occasionally show a weak OH-related band at 3310 cm^{-1} (Figure 40).

Based on these examinations of client stones that were suspected of being HPHT treated (i.e. showing the strong absorption band at 3047 cm^{-1}), we concluded that the general appearance, basic gemmological properties, microscopic features, trace-element composition and visible-range spectra were quite similar to those found in conven-

Figure 39: This non-polarized visible absorption spectrum of a blue sapphire suspected of HPHT treatment shows a typical Fe^{2+} – Ti^{4+} IVCT absorption band. Minor absorption due to Fe^{3+} also is present at 450 nm.



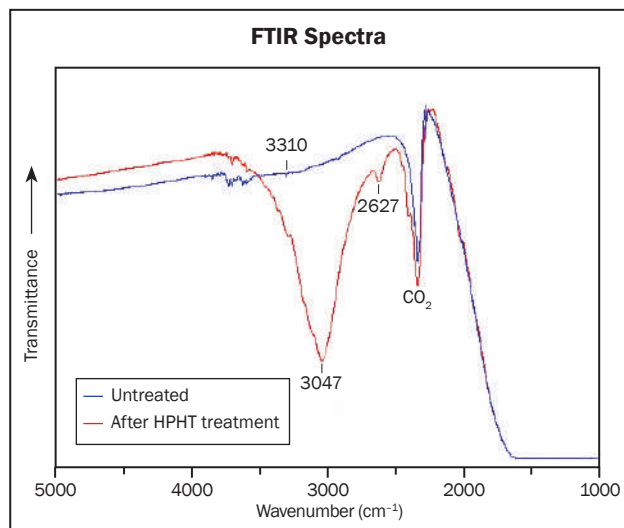


Figure 40: FTIR spectra are shown for blue sapphires that are untreated (blue) and HPHT-processed (red). The treated stone shows a strong absorption band centred at 3047 cm^{-1} with a shoulder at 2627 cm^{-1} .

tionally heated sapphires. In the FTIR spectra, it is likely that the occurrence of the strong absorption band at $3050\text{--}3040\text{ cm}^{-1}$ (Choi et al., 2014a,b) is related to another type of structural OH group that developed as a result of water that was reportedly added during the HPHT treatment.

Acknowledgements: The GIT authors express their sincere thanks to Boontawee Sriprasert for his advice, and also to GIT academic advisors Wilawan Atichat and Dr Visut Pisutha-Arnond for their valuable comments and editing.

Sun-Ki Kim (*skkimmy@hanmail.net*),
Dr Hyun-Min Choi and Dr Young-Chool Kim
Hanmi Gemological Institute Laboratory (GIG)
Seoul, Korea

Dr Pornsawat Wathanakul, Thanong Leelawatanasuk, Nicharee Atsawatapanirom, Papawarin Ounorn and Thanapong Lbuaamporn
GIT, Bangkok

References

- Choi H.M., Kim S.K. and Kim Y.C., 2014a. Appearance of new treatment method on sapphire using HPHT apparatus. *ICGL Newsletter*, No. 4, 1–2.
- Choi H.-M., Kim S.-K. and Kim Y.C., 2014b. New treated blue sapphire by HPHT apparatus, *Proceedings of the 4th International Gem and Jewelry Conference (GIT2014)*, Chiang Mai, Thailand, 8–9 December, 104–105.
- Song J., Noh Y. and Song O., 2015. Color enhancement of natural sapphires by high pressure high temperature process, *Journal of the Korean Ceramic Society*, **52**(2), 165–170.

MISCELLANEOUS

Myanmar Gems Emporium

The 53rd Myanma Jade, Gems & Pearl Emporium took place 24 June–6 July 2016 in Nay Pyi Taw, Myanmar. Under the new government of Aung San Suu Kyi, the Emporium was organized by the Ministry of Natural Resources & Environmental Conservation (a combination of the former Ministry of Mines and Ministry of Forestry and Environmental Conservation). An illustrated catalogue was provided to attendees that listed the programme of events and showed the layout of the Emporium building.

The jade tender consisted of 3,947 lots, with total sales of €527.08 million. In addition to rough material, there were 43 lots of bangles, 20 lots of beads, seven lots of carvings and three lots of cabochons. Highlights included three bangles (190 g total weight) in lot no. 727 with

a floor price of €136,000 and two cabochons (35 carats total weight) in lot no. 815 with a floor price of €100,000. The ‘gems’ tender contained 60 lots with sales of €3.15 million, and the cultured pearl tender consisted of 312 lots that realized €3.2 million.

Attendees came from China (813 companies with 1,866 buyers) and Hong Kong (82 companies with 150 merchants), as well as Australia, India, Japan and Singapore (combined 919 companies with 2,069 buyers). Relatively low sales at this Emporium are blamed on the low turnout of Chinese buyers, as well as the overall lack of high-quality gem material.

Dr U Tin Hlaing (*p.tinblaing@gmail.com*)
Dept. of Geology (retired)
Panglong University, Myanmar




Stone Group Laboratories

Where technology and experience meet.


- Gem Identification
- Treatment Analysis
 - Consultation
 - Research

www.StoneGroupLabs.com

Crown Color

Fine Rubies, Sapphires and Emeralds
Bangkok - Geneva - Hong Kong - New York



Head Office:
Crown Color Ltd.
14/F, Central Building, suite 1408, 1-3 Pedder Street
Central Hong Kong SAR
Tel:+852-2537-8986
New York Office: + 212-223-2363
Geneva Office: +41-22-8100540

Crown Color
is a proud supporter of the
Journal of Gemmology

Join us on social media to keep up-to-date with the latest news, events and offers from Gem-A

 GemAofGB
 @GemAofGB
 [linkd.in/1GisBTP](https://www.linkedin.com/company/gem-a)



Simultaneous High Sensitivity Trace-Element and Isotopic Analysis of Gemstones Using Laser Ablation Inductively Coupled Plasma Time-of-Flight Mass Spectrometry

Hao A. O. Wang, Michael S. Krzemnicki, Jean-Pierre Chalain, Pierre Lefèvre, Wei Zhou and Laurent E. Cartier

GemTOF, installed at the Swiss Gemmological Institute SSEF, is a next-generation chemical analysis technique for gemmology: laser ablation inductively coupled plasma time-of-flight mass spectrometry (LA-ICP-TOF-MS). The system enables full elemental mass-spectrum acquisition at an ultra-high acquisition speed. Nearly all elements in the periodic table can be simultaneously acquired with low limits of detection. Major-to-trace (and even ultra-trace) element compositions can be accurately quantified, and slight concentration differences can be distinguished. The data can be processed with multivariate statistical analysis, thereby increasing the reliability of origin determination as well as the detection of potentially new diffusion treatments. Additionally, higher precision for isotopic analysis is expected than with sequential-acquisition LA-ICP-quadrupole-MS (LA-ICP-Q-MS), especially for short transient signals. Novel research directions in gemstone age dating, analysis of inclusions and chemical zoning will benefit from the advantages of this system.

The Journal of Gemmology, 35(3), 2016, pp. 212–223, <http://dx.doi.org/10.15506/JoG.2016.35.3.212>
© 2016 The Gemmological Association of Great Britain

Introduction

In the past several decades, gem testing has evolved from a rather basic characterization of physical properties (e.g. RI, SG, absorption and fluorescence) into advanced materials science, using sophisticated instrumental technologies for detailed chemical and structural analyses. As gemmology is primarily an applied science, this

analytical evolution was driven by challenging issues confronting the gem trade rather than by fundamental research. From the use of X-ray radiography and X-ray diffraction to detect beaded cultured pearls in the early 20th century (Anderson, 1932), additional technological innovations in gemmology include the chemical characterization of synthetic coloured stones by



Figure 1: Six blue sapphires (various client stones weighing approximately 2–36 ct) are shown on an historical map of the famous gem locality of Mogok, Myanmar. Quantitative chemical data can be helpful for determining the geographic origin of sapphires. Map from Gordon (1888); photo by L. E. Cartier and Julien Xaysongkham, SSEF.

energy-dispersive X-ray fluorescence (EDXRF; Stern and Hänni, 1982; Muhlmeister et al., 1998) and the detection of fissure-filling treatments using Fourier-transform infrared (FTIR) spectroscopy and micro-Raman spectroscopy (Kiefert et al., 1999). Subsequently, the undisclosed appearance of Be-diffusion-treated sapphires, high-pressure, high-temperature (HPHT)-treated diamonds and beadless cultured pearls at the turn of the millennium had major impacts on the evolution of analytical methods in gem laboratories. New and highly sensitive methods have proven very helpful for gemstone and pearl testing, many of them applied for the first time or in a very early stage in the field of gemmology and in actual testing cases. These techniques include photoluminescence spectroscopy at liquid-nitrogen temperature (-196°C) of HPHT-treated diamonds (Chalain et al., 1999; Fisher and Spits, 2000), atomic force microscopy of pearl surfaces (Gutmannsbauer and Hänni, 1994), laser-induced breakdown spectroscopy (LIBS) of Be-diffused corundum (Krzemnicki et al., 2004), X-ray computed microtomography of pearls (Wehrmeister et al., 2008; Krzemnicki et al., 2010), age dating of pearls using accelerator mass spectrometry (Hainschwang et al., 2010; Krzemnicki and Hajdas, 2013), DNA-fingerprinting of pearl species (Meyer et al., 2013), X-ray phase contrast and X-ray scattering imaging of pearls (Krzemnicki et al., 2015; Revol et al., 2016) and neutron imaging of gemstones and pearls (Hanser, 2015; Mannes et al., 2016).

Throughout this period, the chemical analysis of gem materials has been very important not only for material identification (e.g. to identify species within the garnet-group solid solution), but also for identifying synthetics and treatments (e.g. Ti-diffusion of corundum). The main driving force for detailed trace-element analysis of gem materials, however, has been the demand from the trade for laboratories to deliver a scientifically based opinion of geographic origin, particularly for higher-end stones (see, e.g., Figure 1 and the cover of this issue). The demand has resulted from value factors attributed to certain origins (e.g. sapphires from Kashmir), but also from the growing need for traceability of gems due to political (trade bans) or ethical (fair trade) reasons (Dickinson DeLeon, 2008; Cartier, 2010).

Semi-quantitative to quantitative chemical analysis of trace elements in gem materials is typically performed using EDXRF spectroscopy. For the past 15 years, LA-ICP-MS has proven to be a very sensitive and versatile method for trace-element analysis of gem materials (Guillong and Günther, 2001), despite being only quasi-non-destructive. This technique provides access not only to a distinctly wider range of elements than traditional XRF methods, but also to much lower detection limits (especially for light elements such as Li, Be, B and Na) and to different isotopes of the same element. During the past several years, various publications have focused on the chemical characterization of gems from different origins (Giuliani et al., 2000; Rankin et al., 2003; Abduriyim



Figure 2: This LA-ICP-TOF-MS system, named GemTOF, was installed at SSEF in July 2016. The ICP-TOF-MS instrumentation is on the left and the LA unit is on the right. Photo by Vito Lanzafame, SSEF.

and Kitawaki, 2006; Sutherland et al., 2009; Halicki, 2013).

Recently, a novel analytical technique, LA-ICP-TOF-MS, was introduced into the market. In late 2015, the SSEF laboratory in Basel, Switzerland, initiated an evaluation project with three leading companies focusing on implementing such a system for gemstone analysis. The final instrumentation was installed at SSEF in July 2016 (Figure 2) and will be fully operational in winter 2016. This article discusses the capabilities of LA-ICP-TOF-MS compared to conventional ICP-Q-MS. Various potential applications of this new instrumentation are described, and a preliminary case study of sapphire origin determination is briefly presented.

Introduction to LA-ICP-TOF-MS

In general, LA-ICP-MS is a well-known and versatile analytical method for major- to trace-elemental analysis of solids. It consists of a material sampling part (LA) and a chemical analysis part (ICP-MS). The gemstone is placed within a sealed sample chamber in the LA instrument, with no need for sample preparation. Then a high-power pulsed UV laser is focused on the surface of the gem (normally on the girdle). The high laser energy accumulates on a tiny spot, and the ablated particles are instantaneously ejected into the sealed chamber. The resulting crater is too small (commonly less than 100 µm in diameter) to be visible to the naked eye and too shallow (e.g. 18 µm for a 30 s ablation on sapphire; Guillong and Günther, 2001) to produce any significant weight loss. The released particles are transported in a

flow of He gas into the plasma source. Inductively coupled plasma (ICP), created from Ar gas, is a robust ionization source. The temperature of this plasma is comparable with the surface temperature of the sun, causing almost all fine particles to become dissociated, atomized and finally ionized. The stream of ions is then extracted into the mass spectrometer (MS), which separates them based on their mass-to-charge ratio (m/Q). Most ions measured by ICP-MS have a charge of +1, and therefore m/Q is of equal value to mass m . A detector separately registers the intensities of ions with different m/Q values. External calibration is performed using standard reference materials, through which quantitative results for various elements can be calculated. The capability to precisely quantify multiple elements in a wide range of concentrations is the key benefit of LA-ICP-MS.

Commonly, LA instruments are equipped with either a 213 nm solid-state Nd:YAG laser or a 193 nm ArF excimer laser. An excimer laser is preferred for universal applications because finer particles are produced during ablation (Guillong et al., 2003).

There are several types of ICP-MS instruments based on different mass-separation schemes. The quadrupole type is one of the most popular, and is typically used for gemstone research. In such instrumentation, only one selected m/Q is collected by the detector at a time, while others are deflected and lost. To measure several isotopes, the mass spectrometer has to jump from one selected m/Q (isotope) to another.

ICP-TOF-MS is one of the latest and most advanced technologies in the ICP-MS family. The key difference between TOF and quadrupole setups is the mass-separation scheme. TOF uses the principle that the ‘flight’ duration for one ion passing through a fixed flight tube is related to its m/Q . Lighter ions take less time to travel the same distance compared to their heavier counterparts with the same charge, provided they have identical kinetic energy; hence mass separation is achieved. The flight time difference between the lightest and the heaviest ions travelling to the detector is so minimal that one may even consider them to arrive at almost the same time (i.e. simultaneously) at the detector. Benefiting from recent developments in ultra-fast electronics and optimized ion optics, ICP-TOF-MS acquires spectra from the lightest to the heaviest isotopes at a

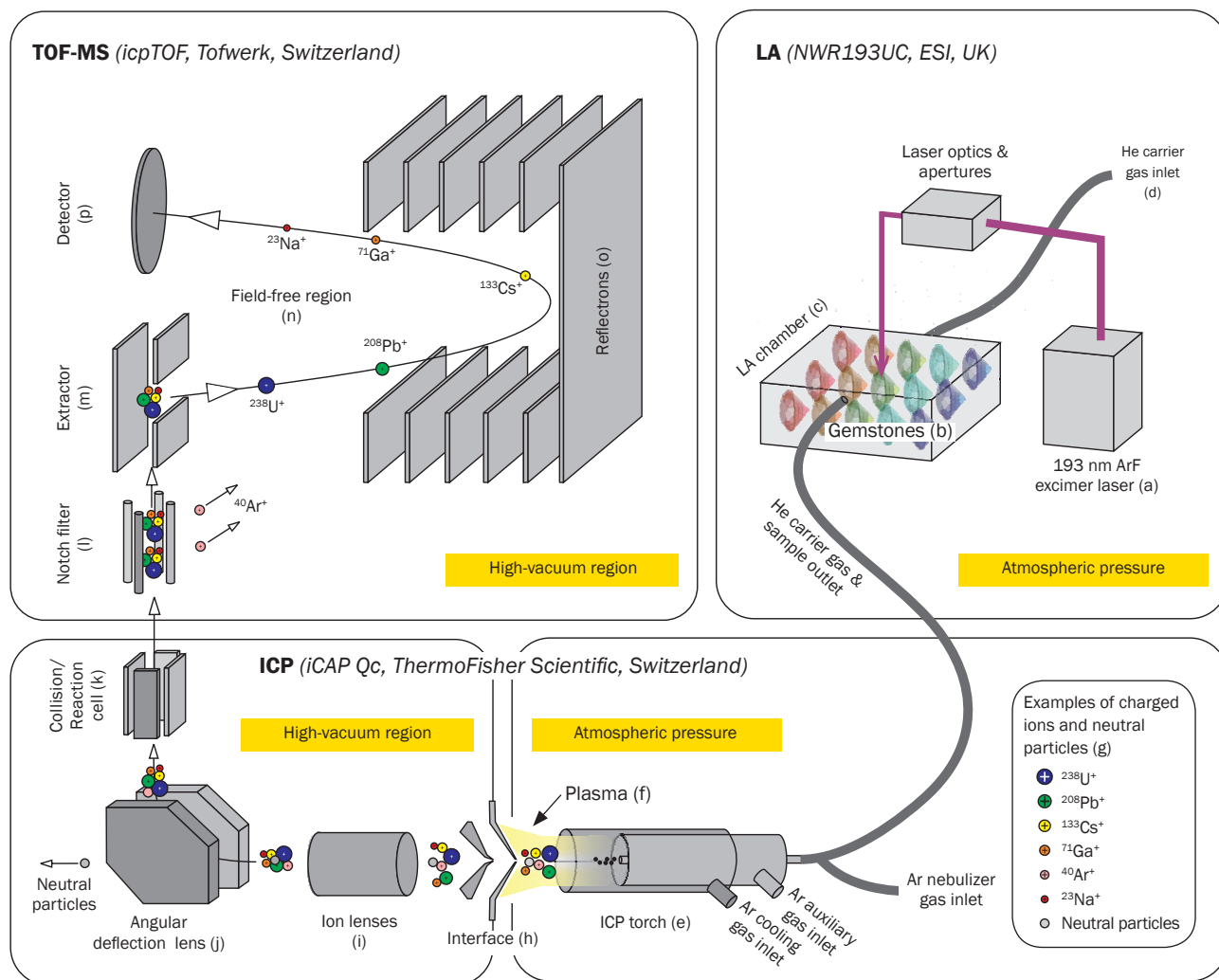


Figure 3: This schematic diagram shows a typical LA-ICP-TOF-MS setup (e.g. GemTOF at SSEF). The beam from a 193 nm ArF excimer laser (a) is focused on the gemstone or pearl (b) that is sealed in a sample chamber (c). The LA chamber is flushed by He gas (d), which transports the ablated particles to the ICP torch (e). The plasma (f) dissociates, atomizes and ionizes the particles into preferably singly-charged ions (g), which are sampled at an interface (h) from atmospheric pressure to a high-vacuum region. The stream of ions is extracted through a series of ion lenses (i), and neutral particles are separated from ions by an angular deflection lens (j). A collision/reaction cell (k) can be used to reduce interferences. At the entrance to the TOF-MS, a notch filter (l) first rejects selected dominant ions (e.g. Ar⁺) from the ion stream, and then the extractor (m) pushes the ions orthogonally at a high frequency into the field-free time-of-flight region (n). The ions are mirrored by reflectrons (o) and finally registered at a detector (p).

higher speed as well as achieving a better resolving power (or higher mass resolution) than conventional Q-MS (see www.tofwerk.com/icp). A schematic diagram showing the components and procedures of the LA-ICP-TOF-MS instrumentation at SSEF is shown in Figure 3.

Key Features of LA-ICP-TOF-MS

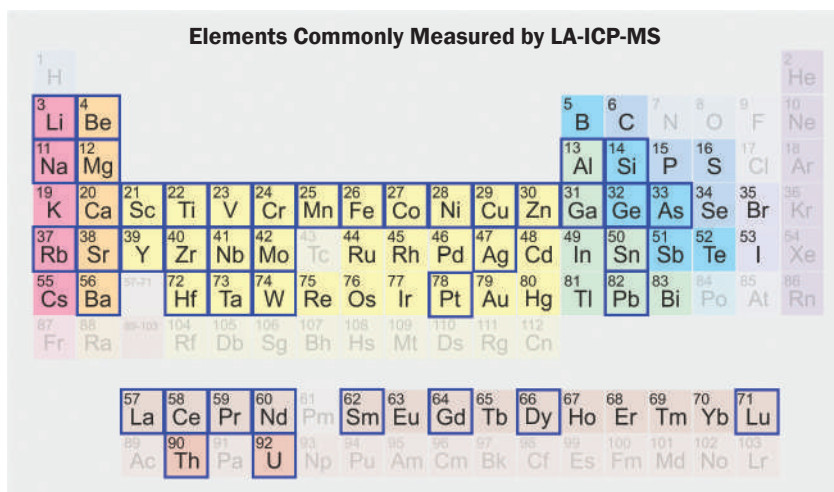
Full Mass-Spectrum Acquisition

Argon ICP has a high ionization potential, so almost all elements can be ionized efficiently. But to detect all these elements, an adequate mass

spectrometer should be employed. Conventional Q-MS has limitations. Because of sequential acquisition, it measures the intensity of one m/Q during a certain dwell time (integration time) before jumping to the next one. Although Q-MS is able to scan the full mass range by hopping through the entire spectrum, it is time consuming. Therefore, in practice, elements from Li to U (Figure 4) are commonly measured using only a selected number of isotopes within a limited measurement time. After measurement, if the selection of isotopes needs to be readjusted, the sample has to be re-ablated.

Figure 4: ICP-MS can measure most of the elements in the periodic table (shown in solid colours, with the atomic number indicated in the top-left corner for each element). The greyed-out elements are difficult to ionize, have strong interferences and high backgrounds, or are not commonly seen in geological samples.

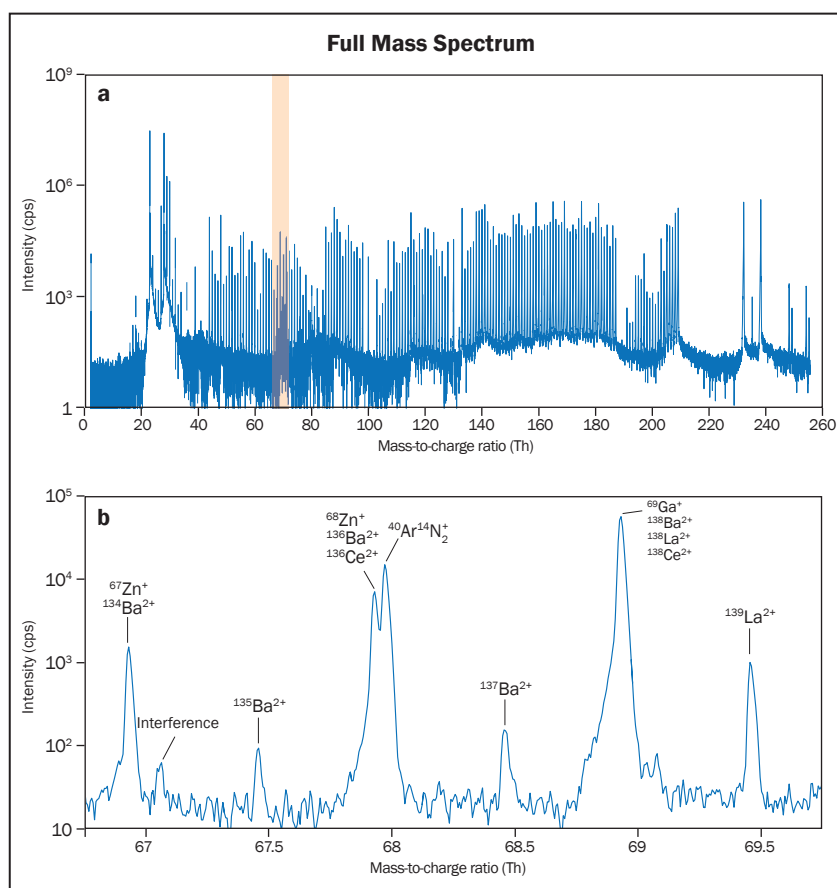
For LA-ICP-Q-MS measurements, only some of the elements (e.g. those with blue outlines) are selected using one of the isotopes from each element. By contrast, LA-ICP-TOF-MS measurements not only analyse all of the (solid coloured) elements simultaneously, but also almost all isotopes of those elements.



By comparison, LA-ICP-TOF-MS ‘snaps pictures’ of the full and continuous mass spectrum without the need to assign isotopes of interest (e.g. an ‘averaged picture’ from a 20 s ablation signal is shown in Figure 5a). Details of the ‘picture’ can be revisited at any time, and the isotopes of interest also can be changed, even after the measurement has been completed. Such a spectrum reveals almost the full elemental composition, reaping the benefits of the robust

plasma source. As a further consequence of this ‘picture snapping’, it is possible to considerably reduce the amount of ablated material required from the sample, thus creating a smaller and shallower crater on the analysed gemstone. In contrast to commonly used quadrupole mass spectrometers, there is no risk of needing to re-ablate the stone due to an incomplete or ‘badly’ chosen predefined list of isotopes, because the full mass spectrum is registered.

Figure 5: (a) An averaged full elemental mass spectrum is shown from a 20 second LA-ICP-TOF-MS measurement of NIST610, a silicate standard reference material. Mass-to-charge ratios (in units of Thomson) through the entire elemental range were acquired simultaneously. (b) Details of the orange region in (a) illustrate the mass resolving power of TOF-MS ($m/\Delta m \approx 3,000$), which is better than quadrupole MS (normally $m/\Delta m \approx 300$) in resolving some interferences.



Due to technical limitations, the ICP-TOF-MS model described in this article cannot measure light isotopes (e.g. ${}^7\text{Li}$, ${}^9\text{Be}$, ${}^{10}\text{B}$, ${}^{11}\text{B}$, etc.) while maintaining a high sensitivity for heavy isotopes (e.g. ${}^{232}\text{Th}$ and ${}^{238}\text{U}$, etc.). In these situations where access to a low m/Q range is required, another set of ion optic voltage settings can be applied. Since the parameters can be pre-set and changed quickly, it is hence feasible to complete the full elemental analysis from Li to U with two measurements (each focused on either low or high m/Q). Taking advantage of simultaneous acquisition, this limitation may not necessarily increase measurement time or have more impact on a sample compared to sequential LA-ICP-Q-MS.

High Mass-Resolving Power

As depicted in Figure 5b, the full mass spectrum ‘picture’ is taken at a high mass-resolving power (i.e. $m/\Delta m \approx 3,000$, where m is the nominal mass of the peak and Δm defines the mass difference between two resolved peaks), and this may help with potential interference problems. For example, when analysing ${}^{68}\text{Zn}^+$, the polyatomic ion ${}^{40}\text{Ar}{}^{14}\text{N}_2^+$ at nominal $m/Q = 68$ as well as doubly charged ions ${}^{135}\text{Ba}^{2+}$ and ${}^{137}\text{Ba}^{2+}$ present at $m/Q = 67.5$ and 68.5 cause interference when using Q-MS (resolving power $m/\Delta m \approx 300$). The higher resolving power of TOF-MS separates ${}^{40}\text{Ar}{}^{14}\text{N}_2^+$ from ${}^{68}\text{Zn}^+$. The doubly-charged species are, however, close in mass to ${}^{68}\text{Zn}^+$, and their separation requires higher resolving power or the application of various mathematical correction models.

High-Speed Mass Spectrum Acquisition

ICP-TOF-MS is capable of ‘snapping’ a full elemental mass spectrum at a maximum speed of 33,000 ‘pictures’ per second, but the data transfer speed from instrument to computer is limited. Therefore, the ‘pictures’ are commonly averaged and downloaded to a computer at a maximum speed of $\sim 1,000$ ‘averaged pictures’ per second. By contrast, Q-MS commonly measures only 2–5 sweeps per second (i.e. complete analysis over the list of predetermined isotopes, analogous to ‘averaged pictures’). The fast ‘frame rate picture snapping’ from TOF-MS can capture more details of a continuous change of sample concentration (e.g. local chemical zoning in gems), and any instantaneous short-signal events (e.g. tiny inclusion, nanoparticle, etc.) also can be resolved.

It is worth mentioning that not all ions from the continuous mass spectrum are eventually detected due to the discrete sampling nature of TOF. The detection efficiency of ICP-TOF-MS is less than 100%, but generally higher than Q-MS (Borovinskaya et al., 2013).

Limit of Detection (LOD)

The LOD is a figure of merit when describing the detection capability of an analytical instrument. During routine LA-ICP-MS analyses, LOD is often given in the unit of parts per million (ppm) or parts per billion (ppb), indicating the lowest concentration of analyte that is sufficient to provide a significant signal above background. There are two major factors for determining LOD: the sensitivity of the instrument and its background signal level. In general, higher sensitivity and lower background noise are necessary for a better LOD. As a result of recent instrumental developments, LA-ICP-TOF-MS has an improved multi-element sensitivity. While benefiting also from lower background noise, it provides better LOD than Q-MS (Borovinskaya et al., 2013).

As summarized in Figure 6, the LOD values of LA-ICP-TOF-MS, calculated using a widely accepted method (Pettke et al., 2012), range from single-digit ppb for heavy elements to low ppm for light elements. Although this is satisfactory for most gemmological studies, a larger laser spot size or a higher laser repetition rate can further boost the sensitivity, thereby further improving LOD values. Specifically for GemTOF at SSEF, it is possible to enlarge the spot size up to $150\ \mu\text{m}$ in diameter and increase the laser repetition rate up to 200 Hz (theoretically giving one to two orders of magnitude better LOD). This will, however, produce a larger and deeper crater on the girdle of the gem. In case both minimized ablation impact and improved LODs are required, then collision/reaction cell technology can be used (e.g. QCell by ThermoFisher Scientific; see ‘k’ in Figure 3). A QCell is an inert or reactive gas-flushed container that is installed on the ICP-TOF-MS. When ions fly through this device, they collide and/or react with gas molecules. In collision mode, polyatomic ions (which may cause interferences) run into inert gas molecules and lose energy more efficiently than the elemental ions of interest; then they can be removed from the beam by using energy filtering. Moreover, less-energetic ions also improve the

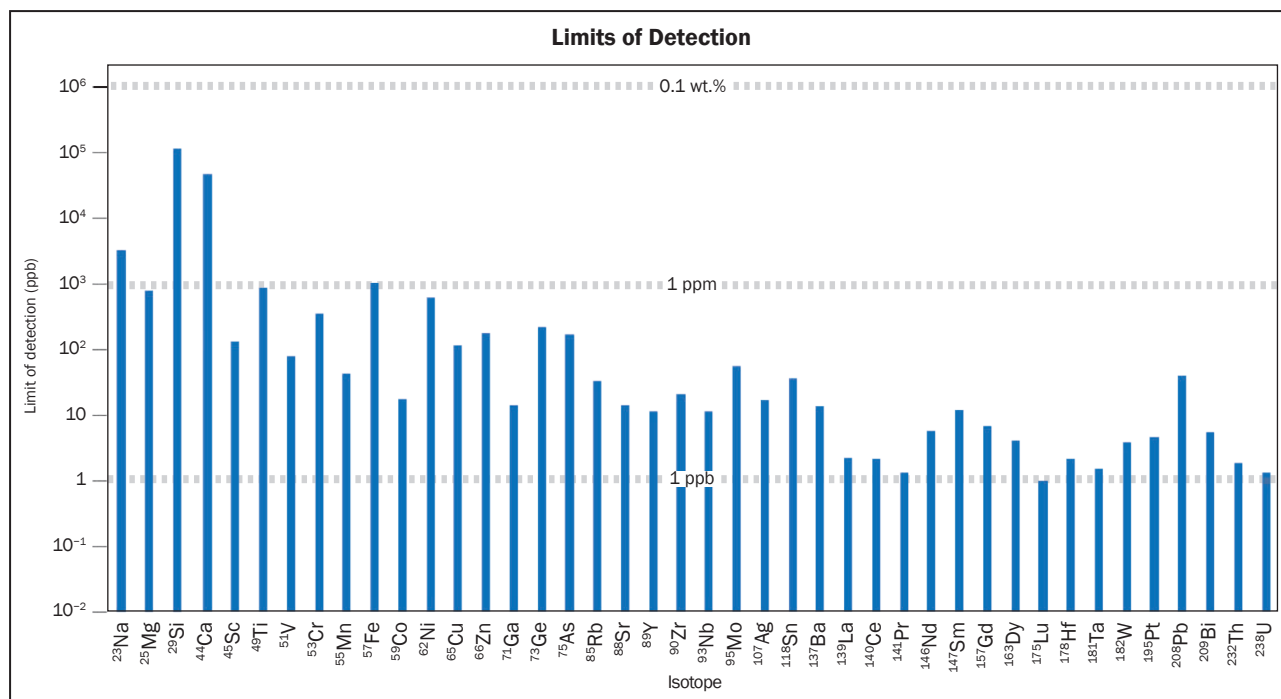


Figure 6: Limits of detection are shown for the LA-ICP-TOF-MS measurement of NIST610 reference material (most elements are ~450 ppm in concentration) in Figure 5 using a 40 μm diameter laser spot size and a 20 Hz laser repetition rate. Only a selected list of isotopes are displayed in the figure.

mass-resolving power of ICP-TOF-MS. Alternatively, interferences may selectively react with gas molecules (e.g. H₂) and disassociate to neutral particles or ions of a different m/Q.

Isotopic Analysis

Isotopes of an element differ in their masses but are naturally present at constant ratios of abundance. Considering fast-varying transient signals, especially from tiny inclusions or from a small area on a gemstone in chemical imaging analysis, it is highly likely that isotope ratios analysed at different sequential time intervals with Q-MS will have high uncertainty. The measurement of isotopic ratios using simultaneous acquisition of TOF-MS is thus expected to be better than that using Q-MS.

Isobaric interferences (isotopes appearing at the same nominal mass) create difficulties for determining the actual contribution of an isotope of interest. Intrinsicly with TOF-MS, all other isotopes of the same elements of interest and interference are collected at the same time. Based on their constant natural abundance, mathematical corrections can be applied in order to improve accuracy of the trace-element quantification.

However, slight differences in isotopic ratios may result from the unique natural formation/production history of gemstones and pearls. This uniqueness could help to answer the question of carbon source for diamonds (e.g. Cartigny, 2005), to determine a gem’s origin (e.g. Coenraads et al., 1990) or to separate synthetic from natural gemstones. Again, high-precision isotopic ratio determination is mandatory for such applications.

Methodology

The GemTOF system used at SSEF includes a high-performance 193 nm laser ablation unit (model NWR193UC from ESI, Huntingdon, UK) and an ICP-TOF-MS (model icpTOF from ToFwerk AG, Thun, Switzerland) upgraded from an optimized ICP-Q-MS unit (model iCAP Qc from ThermoFisher Scientific, Reinach/Basel, Switzerland). Due to installation limitations at the instrument demonstration site, it was not possible to test a combined setup of a NWR193UC laser ablation unit and ICP-TOF-MS. The results summarized in this article used a NWR213 LA system (from ESI) operating at 213 nm wavelength and an ICP-TOF-MS (same model as GemTOF). SSEF conducted a separate

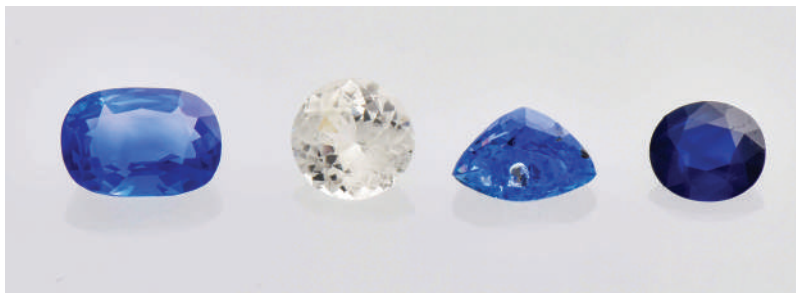


Figure 7: These four sapphires (1.40–3.06 ct) were analysed by LA-ICP-TOF-MS. From left to right, their documented origins are Kashmir (LABc_126), Sri Lanka (LABc_899 and LABc_906) and Myanmar (LABc_926). All samples are from the H. A. Hänni collection at SSEF. Photo by Vito Lanzafame, SSEF.

evaluation of the NWR193UC system and found it to be more suitable for gemstone analysis than the NWR213 unit. Given the focus of the current research on the mass spectrometer, the comparison of different laser wavelengths is not included in this article, and related information can be found elsewhere (Guillong et al., 2003). Notably, these two laser-ablation instruments do not change the qualitative picture of the key points highlighted.

For the experiments described in this article, the 213 nm laser was focused into a 40- μm -diameter spot, ablating in single-hole-drilling mode at a repetition rate of 20 Hz. The laser fluence was set to 15 J/cm². Helium was used as the carrier gas, with a flow rate of 1.0 L/min. Before each measurement, five pre-ablation shots were done to clean any surface contamination from the sample. In all measurements, the first 30 s were recorded as background without ablation, and then the sample was ablated for 20 s.

The ICP-TOF-MS unit was operated at a power of 1,400 W. Argon was used as the nebulizer gas at a flow rate of 0.8 L/min. Without losing key information, the TOF detector collected 10,000 spectra and then reported one averaged spectrum (3.3 spectra per second, maximum 1,000 spectra per second). Though demonstrated in ‘slow’ acquisition mode, the importance of being able to acquire full spectra at the highest speed will be discussed below in the ‘Analysis of Inclusions’ and ‘Imaging of Chemical Zoning for Gem Research’ sections.

NIST610 standard reference material was used for external calibration and Al was used as an internal standard for sapphire quantification. Element concentrations and LOD values were calculated using the methods of Longerich et al. (1996) and Pettke et al. (2012), respectively.

The settings described above are comparable with routine LA-ICP-Q-MS measurements.

Applications of LA-ICP-TOF-MS

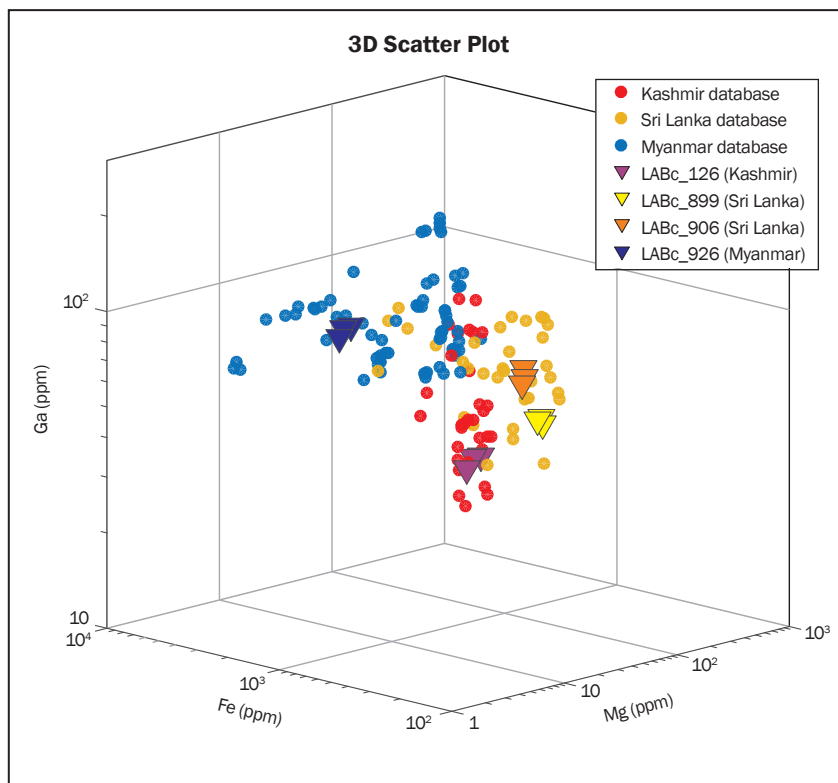
Gemstone Origin Determination: A Preliminary Case Study

The main application of LA-ICP-MS in gemmology is the chemical characterization of gems from various origins according to their major, trace and even ultra-trace elemental composition. The acquired chemical information can be displayed in a binary diagram, ternary plot or 3D plot in order to categorize the data into groups (i.e. geographic origins).

In a preliminary case study using LA-ICP-TOF-MS, we recorded full-mass spectra of four sapphires of documented provenance (Kashmir LABc_126, Sri Lanka LABc_899 and 906, and Myanmar LABc_926; Figure 7) from the H. A. Hänni collection at SSEF. The quantitative results for the trace elements Mg, Fe and Ga were plotted in a three-dimensional scatter plot (Figure 8) together with data from a previous study (Halicki, 2013) that used LA-ICP-Q-MS to analyse sapphires from Kashmir, Sri Lanka and Myanmar in the SSEF reference collection with various colour saturations. The scatter plot reveals that the reference sapphires (circles in Figure 8) plot in separate areas according to their three origins. The four sapphires analysed by TOF-MS (triangles in Figure 8) fit well into the expected plotting areas for the Kashmir, Sri Lanka and Myanmar origins. A drawback of this three-dimensional scatter plot is that only a limited number of trace elements (three in this 3D plot) can be displayed.

By using additional multivariate statistical approaches—such as principle component analysis and linear discrimination analysis—we can in principle take further advantage of the multi-element (multidimensional) information from LA-ICP-TOF-MS and reduce the amount of data to fewer dimensions while maintaining data-set variations in the plot.

Figure 8: This three-dimensional scatter plot shows quantitative LA-ICP-TOF-MS results for the sapphires in Figure 7, together with data for SSEF reference sapphires from Kashmir, Sri Lanka and Myanmar. Trace-element concentrations of Mg, Fe and Ga are displayed using logarithmic scales. Additional plots of this data, seen from different directions, are available in the online data depository on The Journal's website.



Detecting Diffusion Treatments or Coatings

LA-ICP-Q-MS measures a set of preselected elements/isotopes of interest, and ignores all others. This involves choosing the elements/isotopes prior to analysis, and thus one may—by lack of knowledge—omit a crucial element, especially in the case of a previously unknown diffusion treatment or coating. However, LA-ICP-TOF-MS collects all information in the full mass spectrum with no information loss. It is therefore perfectly adapted to detect new and undisclosed chemical treatments. And thus it may help avoid an unprepared situation for gem laboratories such as when Be diffusion-treated corundum entered the market (Emmett et al., 2003).

Analysis of Inclusions

Most gemstones contain various types of inclusions, which may provide key information about the formation conditions of the sample in a minute volume. If the laser is used to analyse a surface-reaching inclusion or to ablate through a shallow surface layer of the host gem to reach an inclusion, such information can be registered by the ICP-MS. The sampling of inclusions by the laser usually lasts for only a very short time (ranging from less than a second to a few seconds of ablation time), as inclusions are commonly very small. The short signal interval often is too

brief for complete sequential acquisition of all isotopes of interest with one sweep using Q-MS. However, since TOF-MS offers simultaneous acquisition at a very high speed, hundreds of full-mass spectra can be collected from a tiny inclusion with only <0.5 s of ablation time. Consequently, TOF-MS provides more accurate concentrations for specific elements and a more reproducible multi-element quantification of the chemical composition of a tiny inclusion in a complex matrix such as a gemstone.

Geological Age Dating

Some elements in nature have constant ratios for their isotopes (only stable isotopes), while others have one or more radiogenic isotopes, which results in a steady change of their isotopic ratios over time due to the radioactive decay from parent to daughter isotopes. The decay process is related to the half-life of the parent radiogenic isotope. By measuring the ratio of the daughter-to-parent isotopes, the elapsed time or age can be calculated using the known half-life constant for the radiogenic pair.

The widely used U-Pb dating system ('geological clock') uses daughter-parent radiogenic pairs of $^{206}\text{Pb}/^{238}\text{U}$ and $^{207}\text{Pb}/^{235}\text{U}$. Zircon is by far the most useful mineral for age dating, as it contains U but no Pb when it forms, with limited contami-

nation from host rocks after formation. Age dating of surface or near-surface zircon inclusions in gem corundum (so far mostly sapphires) has been studied (Coenraads et al., 1990; Sutherland et al., 2002, 2008; Graham et al., 2008). More recently, age dating of zircon inclusions analysed by LA-ICP-Q-MS was performed on faceted sapphires from highly relevant origins to the gem trade (e.g. Link, 2015). These studies show that age dating can be used as a valuable tool for origin determination in gemmological testing, reflecting different formation times for sapphires from particular geological contexts. However, to precisely determine geological age, ratios of parent and daughter isotopes need to be measured at a high reproducibility. At the same time, interfering isotopes from the geological background of a given sample must be monitored and used to correct the ratio of radiogenic isotopes. As discussed previously, higher-precision isotopic ratios are expected when possible interfering isotopes are measured simultaneously by LA-ICP-TOF-MS. Therefore, this technique can be quite suitable for age dating, especially when the zircon inclusions are minute.

Besides a sensitive mass spectrometer, precise age dating relies on proper standard reference materials as well as corrections for laser ablation artefacts (e.g. fractionation). This must be addressed regardless of whether TOF-MS or Q-MS is used.

Imaging of Chemical Zoning for Gem Research

The formation of gem materials is a complex process both spatially and temporally. Chemical (and colour) zoning is common, caused by intrinsic (e.g. oscillatory growth zoning) or extrinsic (e.g. change of rock chemistry due to fluid infiltration) factors. Detailed mapping of elemental distribution may provide valuable information about formation kinetics that cannot be readily perceived based on just a few analytical spots. Quantitative imaging of trace-element distribution thus can be a powerful tool, particularly at high spatial resolution, such as from using homogenized 10 μm (or even smaller) laser spots. The amount of ablated material from such a tiny laser spot is minute and provides a brief transient signal. By controlling the ablation process, it is possible to gain two-dimensional or even three-dimensional elemental distribution images (Burger et al., 2015). Hence LA-ICP-TOF-MS is preferred for chemical mapping at high spatial resolution.

Conclusion and Outlook

The Swiss Gemmological Institute SSEF recently installed an LA-ICP-TOF-MS system, named GemTOF. This system is equipped with a 193 nm LA unit and an ICP-TOF-MS instrument.

LA-ICP-TOF-MS is a relatively new and highly sensitive technique for the chemical analysis of gemstones and pearls. This article discusses the advantages, compared to LA-ICP-Q-MS, as well as limitations of this technique. The main advantage is the simultaneous acquisition of full elemental mass spectra with high mass-resolving power and ultra-high acquisition speed. ICP-TOF-MS does not jump from one mass to the next through a series of preselected isotopes, as Q-MS does. Therefore, it is not necessary to preselect isotopes of interest, which requires assumptions about the trace-element composition of a sample and careful consideration of possible peak interferences before the measurement is performed. Since a full mass spectrum is recorded, TOF-MS allows adjustments for the isotope of interest, even after ablation and analysis, in contrast to Q-MS where re-ablation would be needed.

LA-ICP-TOF-MS yields high-quality elemental analyses, produces multidimensional data and feeds the database for statistical analysis. The combination of improved sensitivity and low background noise guarantees a superior limit of detection for heavy elements in single-digit ppb and for light elements in low ppm concentrations. In addition to routine measurements, this new and sophisticated analytical method complements other gemmological testing instruments. This will enhance applications such as trace-element characterization of gemstones and pearls for origin determination and treatment detection, and will open new research opportunities for age dating, inclusion studies and high-spatial-resolution chemical mapping of gems.

References

- Abduriyim A. and Kitawaki H., 2006. Determination of the origin of blue sapphire using laser ablation inductively coupled plasma mass spectrometry (LA-ICP-MS). *Journal of Gemmology*, **30**(1), 23–36, <http://dx.doi.org/10.15506/JoG.2006.30.1.23>.
- Anderson B.W., 1932. The use of X-rays in the study of pearls. *British Journal of Radiology*, **5**(49), 57–64.
- Borovinskaya O., Hattendorf B., Tanner M., Gschwind S. and Günther D., 2013. A prototype of a new inductively coupled plasma time-of-flight mass

- spectrometer providing temporally resolved, multi-element detection of short signals generated by single particles and droplets. *Journal of Analytical Atomic Spectrometry*, **28**(2), 226–233, <http://dx.doi.org/10.1039/c2ja30227f>.
- Burger M., Gundlach-Graham A., Allner S., Schwarz G., Wang H.A.O., Gyr L., Burgener S., Hattendorf B., Grolimund D. and Günther D., 2015. High-speed, high-resolution, multielemental LA-ICP-TOFMS imaging: Part II. Critical evaluation of quantitative three-dimensional imaging of major, minor, and trace elements in geological samples. *Analytical Chemistry*, **87**(16), 8259–8267, <http://dx.doi.org/10.1021/acs.analchem.5b01977>.
- Cartier L.E., 2010. Environmental stewardship in gemstone mining: Quo vadis? *InColor*, No. 15, Fall/Winter, 2–9.
- Cartigny P., 2005. Stable isotopes and the origin of diamond. *Elements*, **1**(2), 79–84, <http://dx.doi.org/10.2113/gselements.1.2.79>.
- Chalain J.-P., Fritsch E. and Hänni H.A., 1999. Detection of GE POL diamonds: A first stage. *Revue de Gemmologie AFG*, **138**(9), 30–33.
- Coenraads R.R., Sutherland F.L. and Kinny P.D., 1990. The origin of sapphires: U-Pb dating of zircon inclusions sheds new light. *Mineralogical Magazine*, **54**(374), 113–122, <http://dx.doi.org/10.1180/minmag.1990.054.374.13>.
- Dickinson DeLeon S.W., 2008. Jewels of Responsibility from Mines to Markets: Comparative Case Analysis in Burma, Madagascar and Colombia. M.S. thesis, University of Vermont, Burlington, USA, 190 pp.
- Emmett J.L., Scarratt K., McClure S.F., Moses T., Douthit T.R., Hughes R., Novak S., Shigley J.E., Wang W., Bordelon O. and Kane R.E., 2003. Beryllium diffusion of ruby and sapphire. *Gems & Gemology*, **39**(2), 84–135, <http://dx.doi.org/10.5741/gems.39.2.84>.
- Fisher D. and Spits R.A., 2000. Spectroscopic evidence of GE POL HPHT-treated natural type IIa diamonds. *Gems & Gemology*, **36**(1), 42–49, <http://dx.doi.org/10.5741/gems.36.1.42>.
- Giuliani G., Chaussidon M., Schubnel H.-J., Piat D.H., Rollion-Bard C., France-Lanord C., Giard D., de Narvaez D. and Rondeau B., 2000. Oxygen isotopes and emerald trade routes since antiquity. *Science*, **287**(5453), 631–633, <http://dx.doi.org/10.1126/science.287.5453.631>.
- Gordon R., 1888. On the ruby mines near Mogok, Burma. *Proceedings of the Royal Geographical Society and Monthly Record of Geography*, **10**(5), 261–275, <http://dx.doi.org/10.2307/1801309>.
- Graham I., Sutherland L., Zaw K., Nechaev V. and Khanchuk A., 2008. Advances in our understanding of the gem corundum deposits of the West Pacific continental margins intraplate basaltic fields. *Ore Geology Reviews*, **34**(1–2), 200–215, <http://dx.doi.org/10.1016/j.oregeorev.2008.04.006>.
- Guillong M. and Günther D., 2001. Quasi ‘non-destructive’ laser ablation-inductively coupled plasma-mass spectrometry fingerprinting of sapphires. *Spectrochimica Acta Part B: Atomic Spectroscopy*, **56**(7), 1219–1231, [http://dx.doi.org/10.1016/s0584-8547\(01\)00185-9](http://dx.doi.org/10.1016/s0584-8547(01)00185-9).
- Guillong M., Horn I. and Günther D., 2003. A comparison of 266 nm, 213 nm and 193 nm produced from a single solid state Nd:YAG laser for laser ablation ICP-MS. *Journal of Analytical Atomic Spectrometry*, **18**(10), 1224–1230, <http://dx.doi.org/10.1039/b305434a>.
- Gutmannsbauer W. and Hänni H.A., 1994. Structural and chemical investigations on shells and pearls of nacre forming salt- and fresh-water bivalve molluscs. *Journal of Gemmology*, **24**(4), 241–252, <http://dx.doi.org/10.15506/JoG.1994.24.4.241>.
- Hainschwang T., Hochstrasser T., Hajdas I. and Keutschegger W., 2010. A cautionary tale about a little-known type of non-nacreous calcareous concretion produced by the *Magilus antiquus* marine snail. *Journal of Gemmology*, **32**(1–4), 15–22, <http://dx.doi.org/10.15506/JoG.2010.32.1-4.15>.
- Halicki P., 2013. Part I: Chemical Characterisation of Gem-Quality Sapphires from Metamorphic and Magmatic Host Rocks: LA-ICP-MS Study. M.S. thesis, University of Basel, Switzerland, 180 pp.
- Hanser C., 2015. Comparison of Imaging Techniques for the Analysis of Internal Structures of Pearls. M.S. thesis, University of Freiburg, Germany, 140 pp.
- Kiefert L., Hänni H.A., Chalain J.-P. and Weber W., 1999. Identification of filler substances in emeralds by infrared and Raman spectroscopy. *Journal of Gemmology*, **26**(8), 501–520, <http://dx.doi.org/10.15506/JoG.1999.26.8.501>.
- Krzemnicki M.S. and Hajdas I., 2013. Age determination of pearls: A new approach for pearl testing and identification. *Radiocarbon*, **55**(3–4), http://dx.doi.org/10.2458/azu_js_rc.55.16389.
- Krzemnicki M.S., Hänni H.A. and Walters R.A., 2004. A new method for detecting Be diffusion-treated sapphires: Laser-induced breakdown spectroscopy (LIBS). *Gems & Gemology*, **40**(4), 314–322, <http://dx.doi.org/10.5741/gems.40.4.314>.
- Krzemnicki M.S., Friess S.D., Chalus P., Hänni H.A. and Karampelas S., 2010. X-ray computed microtomography: Distinguishing natural pearls from beaded and non-beaded cultured pearls. *Gems & Gemology*, **46**(2), 128–134, <http://dx.doi.org/10.5741/gems.46.2.128>.
- Krzemnicki M.S., Revol V., Hanser C., Cartier L. and Hänni H.A., 2015. X-ray phase contrast and X-ray scattering images of pearls. *Proceedings of the 34th International Gemmological Conference*, Vilnius, Lithuania, 26–30 August, 117–120.
- Link K., 2015. Age determination of zircon inclusions in faceted sapphires. *Journal of Gemmology*,

- 34**(8), 692–700, <http://dx.doi.org/10.15506/JoG.2015.34.8.692>.
- Longerich H.P., Jackson S.E. and Günther D., 1996. Inter-laboratory note: Laser ablation inductively coupled plasma mass spectrometric transient signal data acquisition and analyte concentration calculation. *Journal of Analytical Atomic Spectrometry*, **11**(9), 899–904, <http://dx.doi.org/10.1039/ja9961100899>.
- Mannes D., Hanser C., Krzemnicki M., Harti R., Jerjen I. and Lehmann E., 2016. Gemmological investigations on pearls and emeralds using neutron imaging. *Abstract Proceedings of the 8th International Topical Meeting on Neutron Radiography (ITMNR-8)*, Beijing, China, 4–8 September, poster no. PA9, p. 97.
- Meyer J.B., Cartier L.E., Pinto-Figueroa E.A., Krzemnicki M.S., Hänni H.A. and McDonald B.A., 2013. DNA fingerprinting of pearls to determine their origins. *PLoS ONE*, **8**(10), article e75606, 11 pp., <http://dx.doi.org/10.1371/journal.pone.0075606>.
- Muhlmeister S., Fritsch E., Shigley J.E., Devouard B. and Laurs B.M., 1998. Separating natural and synthetic rubies on the basis of trace-element chemistry. *Gems & Gemology*, **34**(2), 80–101, <http://dx.doi.org/10.5741/gems.34.2.80>.
- Pettke T., Oberli F., Audétat A., Guillong M., Simon A.C., Hanley J.J. and Klemm L.M., 2012. Recent developments in element concentration and isotope ratio analysis of individual fluid inclusions by laser ablation single and multiple collector ICP-MS. *Ore Geology Reviews*, **44**, 10–38, <http://dx.doi.org/10.1016/j.oregeorev.2011.11.001>.
- Rankin A.H., Greenwood J. and Hargreaves D., 2003. Chemical fingerprinting of some East African gem rubies by laser ablation ICP-MS. *Journal of Gemmology*, **28**(8), 473–482, <http://dx.doi.org/10.15506/JoG.2003.28.8.473>.
- Revol V., Hanser C. and Krzemnicki M., 2016. Characterization of pearls by X-ray phase contrast imaging with a grating interferometer. *Case Studies in Nondestructive Testing and Evaluation*, **6**, 1–7, <http://dx.doi.org/10.1016/j.csndt.2016.06.001>.
- Stern W.B. and Hänni H.A., 1982. Energy dispersive X-ray spectrometry: A non-destructive tool in gemmology. *Journal of Gemmology*, **18**(4), 285–296, <http://dx.doi.org/10.15506/JoG.1982.18.4.285>.
- Sutherland F.L., Bosshart G., Fanning C.M., Hoskin P.W.O. and Coenraads R.R., 2002. Sapphire crystallization, age and origin, Ban Huai Sai, Laos: Age based on zircon inclusions. *Journal of Asian Earth Sciences*, **20**(7), 841–849, [http://dx.doi.org/10.1016/s1367-9120\(01\)00067-0](http://dx.doi.org/10.1016/s1367-9120(01)00067-0).
- Sutherland F.L., Duroc-Danner J.M. and Meffre S., 2008. Age and origin of gem corundum and zircon megacrysts from the Mercaderes–Rio Mayo area, south-west Colombia, South America. *Ore Geology Reviews*, **34**(1–2), 155–168, <http://dx.doi.org/10.1016/j.oregeorev.2008.01.004>.
- Sutherland F.L., Zaw K., Meffre S., Giuliani G., Fallick A.E., Graham I.T. and Webb G.B., 2009. Gem-corundum megacrysts from east Australian basalt fields: Trace elements, oxygen isotopes and origins. *Australian Journal of Earth Sciences*, **56**(7), 1003–1022, <http://dx.doi.org/10.1080/08120090903112109>.
- Wehrmeister U., Goetz H., Jacob D.E., Soldati A.L., Xu W., Duschner H. and Hofmeister W., 2008. Visualization of the internal structures of cultured pearls by computerized X-ray microtomography. *Journal of Gemmology*, **31**(1), 15–21, <http://dx.doi.org/10.15506/JoG.2008.31.1.15>.

The Authors

Dr Hao A. O. Wang, Dr Michael S. Krzemnicki, Jean-Pierre Chalain, Pierre Lefèvre, Dr Wei Zhou and Dr Laurent E. Cartier
Swiss Gemmological Institute SSEF
Aeschengraben 26, 4051 Basel, Switzerland
Email: hao.wang@ssef.ch

Acknowledgements

The authors thank all parties who contributed to the LA-ICP-TOF-MS evaluation project, especially Dr Martin Tanner and Dr Olga Borovinskaya from Tofwerk AG (Thun, Switzerland), Dr Robert Hutchinson and Kevin Boyce from ESI (Huntingdon, UK) and Dr Serge Bilger from ThermoFisher Scientific (Reinach/Basel, Switzerland). We thank the Board of the Swiss Foundation of Gemstone Research (SSEF) for their support of this research. The Swiss Association of Gemstone Dealers is appreciated for their generous financial donation. The authors appreciate helpful comments on this article from three anonymous reviewers and Dr Borovinskaya. Thanks also to the entire SSEF team for their support and fruitful discussions.

Synthetic Emeralds Grown by IG Farben: Historical Development and Properties Related to Growth Technology

Karl Schmetzer, H. Albert Gilg and Elisabeth Vaupel

Developments in emerald synthesis occurred over a period of nearly five decades (1911–1958) at a facility in Bitterfeld, Germany, operated primarily under the name IG Farben. Initial experiments involving the flux method of growth performed by H. Wild in Idar-Oberstein led to collaborations with Bitterfeld scientist O. Dreibrodt in the 1910s and 1920s. Almost two decades of research then ensued, culminating in a breakthrough by H. Espig of IG Farben in 1929 that permitted the growth of larger synthetic emerald crystals. A standard synthesis process was developed between 1930 and 1935, and production on a limited scale lasted until 1942. Although the possibility of restarting production was explored in the 1950s, those initiatives were abandoned without further operations. The evolution of the company's flux-growth technology from the first trials before 1914 through the standardized production after 1935 is recorded in variations in the properties of the resulting synthetic emeralds. While Cr was always present as a colour-causing trace element, in later eras Ni was added as well. Growth was performed in platinum crucibles with the nutrient at the bottom, seeds centrally located in a molybdate melt and silica plates floating on top of the melt. To create a barrier between the seeds and the silica plates, a platinum net was originally employed but was subsequently replaced by a platinum baffle. Natural beryl seeds were used in the early years, followed by flat synthetic emerald plates. As a consequence, the morphology of the synthetic emerald crystals changed from prismatic to thick tabular or short prismatic.

The Journal of Gemmology, 35(3), 2016, pp. 224–246, <http://dx.doi.org/10.15506/JoG.2016.35.3.224>
© 2016 The Gemmological Association of Great Britain

Introduction

In February 1935, the trade press first announced that scientists at Interessen-Gemeinschaft Farben-industrie Aktiengesellschaft, known as IG Farben AG, in Bitterfeld, Germany, had succeeded in growing synthetic emeralds of facetable size and quality (e.g. Figure 1), denominated 'Igemerald'

(for **IG** Farben synthetic **emerald**; Anonymous, 1935a). The first gemmological and mineralogical descriptions were published by M. Jaeger, the director of the IG Farben plant at Bitterfeld, and H. Espig, the technical leader of synthetic gemstone production at the company, which mainly grew rubies, sapphires and spinels by

the Verneuil technique (Espig, 1935; Jaeger and Espig, 1935).¹ These initial descriptions were soon followed by additional studies by a few gemmologists or mineralogists who were able to obtain samples for scientific research (Anderson, 1935; Eppler, 1935, 1936; Schiebold, 1935). A general summary, with short contributions by K. Schlossmacher, B. W. Anderson and G. O. Wild, also was published by the Gemological Institute of America (Anonymous, 1935b).

Jaeger and Espig (1935) further indicated that commercialization of the growth process through the release of the synthetic emeralds freely to the trade was not intended at that time. Rather, they indicated that samples would be given to a limited number of highly qualified goldsmiths for production of a small quantity of special jewellery items. In reality, it appears that samples were received only by K. B. Berthold, who published a note in *Deutsche Goldschmiede-Zeitung* (German Goldsmiths' Journal) describing the extraordinary "beauty, quality and value" of the synthetic emeralds (Berthold, 1935). Such statements could certainly support use of the new synthetic material exclusively for advertisement and public relations purposes (see Metzger, 2000).

In the early works cited above, as well as in subsequent reports discussing ways to distinguish natural and synthetic emeralds, the growth method used at Bitterfeld was not mentioned even in general terms. Instead, it was simply assumed through the 1950s that a hydrothermal technique

¹ Verneuil synthesis of ruby and sapphire in Bitterfeld commenced in 1910 at Elektrochemische Werke Bitterfeld (see footnote 2). The initial attempts at growing synthetic emerald by this company can be traced back to around 1911 and, later, to the work of O. Dreibrodth beginning in ~1913–1914 (see footnotes 4–6). In 1925, this company, including the plant for producing synthetic gem materials, was incorporated into the IG Farben group of companies. Later, under communist rule, the state-owned entity VEB Elektrochemisches Kombinat Bitterfeld took control of synthetic ruby, sapphire and spinel production at Bitterfeld. Business files from all three periods are preserved in the Landesarchiv Sachsen-Anhalt (LASA), Abteilung Merseburg (archives of the German federal state Saxony-Anhalt, Department Merseburg) and at Kreismuseum Bitterfeld. In Merseburg, the documents attributed to Elektrochemische Werke Bitterfeld and IG Farben Bitterfeld are filed as LASA, MER, I 506; the documents attributed to VEB Elektrochemisches Kombinat Bitterfeld are filed as LASA, MER, I 507; and a mixed file containing documents from different eras is filed as LASA, MER, I 509. The documents collected at Kreismuseum Bitterfeld are filed as SE (synthetische Edelsteine = synthetic gemstones).



Figure 1: This cluster consisting of five synthetic emerald crystals (type 3) was produced by IG Farben at Bitterfeld, and is from the collection of the Museum für Naturkunde, Berlin. The size of the crystal group is approximately 19.3 × 15.4 mm, and it weighs 15.54 ct; the largest crystal measures 13.8 mm long, with a diameter of 9.3 mm. Photo courtesy of R.-T. Schmitt.

had been used (Webster, 1952, 1955, 1958; for an overview of methods applied for emerald synthesis, see also Fischer, 1955; Cannawurf, 1964; Nassau, 1976a,b; Diehl, 1977; Schmetzer, 2002). Only in the 1960s did a series of publications by Espig (1960, 1961, 1962) correct the record, detailing flux growth in lithium molybdate. An analogous flux-growth process had already been used by French scientists in the 19th century (Hautefeuille and Perrey, 1888, 1890), but the resulting synthetic emerald crystals were heavily included and only in the millimetre range or below.

Based upon the descriptions given by Espig (1960, 1961, 1962), the growth technique for synthetic emeralds applied at Bitterfeld was more recently depicted schematically (Recker, 1973; Schmetzer and Kiefert, 1998). The 'secret ingredient' alluded to by Espig as the means for obtaining a more desirable slightly yellowish green colour was also identified as a Ni-bearing compound by X-ray fluorescence and absorption spectroscopy (Schmetzer and Kiefert, 1998).

Yet much about the development and history of emerald synthesis at Bitterfeld has remained a mystery. Although Espig (1960, 1961, 1962) indicated that efforts began as early as 1911,

until now our knowledge has been restricted to those facts that he decided to publish in the early 1960s. Almost nothing is known about work prior to the 1930s, and equally absent is information about possible developments after production at Bitterfeld was terminated in 1942 because of World War II. Also limiting is the fact that the modern analytical examinations undertaken by Schmetzer and Kiefert (1998) were performed using only a small number of samples from a single collection (i.e. that of the late E. Gübelin, Lucerne, Switzerland).

However, the foregoing dearth of available information was recently altered when, during research by one of the authors into the industrial history of Verneuil synthesis at Bitterfeld (see footnote 1 and Vaupel, 2015), some internal IG Farben reports and related documents were discovered pertaining to emerald synthesis. Additional samples were then located and obtained from the museum of the Technische Universität Bergakademie (University of Mining and Technology) in Freiberg, Saxony, Germany; from the Museum für Naturkunde (Natural History Museum) in Berlin (Figure 1); from the Naturhistorisches Museum (Museum of Natural History) in Vienna, Austria; from the reference collection of the German Gemmological Association in Idar-Oberstein, Germany; and from private collections (e.g. from S. Fordemann, the granddaughter of Berthold). Thus, with these samples and the new documents, the present study was undertaken to fill historical gaps regarding emerald production in Germany and to add further gemmological and mineralogical data about the synthetic emeralds grown primarily in connection with the Bitterfeld operations.

² Hermann Wild (1859–1938) developed technology for growing Verneuil synthetic rubies together with Dr Adolf Miethe (1862–1927), professor at the Technical University of Berlin-Charlottenburg, Germany (Conradt, 1959). They first grew synthetic rubies in 1906 and developed recipes for producing synthetic sapphires of various colours in the following years. Samples grown on an experimental basis were cut in Idar-Oberstein and put on the market. Beginning in 1907, Wild and Miethe collaborated with Elektrochemische Werke Bitterfeld, then a subsidiary of Allgemeine Elektrizitäts-Gesellschaft AEG (General Electricity Company), one of the major producers of electrical equipment in Germany at that time. In 1909, Wild's gem trading company, including the equipment for experimental corundum synthesis, became a subsidiary of Elektrochemische Werke Bitterfeld, and the new joint enterprise worked under the designation Deutsche Edelsteingesellschaft (DEG; German Gemstone Company).



Figure 2: Hermann Wild began producing synthetic rubies and sapphires by the Verneuil technique in Idar-Oberstein in 1906, and the operations were transferred to Bitterfeld in 1910. Wild also experimented with emerald synthesis and submitted some small crystals he produced to R. Brauns in 1912. Photo taken ~1900; courtesy of D. Jerusalem.

History

Emerald Synthesis by H. Wild (~1912)

Hermann Wild², a gem merchant from Idar-Oberstein (Figure 2), was the first to grow synthetic rubies and sapphires by the Verneuil method in Germany, beginning in 1906 (Miethe, 1908; Bauer, 1909; Doelter, 1909; *Mitteilungen der Wiener Mineralogischen Gesellschaft*, 1909). He cooperated with Elektrochemische Werke Bitterfeld in these efforts from 1907 until 1909, when his synthetic corundum operations were acquired by that company. In 1910 the synthetic corundum production was transferred from Idar-Oberstein to Bitterfeld, but Wild continued to collaborate with Elektrochemische Werke Bitterfeld by giving technical advice, observing the market, and distributing the synthetic materials grown by them (for further details see Vaupel, 2015). Also in 1910, Wild discussed emerald synthesis experiments with F. Rothe



Figure 3: Hermann Espig joined Elektrochemische Werke Bitterfeld in 1921 and from 1924 onwards was involved in experiments related to emerald synthesis. After a breakthrough in 1929 enabled the growth of larger crystals, he developed the final production technique between 1930 and 1935. Photo taken in the 1950s; courtesy of K.-D. Heinrich.

and H. Röhler, leading representatives from Bitterfeld (file LASA, MER, I 506, No. 96). This corresponds with the dates given by Espig (1945, 1960), who mentioned the years 1910 and 1911 in connection with the start of experimental studies on emerald synthesis at Bitterfeld. While maintaining his own emerald-growth operations in Idar-Oberstein, Wild additionally became privy to details regarding the experiments at Bitterfeld, such as learning in 1915 about the use of Otto Dreibrodt's³ apparatus in the early years of experimental mineral synthesis (see below).

In August 1912, Wild submitted a number of small synthetic emerald crystals to R. Brauns, professor of mineralogy at the University of Bonn, Germany. Brauns published a short note about this synthetic gem material in 1913, and a more detailed study followed in 1936. The full text of that study, including the three original figures, was later republished in the *Zeitschrift der Deutschen Gesellschaft für Edelsteinkunde*

(Journal of the German Gemmological Association), together with general notes and comments by H. Bank (1965).⁴ The synthetic emeralds produced by Wild also were briefly mentioned in Doelter (1913) and in Michel (1914, 1915), and some of the material was used for a luminescence study (Michel and Riedl, 1925). Nevertheless, none of the works divulged anything about Wild's production technique.

Emerald Synthesis at Bitterfeld by O. Dreibrodt (~1913–1926) and H. Espig (~1924–1928)

As noted above, in describing the method for emerald synthesis invented at Bitterfeld, Hermann Espig (1960, 1961, 1962; Figure 3) dated the first experiments in that endeavour as early as 1910–1911. It is likely that such comments also referred to the collaboration with and early experiments by Wild, because experiments in Bitterfeld, as performed by Dreibrodt and described below, are documented only from 1913 or even somewhat later.

In 1913, Otto Dreibrodt (Figure 4), a young mineralogist, was hired by Elektrochemische Werke Bitterfeld, which in turn became part of IG Farben in 1925. Prior to this employment, Dreibrodt had already invented an apparatus for crystal growth in solutions or melts, and in his new position he

³ Dr Otto Dreibrodt (1887–1941) studied mathematics and mineralogy at the Universities of Halle and Leipzig, Germany, graduating from the latter in 1912. Dreibrodt joined Elektrochemische Werke Bitterfeld in August 1913. Numerous German and international patents by Dreibrodt and assigned to Elektrochemische Werke Bitterfeld dealt with developments and improvements in the Verneuil technique, such as for producing sapphires and spinels of various colours, as well as for chemical technology not related to gem synthesis. He became the technical leader for synthetic gemstone production at Elektrochemische Werke Bitterfeld in 1919 but left the company at the end of 1926. His personnel records still exist (files LASA, MER, I 506, Nos. 1068 and 1069), but no grounds for his departure were disclosed. Several Verneuil boules from his work remain with the family, having been left by his daughter L. Dreibrodt at her death, but no synthetic emerald samples are included (E. Schlatter, pers. comm., 2015).

⁴ In his comments, H. Bank (1965) mentioned that he borrowed the samples produced by H. Wild and described by R. Brauns from the mineralogical collection at the University of Bonn, Germany, and he announced the forthcoming publication of his own study. Unfortunately, this paper was never published, and the samples can no longer be located in the mineralogical collection at the University of Bonn (A. Zacke, pers. comm., 2015).

was tasked with developing novel techniques for crystal growth and with applying known methods to new materials, including synthetic emerald. Elektrochemische Werke Bitterfeld also applied for German and international patents covering the apparatus previously invented by Dreibrodts, after rights to the device had been transferred to the company by contract.⁵ A German patent was granted in 1914, and the corresponding U.S. patent was published in 1920. The U.S. patent for Dreibrodts apparatus was apparently considered worthy of attention, as it was reviewed briefly in the *American Mineralogist* (Hunt, 1921)—not a common practice at that time.

In that device, called a ‘rotation apparatus’ (Figure 5a), a solution or melt was placed in a vessel with the nutrient at the bottom and a seed (‘k’ in Figure 5a) in an upper crystallizing chamber (f). A temperature gradient was created between the seed and nutrient by an external heat source. An outer tube (b) was suspended over the crystallizing chamber and connected by special holders to an inner tube (g), which terminated in a T-piece (h). When the bottom portion of the apparatus containing the nutrient was heated and the outer and inner tubes were rotated (with the T-piece), hotter solution or melt was drawn up through the outer tube, thereby transporting dissolved nutrient to the cooler seed. To work



Figure 4: Otto Dreibrodts worked from August 1913 to December 1926 for Elektrochemische Werke Bitterfeld and was involved in the first experiments dealing with emerald synthesis. His projects also encompassed the growth of synthetic rubies, sapphires and spinels by the Verneuil technique. Photo taken about 1913; Landesarchiv Sachsen-Anhalt, Merseburg, file LASA, MER, I 506, No. 1068; reproduced by permission.

⁵ The rights to use and to file national and international patent applications for the apparatus Dreibrodts invented for crystal growth were sold to Elektrochemische Werke Bitterfeld for 3,000 Reichsmark. Dreibrodts was hired by the company at a monthly wage of 300 Reichsmark in 1913 (file LASA, MER, I 506, No. 1068).

⁶ Dr Hermann Espig (1895–1969) studied mathematics and natural sciences, primarily mineralogy, chemistry and physics, from 1916 to 1920 at the University of Leipzig. He graduated in 1920 with a thesis addressing X-ray diffraction patterns of silicon carbide, prepared under the academic supervision of F. Rinne and E. Schiebold (archives of the University of Leipzig). Espig joined Elektrochemische Werke Bitterfeld in March 1921 and became O. Dreibrodts assistant in 1922. During his early years with the firm, Espig was also tasked with carrying out experiments suggested by A. Miethe (see footnote 2). After Dreibrodts left the company at the end of 1926, Espig became the leader of synthetic gemstone production at Bitterfeld. (Espigs personnel file is available in Merseburg, LASA, MER, I 506, No. 1064.) The cooperation between Espig and Dreibrodts in the early 1920s is evidenced by German patents 385 374 (granted 1923) and 390 794 (granted 1924). Both applications, which dealt with the production of green synthetic sapphires, were filed in December 1922 and listed Dreibrodts, Espig and D. Strauss as the inventors.

with a melt and not only with hydrous solutions, the apparatus was constructed of platinum and used, at least temporarily, in Bitterfeld for emerald synthesis experiments (file LASA, MER, I 506, No. 475, dated 1915; see footnote 1 for an explanation of LASA references).

However, problems with oversaturation of the melt and spontaneous nucleation of tiny synthetic emerald crystals or aggregates could not be solved, and no samples of facetable size were obtained from the experiments.

Hermann Espig⁶ (see again Figure 3) was involved in experiments dealing with emerald synthesis at Bitterfeld beginning in 1924. In an internal report, Espig (1930) presented a short summary of the work before 1929. He described the problem of oversaturation and mentioned another apparatus, also made of platinum, that was developed to obtain synthetic emerald

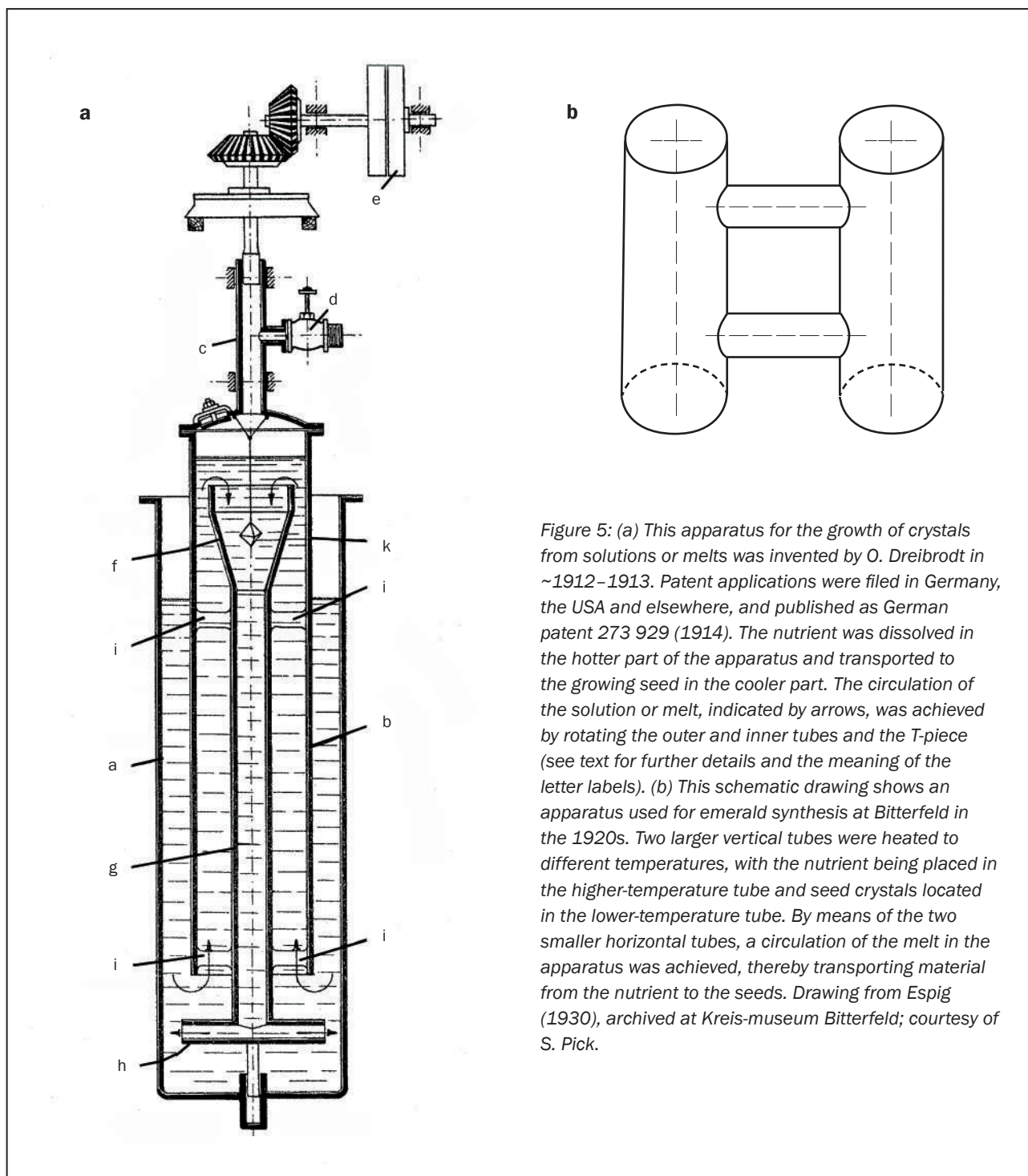


Figure 5: (a) This apparatus for the growth of crystals from solutions or melts was invented by O. Dreibrod in ~1912–1913. Patent applications were filed in Germany, the USA and elsewhere, and published as German patent 273 929 (1914). The nutrient was dissolved in the hotter part of the apparatus and transported to the growing seed in the cooler part. The circulation of the solution or melt, indicated by arrows, was achieved by rotating the outer and inner tubes and the T-piece (see text for further details and the meaning of the letter labels). (b) This schematic drawing shows an apparatus used for emerald synthesis at Bitterfeld in the 1920s. Two larger vertical tubes were heated to different temperatures, with the nutrient being placed in the higher-temperature tube and seed crystals located in the lower-temperature tube. By means of the two smaller horizontal tubes, a circulation of the melt in the apparatus was achieved, thereby transporting material from the nutrient to the seeds. Drawing from Espig (1930), archived at Kreis-museum Bitterfeld; courtesy of S. Pick.

crystals of larger sizes. A simple schematic drawing showed two larger vertical tubes that were connected by two smaller horizontal tubes (Figure 5b). By heating one of the vertical tubes to 600°C and the second to 800°C, a temperature gradient and a circulation of the melt could be established, with the nutrient being added to the higher-temperature tube. Nonetheless, the experiments performed with that equipment

likewise did not succeed in growing larger crystals.

Obviously, the small synthetic emerald crystals produced by Elektrochemische Werke Bitterfeld/IG Farben Bitterfeld before 1929 were not distributed on a significant scale. Only a few short descriptions of the small hexagonal prisms are found in the literature (Michel, 1927; Doerner, 1929; see Figure 6).

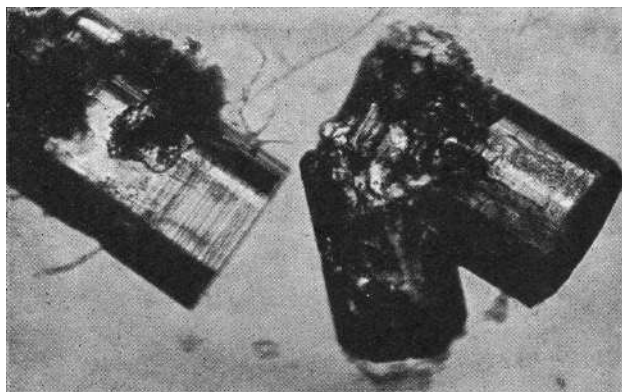


Figure 6: Small synthetic emerald crystals were grown in various experiments at the Bitterfeld facility in the 1920s. The diameter of the crystals is about 0.5 mm. From Doermer (1929).

Breakthrough by H. Espig (1929) and Efforts Toward Commercial Production (1930–1935)

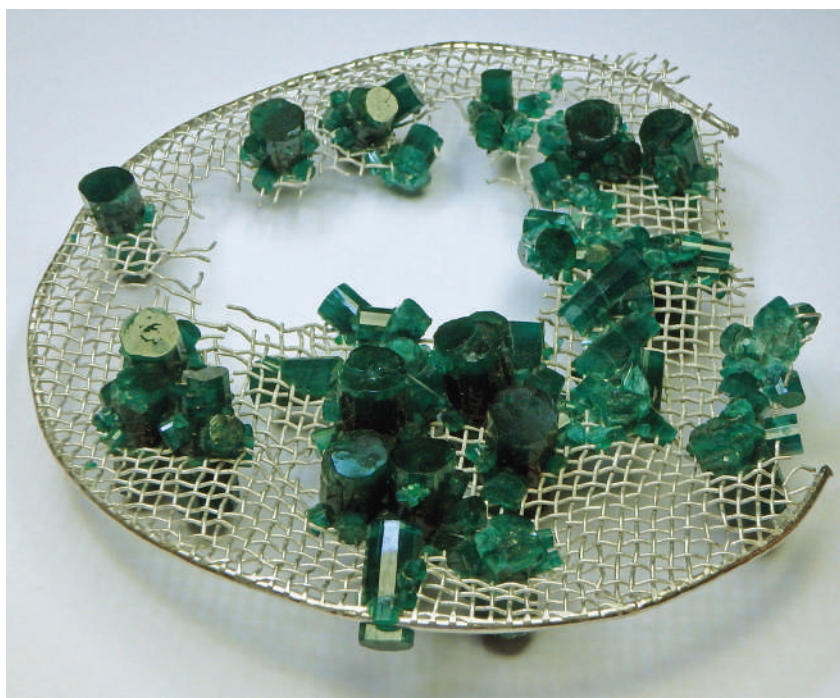
Espig (1930) described an experiment in which two of the components of beryl, Al_2O_3 and BeO , were separated from SiO_2 powder in a platinum dish. That experiment, performed in February 1929, led to the growth of synthetic emerald crystals that were larger than those obtained before. Additional developments resulted in the Al_2O_3 and BeO being placed on the bottom of a crucible with silica plates (composed of quartz or vitreous silica) being floated on top of the molten flux. The silica was dissolved by the flux to supply the SiO_2 component for synthetic emerald growth. With that arrangement, however, small synthetic

emerald crystals were found to grow on the silica plates.

Next, in an attempt to avoid nucleation on the silica plates, a platinum net was placed in the crucible, with beryl seeds below the net. The disadvantage was that the synthetic emerald crystals tended to adhere to and grow on both sides of the platinum net (Figure 7). They consequently had to be sawn into pieces to separate them from the net. This was addressed by replacing the platinum net with a platinum baffle (disc) punctured by small holes to allow circulation of the SiO_2 -bearing flux. Finally, to ensure that crystal growth would not need to be interrupted every 2–3 days due to consumption of the initial nutrient, a platinum tube was placed in the centre of the crucible to allow nutrient to be added to the bottom as the growth process continued (Figure 8). After a growth period of about 20 days, the synthetic emeralds were removed from the flux and inspected visually. Any extremely impure layers were removed and the synthetic emeralds so prepared were used for further growth cycles. Facetable-sized crystals were obtained after a total period of about one year (for further details, see Schmetzer and Kiefert, 1998).

Additional information regarding the seeding technique, which influenced the properties of the final product, is found in some of Espig's later works (1960, 1962). During the early years, after the clusters or druses were sawn from the

Figure 7: Multiple IG Farben synthetic emerald crystals and crystal clusters are shown attached to a platinum net. The size of the item is approximately 11 × 9 cm, and it is part of the collection of the Museum für Naturkunde, Berlin. Photo courtesy of R.-T. Schmitt.



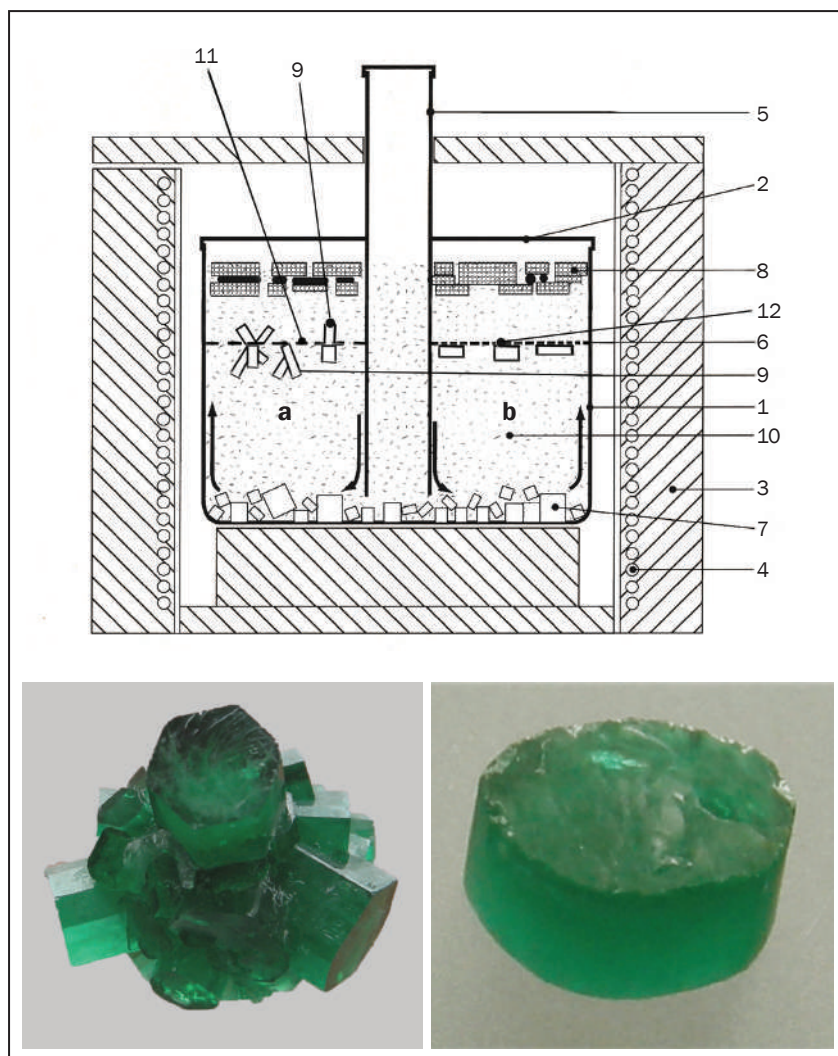


Figure 8: In this schematic diagram for the flux growth of synthetic emerald by IG Farben at Bitterfeld from 1929 to 1942, (a) represents the earlier method using a platinum net to separate seeds of natural beryl or synthetic emerald from silica plates floating on the melt, and (b) represents the later method using platinum baffles to separate seeds of synthetic emerald from the silica plates. For (a), the synthetic emerald crystals and crystal clusters grew on both sides of the net, while in (b) single crystals grew only on one side of the baffle. 1—platinum crucible, 2—platinum lid, 3—insulation, 4—heating system, 5—central platinum tube for the addition of nutrient material, 6—platinum baffle, 7—nutrient, 8—silica plates, 9—growing prismatic synthetic emerald crystals, 10—lithium molybdate flux, 11—platinum net, 12—growing tabular synthetic emerald crystals (adapted from Schmetzer and Kiefert, 1998). The photos show a crystal cluster (left, approximately 20.4 × 17.3 × 13.6 mm) and a single crystal with short columnar habit (right, approximately 13.8 × 12.9 × 6.3 mm), representing typical products grown with the two variants drawn schematically above. Photos by K. Schmetzer.

platinum nets, they were used to create synthetic seeds. Specifically, the ends of the larger crystals within the clusters were cut perpendicular to the c-axis. These short prismatic seeds were then placed in the melt for further crystal growth, and this practice continued after the platinum net was replaced by a platinum baffle. The morphology of the resulting single crystals was described by Espig (1962) as prismatic to thick tabular.

Overall, many details given in the above-cited early internal report prepared by Espig (1930) are consistent with later data published in the early 1960s. Obvious examples include a $\text{BeO-Al}_2\text{O}_3\text{-SiO}_2$ phase diagram and a description of the various mineral phases and their stability fields in a triangular diagram, which are identical across the sources. Conversely, one notable aspect of the history found only in Espig's 1930 report is the filing of two patent applications, the first in October 1929 and a second shortly thereafter. Espig stated that both applications had already

received positive reports from the examiner at the German patent office in Berlin responsible for inorganic synthesis technologies and were awaiting publication. However, given that those patents were never published, it can be concluded that they were abandoned by the applicant, likely to avoid having the processes for emerald synthesis made publicly available. Other internal IG Farben documents dated between 1931 and 1942 confirm this presumption (see below).⁷

⁷ Two documents preserved in the archives of Bayer AG at Leverkusen, Germany (dated 1931 and 1935, in file 186/9) and one document archived at Merseburg (dated 1942, in file LASA, MER, I 506, No. 9580) record statements by IG Farben managers and by staff members of the patent department about filing patent applications dealing with emerald synthesis. (From 1925 onwards, Bayer AG was one of the larger companies within the IG Farben group.) Together with the internal report by Espig (1930), these documents show that at least three patent applications were filed and then subsequently withdrawn to avoid publication.

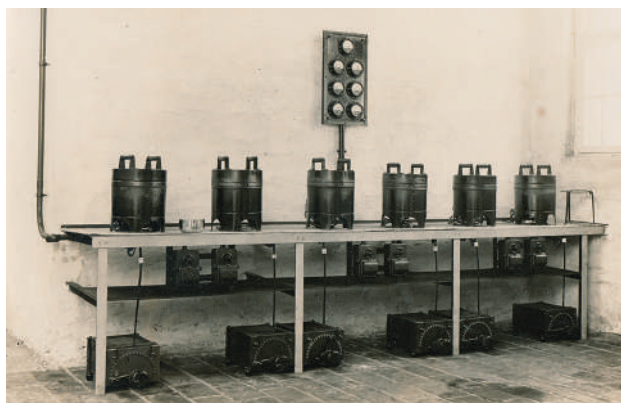


Figure 9: The production facility at the IG Farben plant in Bitterfeld for growing synthetic emeralds in 1930 is shown here. Six apparatus are seen, each corresponding to the assembly shown schematically in Figure 8. Photo from Espig (1930), archived at Kreismuseum Bitterfeld; courtesy of S. Pick.

The use of a Ni-bearing compound together with yttrium oxide (see below)—in addition to Cr—as the cause of colour was not mentioned in Espig’s 1930 report. This may indicate that the “hundreds of experiments to establish the desired slightly yellowish green coloration of the synthetic emeralds”, as described by Espig in his papers of the early 1960s, were performed between 1930 and 1935. As noted at the outset, 1935 was the year that IG Farben announced the successful development of a process for Igmerald synthesis and made available to the public a limited number of samples, especially for gemmological examination.

IG Farben in the 1930s

Although the IG Farben board of directors in 1935 proudly announced their company’s work as a breakthrough in synthetic emerald production, the result achieved actually fell short of the goal underlying the more than two decades of effort that preceded the announcement. The aim had been to develop a process for cheap mass production of synthetic emerald (comparable with the Verneuil synthesis of ruby and sapphire) that could meet the demand of the jewellery industry for a green gem material. However, the high production cost, the required growth time of one year or more in total and the relatively low yield failed to meet the vision of IG Farben leadership.

Various calculations of the production cost, based upon different assumptions, exist in the historical documents from 1937 (50 or 60

Reichsmark per carat of faceted material) and from 1940 (100 Reichsmark per carat of faceted material).⁸ The production capacity from the established facility (Figure 9) was given in a 1938 document as only 200 carats per year. The consequent high cost of production resulted in a selling price in the trade of at least ~100 Reichsmark per carat for smaller gems and ~140 Reichsmark per carat for larger ones.⁸ At those prices, distribution via the established German gem trade in Idar-Oberstein would have been uneconomical. Moreover, none of the companies dealing in faceted natural emeralds wanted to offer synthetics for sale, in addition to their established product range of natural stones. Such facts led the IG Farben board of directors to consider using the Igmeralds for public relations purposes,⁹ as opposed to releasing them for sale. However, the officially stated reason offered in 1934 for the company’s decision not to engage in commercial production was that IG Farben sought to protect the trade in natural stones.¹⁰ Nonetheless, several efforts to explore placing the synthetic material into the trade are documented to have taken place in the years after 1935.

⁸ The various estimations or calculations of production cost for 1937 and 1940 are found in file LASA, MER, I 509, No. 9850. The production capacity and possible selling prices are mentioned in the same files. For comparison, the monthly wage of an average worker in Germany in 1937 was about 150 Reichsmark, and the average monthly income of a university professor was approximately 800 Reichsmark.

⁹ A contract between IG Farben and goldsmith Prof. Karl Borromäus Berthold (1889–1975) for the supply of synthetic emeralds is dated January 1935, and Berthold produced several jewellery pieces containing Igmerald. Some of the pieces were displayed at major exhibitions, such as the 1937 world exposition in Paris. Others were ultimately donated to high-ranking officials within the German government. For example, one item called the ‘Golden Shrine’, which incorporated 161 Igmeralds, was presented to A. Hitler on the occasion of his 50th birthday (1939) by the city of Cologne. See files LASA, MER, I 506, No. 2547 and LASA, MER, I 509, No. 9580; several items also were depicted and described in detail by Metzger (2000).

¹⁰ A short note was published in 1952 by C. Rühle, editor of *Deutsche Goldschmiede-Zeitung* from 1922 to 1953. Rühle mentioned that he had been told in 1934 by several people involved in Igmerald production that the primary rationale for limiting output was to avoid causing a drop in the prices for natural emerald. The market for ruby and sapphires had seen such a drop with the introduction of Verneuil-grown synthetics in the first decades of the 20th century.

This ambiguity between official statements and proprietary activities was also reflected in the patent policy of the company (again see footnote 7). As indicated previously, Espig's June 1930 internal report referenced two patent applications filed in the German patent office, the first one in October 1929, and a possible application in the USA also was considered. Both German applications were abandoned by the company, and at least one further application, filed about 1934, also was abandoned in 1935. The rationale behind these abandonments is suggested in the minutes from a meeting of IG Farben management in 1931: The company leaders were afraid that it would be impossible to control the worldwide use of the growth technology and especially to prevent possible patent infringement. Several letters dated after 1935 evidence consent amongst management regarding these policies.

IG Farben After 1942

According to all available information, the synthesis technique as established by 1935 remained essentially unchanged, and production continued on a limited scale until being terminated in 1942 because of World War II. Although Espig (1960, 1961, 1962) published that production of synthetic emeralds did not resume after 1942, two noteworthy events after 1945 should be mentioned for completeness.

Archived at Kreismuseum Bitterfeld is an internal report by Espig (1946) that recounted an experiment for growing synthetic emeralds. Specifically, a description of the growth process had been prepared in October 1945 for the Russian commander of the synthetic gemstone plant at Bitterfeld, and a practical demonstration also was required by the Russians. The February 1946 document reported that the original platinum apparatus used in emerald synthesis had ceased to be available. Therefore, at least one platinum crucible had to be manufactured from some residual sheet material. The experiment was performed successfully in January 1946 with a growth period of approximately one month. Most interestingly, the recipe for the various ingredients was given, and that recipe included nickel carbonate, the 'secret' ingredient not otherwise disclosed until the late 1990s (Schmetzer and Kiefert, 1998). Surprisingly, the list of ingredients also contained yttrium oxide, an Igemerald component not previously recognized. As a consequence of these activities, Espig would later remark in a letter dated 1952 that the production

technology for synthetic emerald was no longer secret because his 1946 report had been sent to Moscow.

In a further internal report, which was recently obtained by the authors from K.-D. Heinrich (the final director of the Bitterfeld plant before its closure in 1990), Espig (1945) stated that the yttrium oxide mentioned above was used in addition to lithium chromate and nickel carbonate as a colour-causing trace element to obtain the desired slightly yellowish green coloration of the synthetic emeralds.

In the Landesarchiv Sachsen-Anhalt, Abteilung Merseburg, a series of documents dated March 1954 to December 1958 revealed several exploratory efforts toward restarting synthetic emerald production after 1945. Included in them were calculations regarding the profitability of a small production of synthetic emerald comprising about 15–20 carats of faceted material per month (i.e. close to the yield obtained in the late 1930s), with an estimated production expense of 200 DM per carat (using the currency of the German Democratic Republic) and a selling price that was equivalent to that of Chatham synthetic emeralds at the time. The investment for the apparatus, including 15 kg of platinum,¹¹ was computed by Espig in 1955 to be about 118,500 DM.

Obviously, Espig never succeeded in obtaining permission for such a restart. However, samples of the remaining pre-1942 production (an inventory from 1951 mentioned 159 faceted pieces totalling 15.1 carats and 623 crystals totalling 3,124.7 carats) were used as state gifts for important visitors to the German Democratic Republic, mostly from the Soviet Union and other socialist countries.

Materials and Methods

The present study involved flux-grown synthetic emerald samples grown by four early producers. The oldest were some small crystals produced in the late 19th century from a lithium molybdate

¹¹ Espig listed 15 kg of platinum as well as several ingredients (beryllium oxide, lithium carbonate and yttrium oxide) that had to be purchased from foreign countries using Western currencies. Such complications in the supply chain, the high investment required and the minimal production output of only 15–20 carats per month culminated to suggest only a small possible profit. The combined disadvantages may explain why Espig was never successful in obtaining permission to restart synthetic emerald production. See file LASA, MER, I 507, No. 591, dated 1950s.

Table I: Properties of some early flux-grown synthetic emeralds.

Samples prepared by	P. G. Hautefeuille and A. J. E. Perrey, Paris, late 19th century	H. Wild, Idar-Oberstein, ~1912	K. A. Hofmann, Berlin, ~1926
Source of samples	Naturhistorisches Museum, Vienna	German Gemmological Association, Idar-Oberstein	Museum für Naturkunde, Berlin; Inv. No. 2015 00055
Description	Minute crystals or clusters, embedded between two glass slides	5 minute crystals or clusters, loose	Numerous minute crystals or clusters, loose
Crystal morphology	Short prismatic single crystals or clusters	Long prismatic single crystals or clusters	Long prismatic single crystals or clusters
Size	Up to ~0.5 mm	Up to ~1 mm	Up to ~1 mm
Growth zoning	Very impure, heavily included cores, clearer rims	None	None
Inclusions	Residual flux in various forms	Residual flux in various forms	Residual flux in various forms
Cause of colour	(Analysis not possible because embedded between glass slides)	Cr, minor Fe	Cr, minor Fe
Element(s) related to flux		Mo	Mo

flux by P. G. Hautefeuille¹² and A. J. E. Perrey in Paris, France. These were examined principally for comparison purposes and came from the Naturhistorisches Museum in Vienna. Five small crystals grown by Wild around 1912 were made available from the reference collection of the German Gemmological Association, Idar-Oberstein. Several synthetic emerald crystals produced in the 1920s by K. A. Hofmann,¹³ professor at the Technical University of Berlin-Charlottenburg, were provided by the Museum für Naturkunde in Berlin (Inv. No. 2015 00055). An overview of these three groups is presented in Table I.

¹² Dr Paul Gabriel Hautefeuille (1836–1902) was a French mineralogist and chemist. In 1865 he earned doctorates in physical sciences and medicine. From 1870 to 1885, he then served as co-director of the chemical laboratory at the École Normale Supérieure in Paris. He was appointed professor of mineralogy at the Faculté des Sciences in Paris in 1885 and, during the same year, was named director of the mineralogical laboratory at the École des Hautes Études. He published a number of papers that dealt with mineral synthesis, often in collaboration with the *ingénieur* Adolphe Jean Edme Perrey, vice-director of the laboratory at the École des Hautes Études (see Wisniak, 2014). Modern analytical and spectroscopic data for synthetic emeralds grown by Hautefeuille and Perrey were published by Bellatreccia et al. (2008).

¹³ Dr Karl Andreas Hofmann (1870–1940) was professor of inorganic chemistry at the Technical University of Berlin-Charlottenburg, Germany. He worked at the same university as A. Miethé (see footnote 2), so it is likely that the two scientists interacted. Additionally, Hofmann was in contact in the 1920s with staff members at the Bitterfeld production facility, discussing various aspects of mineral synthesis (including diamond).

The fourth group consisted of rough and faceted Igemeralds that were obtained from six different sources. The German Gemmological Association loaned two crystals and one faceted sample, and from the private collections of C. Weise, Munich, and E. Gübelin, Lucerne, came one crystal cluster and one faceted sample, respectively. The Museum für Naturkunde in Berlin offered one crystal and one cluster submitted by Espig in 1962 (e.g. Figure 1), plus a platinum net with multiple attached synthetic emerald crystals and clusters (Figure 7). The Technische Universität Bergakademie Freiberg provided 10 faceted samples and 10 rough crystals, which had been bequeathed by an individual involved in the production at Bitterfeld during the 1960s and 1970s. Five faceted Igemeralds set in jewellery by Berthold in the 1930s were made available by his granddaughter S. Fordemann of Herford, Germany. Thus, in summary and without counting the samples attached to the platinum net, the authors were able to examine 15 crystals or crystal clusters and 17 faceted synthetic emeralds produced by IG Farben.

All of the rough and faceted Igemeralds were examined with a gemmological microscope (magnification up to 100×), both with and without immersion. The early flux-grown synthetic emeralds were examined without immersion. All of the samples also were examined at higher magnification (up to 1,000×) using a Leica DM LM polarizing microscope with a transmitted light source. For photo documentation, we used an Olympus DP25 digital camera with Olympus Stream Motion software 1.6.1. For all faceted samples,

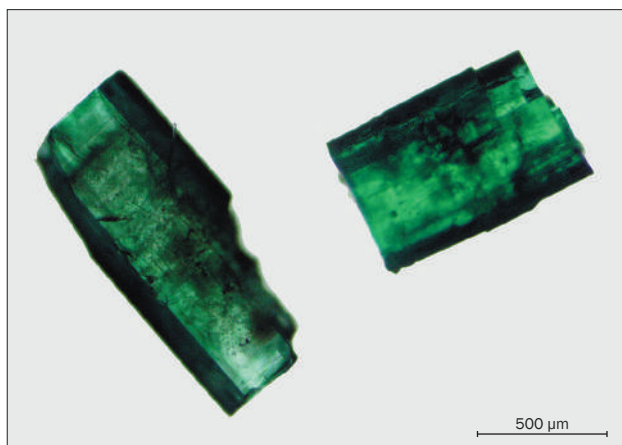


Figure 10: These tiny crystals from the synthesis experiments of H. Wild, about 1912, are kept in the reference collection of the German Gemmological Association, Idar-Oberstein. These single crystals contain dark inclusions of residual flux. (The dark edges along the prism faces are due to internal reflections.) Transmitted light; photomicrograph by H. A. Gilg.

refractive indices were measured; in addition, hydrostatic specific gravity was determined for samples without natural seed plates.

The 32 rough and faceted Igemeralds were examined by energy-dispersive X-ray fluorescence (EDXRF) spectroscopy using a Bruker Tracer III-SD mobile unit, as were the five synthetic emeralds grown by Wild and a similar number of tiny synthetic emerald crystals grown by Hofmann.

The platinum net with the attached crystals was not allowed to leave the Museum für Naturkunde in Berlin. Therefore, some of the crystals attached to the platinum net, as well as the single synthetic emerald crystal and the cluster from the same museum (which were also among the 32 samples mentioned above), were analysed by L. Hecht in Berlin using a Bruker Nano Tracer IV-SD EDXRF unit.

Results

Early Flux-grown Synthetic Emeralds

The basic properties of the early flux-grown synthetic emeralds are summarized in Table I.

Brauns (1936) described and depicted samples that were obtained from Wild in 1912. Strong zoning within the tiny prismatic crystals was highlighted, with a heavily included core and a transparent, almost clear rim. Conversely, the five samples grown by Wild available for the present study (e.g. Figure 10) lacked such distinct zoning. Instead, only the synthetic emeralds grown by Hautefeuille and Perrey

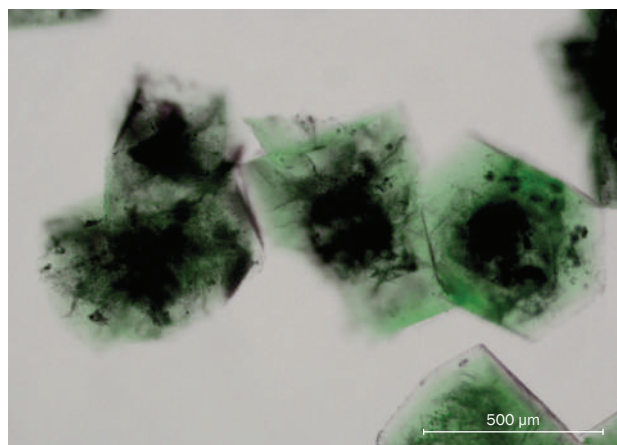
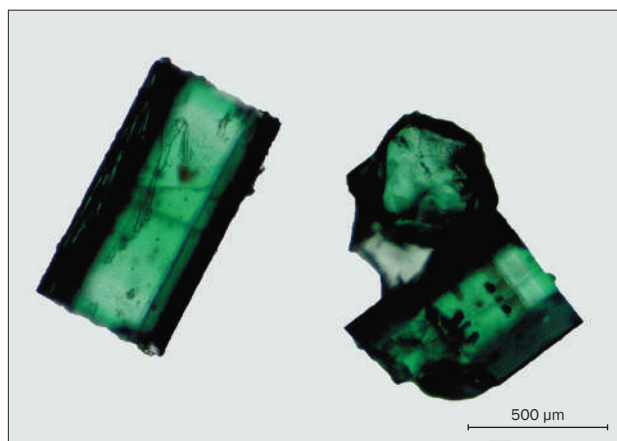


Figure 11: These tiny crystals from the synthesis experiments of P. G. Hautefeuille and A. J. E. Perry, late 19th century, are kept in the collection of the Naturhistorisches Museum, Vienna. The single crystals and crystal aggregates contain inclusions of residual flux, especially in the centre of each crystal. Transmitted light; photomicrograph by H. A. Gilg.

displayed pronounced zoning, with heavily included, almost opaque cores and clear rims, combined with a short prismatic morphology (Figure 11). The morphology and microscopic inclusion scene of the Wild samples instead paralleled the features seen in the Hofmann samples (Figure 12). In addition to the absence of zoning or of heavily included cores, both the Wild and Hofmann samples showed longer prismatic habits. Overall, their visual appearance was similar to that of material produced in Bitterfeld in the mid-1920s (see Figure 6).

The Hofmann material is recorded as having been produced through the same method used by

Figure 12: These tiny crystals from the synthesis experiments of K. A. Hofmann, mid-1920s, are kept in the collection of the Museum für Naturkunde, Berlin. The single crystals contain some inclusions of residual flux. Transmitted light; photomicrograph by H. A. Gilg.



Hautefeuille and Perrey—flux growth in lithium molybdate. Consistent therewith, the Hofmann samples gave a clear signal for Mo in the EXDRF spectrum. A likewise clear Mo spectrum also was obtained for the Wild material. Unfortunately, the samples produced by Hautefeuille and Perrey could not be analysed by EDXRF because they were embedded between two glass slides.

The foregoing results indicate that the synthetic emeralds grown by Wild in the early 20th century were produced by a variant of the method applied by French scientists in the late 19th century. The samples grown by Wild and also by Hofmann demonstrated that it was possible to produce small synthetic emerald crystals without intensely zoned areas of inclusions. Similar unzoned samples produced by the method of Hautefeuille and Perrey were described by Eppler (1961).

Thus, it is possible that Brauns (1936) had received samples from Wild that simply represented a different production run than those crystals available for the present study. Nonetheless, it is equally conceivable that Brauns just selected the samples with the most interesting zoning for description.

Igmerald

The Igmerald samples, based on their respective features, were subdivided into four different types (Table II). These types demonstrate the development of the growth technology at Bitterfeld between 1929 and 1935 (types 1–3) and ultimately represented the last step of the developmental process and the standardized production from 1935 to 1942 (type 4). Samples of types 1 and 4 are depicted in Figure 13.

Table II: Properties of IG Farben flux-grown synthetic emeralds (Igmeralds, ~1929–1942).

Classification		Type 1	Type 2	Type 3	Type 4
Samples		1 cluster of 18 crystals ^a ; 1 crystal ^b	1 faceted sample ^b	1 platinum net with numerous attached clusters, 1 cluster of 5 crystals and 1 single crystal ^c	1 crystal ^b ; 10 crystals and 10 faceted samples ^d ; 1 faceted sample ^e ; 5 faceted samples, set in jewellery by K. B. Berthold ^f
Crystal morphology		Long prismatic (cluster) or short prismatic (crystal), first- and second-order hexagonal prism plus basal faces	(Not applicable)	Long prismatic, first- and second-order hexagonal prism plus basal faces	Tabular or short prismatic
Seed		Irregularly shaped colourless natural beryl seed (crystal)	Colourless natural beryl seed with prism faces	Synthetic emerald seed	Synthetic emerald seed
Growth zoning		Layers parallel to the surface of the seed and parallel to prism faces (crystal)	Layers parallel to the first- and second-order hexagonal prism, in the seed zoning parallel to the basal faces	Layers parallel to prism and basal faces	Layers parallel to the first- and second-order hexagonal prism plus basal faces
Colour zoning		Strong zoning parallel to all crystal faces	Strong zoning parallel to all crystal faces	Strong zoning parallel to all crystal faces	Strong zoning parallel to all crystal faces
Inclusions	Growth tubes with nail-heads	Present (crystal)	None	None	None
	Isolated beryl crystals	Present	Present	Present	Frequently present
	Residual flux in various forms	Present	Present	Present	Always present
Element(s) related to flux		Mo	Mo	Mo ± Y	Mo
Cause of colour		Cr, minor V and Fe	Cr, Ni, minor Fe	Cr, Ni, minor Fe	Cr, Ni, minor Fe

Sources of samples:

^a C. Weise, Munich

^b German Gemmological Association, Idar-Oberstein

^c Museum für Naturkunde, Berlin; Inv. Nos. 2011 04554 and 2015 00054

^d Technische Universität Bergakademie Freiberg

^e E. Gübelin, Lucerne (obtained by author KS in the late 1990s)

^f S. Fordemann, Herford

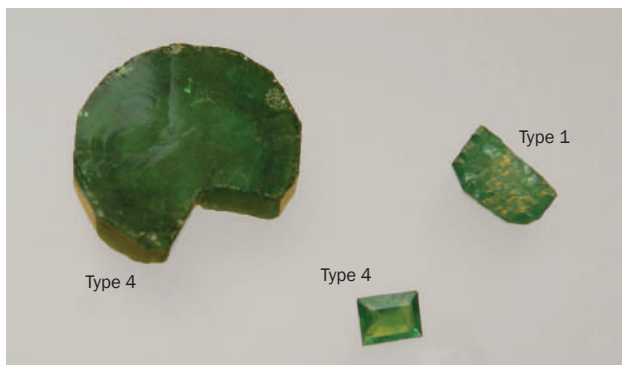


Figure 13: Shown here are rough synthetic emeralds of types 1 and 4 from the reference collection of the German Gemmological Association, as well as a type 4 faceted synthetic emerald from the collection of the late E. Gübelin. The crystal on the left measures 14.0 mm in diameter, with a thickness of 3.5 mm, and weighs 6.05 ct. Photo by K. Schmetzer.



Figure 14: This cluster of type 1 synthetic emerald crystals (20.4 × 17.3 × 13.6 mm) was produced by IG Farben without the addition of a Ni-bearing compound and is from the collection of C. Weise, Munich. Photo by K. Schmetzer.

In the present study, types 1 and 2 were represented by only a few samples. However, when considered together with the more abundant samples of types 3 and 4, a progression became evident that closely paralleled the developments indicated by Espig's descriptions and the IG Farben internal notes. Thus, while it remains highly probable that samples with properties intermediate between these four types were grown as the experiments proceeded, the classification into four types was used to facilitate general chronological understanding of the available samples. The intent was not to strictly circumscribe different categories or types of Igemeralds.

Type 1: Type 1 synthetic emeralds were grown from Mo-bearing fluxes. The two samples found to be of type 1 included a short prismatic crystal (Figure 13, upper right) and a cluster of 18 prismatic synthetic emeralds (Figure 14). With respect to the primary cause of the green colour, Cr-bearing compounds had been added to the nutrient, but Ni-bearing compounds were absent (i.e. not detected by EDXRF spectroscopy; Figure 15). Along with Cr, both samples also contained traces of V and Ga. It is unknown if the small amounts of V might have come from impurities present in chemicals used in the growth process or, alternatively, if V might have been intentionally added to the nutrient to induce colour. The traces

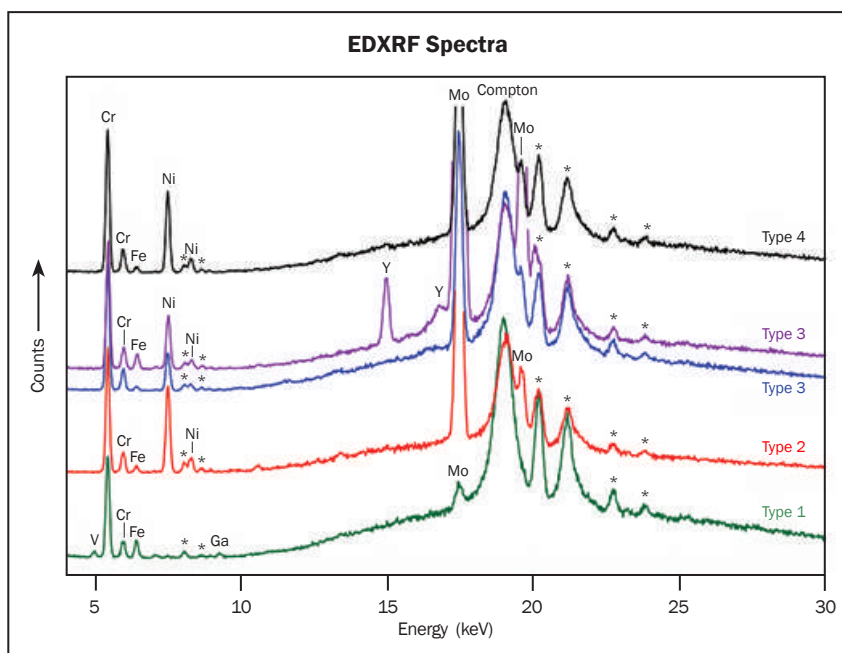


Figure 15: EDXRF spectra of type 1–4 synthetic emeralds produced in Bitterfeld show Cr and Ni as the main colour-causing trace elements and Mo as the main component of the flux. Small amounts of V (but no significant Ni) are present in the spectrum of the type 1 sample. A Y-bearing compound is also demonstrated as an ingredient of the flux used for crystal growth in one type 3 sample. The peaks labelled with an asterisk are related to the X-ray tube (Rh) or to interactions with the instrument (Pd, Cu, Zn); Compton refers to the inelastic scattering of the incident radiation.

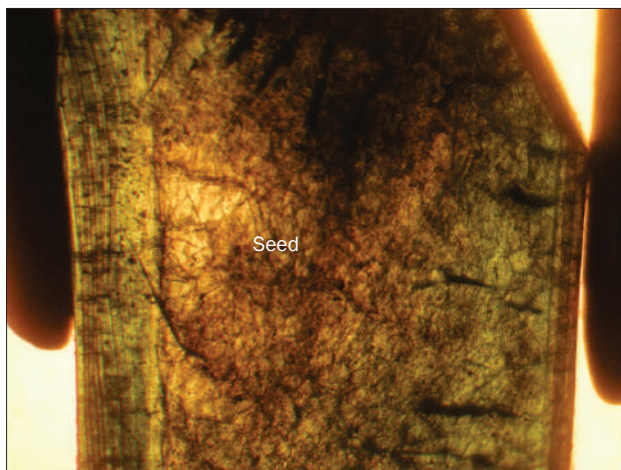


Figure 16: A crystal of type 1 synthetic emerald grown in Bitterfeld shows a natural colourless seed that is overgrown by synthetic emerald. Growth and colour zoning are seen parallel to the boundary between the seed and the synthetic emerald overgrowth. Immersion, field of view 4.6×3.5 mm; photomicrograph by K. Schmetzer.

of Ga most likely originated from somewhat impure chemicals (e.g. from traces of Ga in the aluminium oxide).

The individual crystal contained a colourless, somewhat irregularly shaped seed, and growth zoning was observed parallel to the boundary between the seed and the overgrowth (Figure 16). Amongst the inclusions seen, along with residual flux, were isolated synthetic beryl crystals, occasionally attached to growth tubes (i.e. ‘nail-head spicules’; Figure 17).

Type 2: The one type 2 synthetic emerald studied for this report was produced with the addition of a Ni-bearing compound to the nutrient (see Figure 15). In the immersion microscope, a colourless core with a boundary parallel to various prism faces was observed (Figure 18). The overgrowth displayed intense growth and colour zoning, likewise generally parallel to prism faces. However, in some parts of the crystal, the boundaries between growth zones were inclined to the otherwise typical prism planes. This indicated that the sample had been cut and repolished for subsequent growth runs, most likely to remove impure portions. Besides various forms of residual flux, inclusions of synthetic beryl in an orientation different from that of the host synthetic emerald were seen (Figure 19). Those tiny included synthetic emerald crystals were generated by spontaneous nucleation and, in turn, contained numerous inclusions in their respective cores.

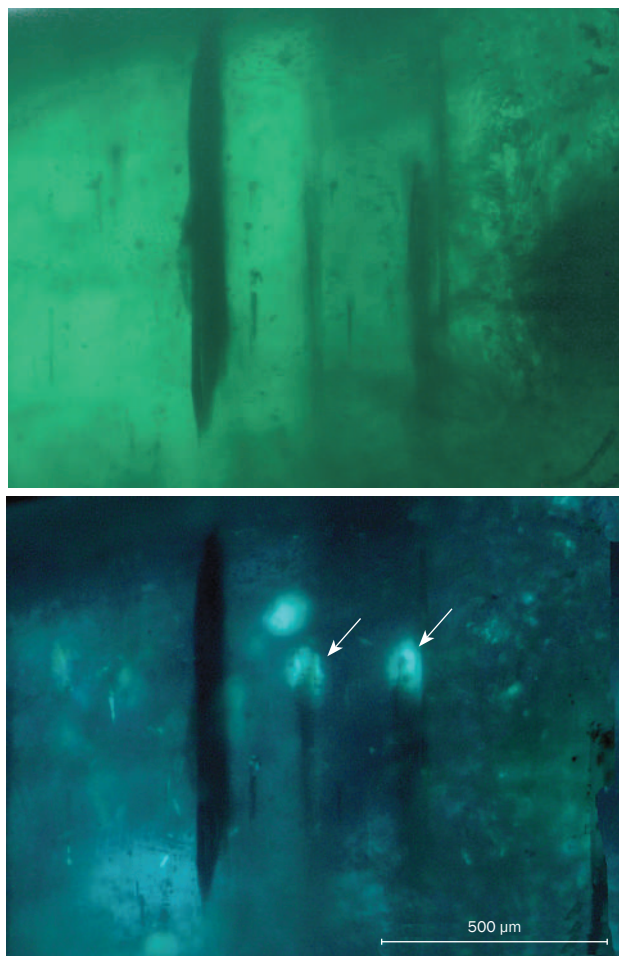


Figure 17: At higher magnification, the type 1 synthetic emerald depicted in Figure 16 shows growth tubes with small birefringent synthetic emerald crystals attached to the wider ends of the channels (see arrows). Top: transmitted light; bottom: transmitted light with crossed polarizers; photomicrographs by H. A. Gilg.

Type 3: The samples assigned to type 3 were grown with seeds having been placed below a platinum net in the crucible. As a consequence of such arrangement, the developing synthetic emerald crystals adhered to the net, even growing through the net (Figure 7). One cluster of five crystals (Figure 1) had been removed from the net and consequently exhibited a planar sawn surface. A single crystal of this type (Figure 20, left) contained residual platinum wires from the net. The prismatic morphology of the crystals (Figure 20, right) typically consisted of first- and second-order hexagonal prism faces **m** ($10\bar{1}0$) and **a** ($11\bar{2}0$), in combination with the basal pinacoid **c** (0001). The single crystal displayed a green seed in the centre, with growth planes parallel to the basal and prism faces (Figure 21). These

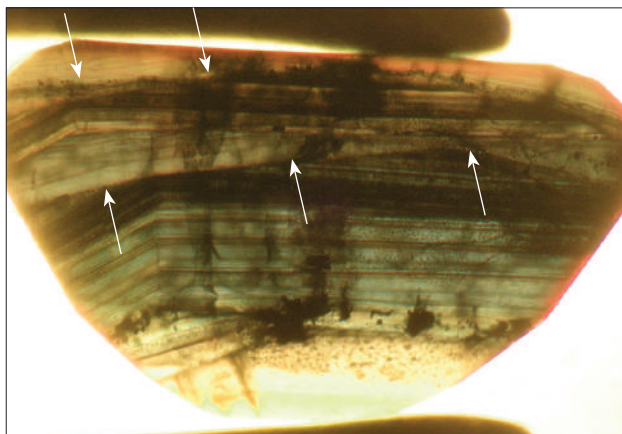


Figure 18: A faceted type 2 synthetic emerald grown in Bitterfeld shows a natural colourless seed (bottom) and multiple layers of synthetic emerald. Growth and colour zoning are seen parallel to prism faces. Between different growth cycles, impure material was removed and a new surface was prepared for subsequent crystal growth. Such surfaces, indicated by arrows, do not exactly follow the morphology of the synthetic emerald crystal. Immersion, field of view 4.2×3.1 mm; photomicrograph by K. Schmetzer.

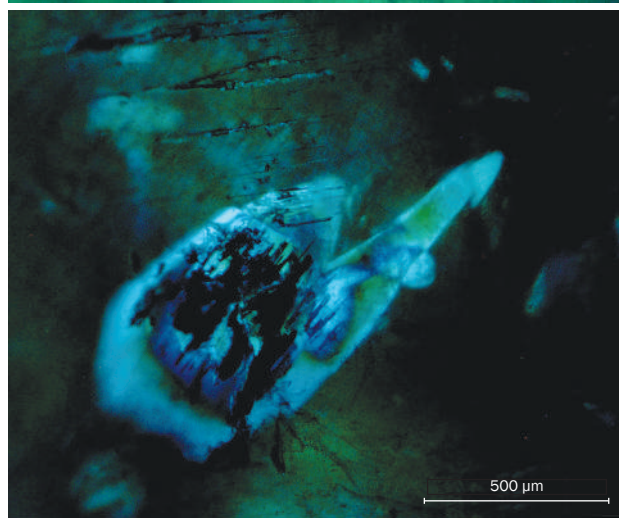
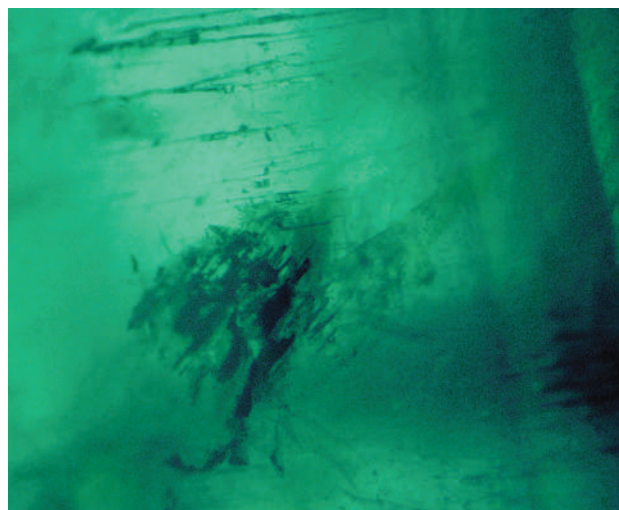


Figure 19: At higher magnification, the type 2 synthetic emerald shown in Figure 18 displays inclusions of small birefringent synthetic emerald crystals. These inclusions were generated by spontaneous nucleation and are heavily included with various forms of residual flux. Top—transmitted light; bottom—transmitted light with crossed polarizers; photomicrographs by H. A. Gilg.

results demonstrated that the crystal grew freely in different directions before becoming attached to the platinum net.

EDXRF chemical analyses performed in Berlin of samples still attached to the platinum net revealed the primary colour-causing elements, Cr and Ni, and the main component of the flux, Mo. The characteristic X-ray lines for Y also were evident in those samples. Analyses of the crystal cluster in Munich and Berlin gave identical results (Figure 15). Surprisingly, the single crystal showing identical habit and with wires of the platinum net still attached did not show any Y signal (again, see Figure 15).

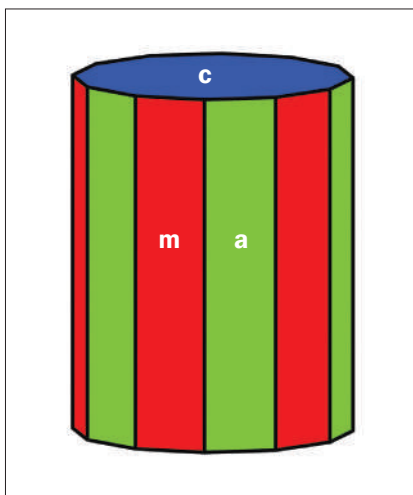


Figure 20: On the left, this type 3 synthetic emerald crystal ($8.4 \times 7.2 \times 6.8$ mm; 3.68 ct) was produced by IG Farben at Bitterfeld and is from the collection of the Museum für Naturkunde, Berlin. At the lower end, two included residual wires from a platinum net are seen. Photo courtesy of R.-T. Schmitt. On the right, a clinographic projection shows the typical crystal habit of the synthetic emeralds grown from Mo-bearing fluxes by IG Farben in Bitterfeld. The idealized drawing shows two hexagonal prism faces, **m** and **a**, as well as the basal pinacoid **c**. Drawing by K. Schmetzer.

Type 4: Refractive indices of the faceted samples were $n_o = 1.562\text{--}1.566$ and $n_c = 1.558\text{--}1.561$, yielding a birefringence of $0.004\text{--}0.005$. Specific gravity was $2.64\text{--}2.66$. These data are consistent with values given by Schmetzer and Kiefert (1998) for Igemerald, as well as with information generally reported for flux-grown synthetic emerald from various producers (see, e.g., Flanigen et al., 1967; Sinkankas, 1981; Henn, 1995).

Type 4 samples proved to be most prevalent amongst the research material. The 10 crystals from the Technische Universität Bergakademie Freiberg consisted of thick tabular plates or short hexagonal columns formed by a 12-sided prism and the basal faces (Figure 22). The one tabular crystal from the reference collection of the German Gemmological Association had a

Figure 22: These photos show some of the samples of type 4 Cr- and Ni-bearing synthetic emerald studied from the collection of the Technische Universität Bergakademie Freiberg. Top: Tabular plates or short prismatic crystals—the crystal in the upper row, centre, measures $8.6 \times 5.7 \times 3.8$ mm and weighs 1.62 ct. Bottom: Faceted samples; the largest at the upper left measures 13.5×7.6 mm and weighs 4.04 ct; shown for comparison is a Cr-bearing synthetic emerald crystal at the lower left from the early Chatham production measuring 5.2×3.6 mm and weighing 0.40 ct. The use of Ni in addition to Cr caused a somewhat more yellowish green coloration for the synthetic emeralds produced by IG Farben. Photos by K. Schmetzer.

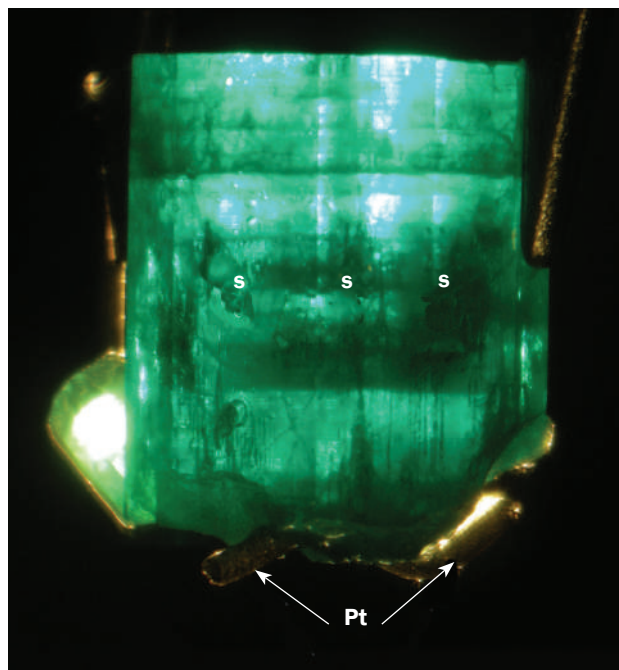


Figure 21: The type 3 synthetic emerald crystal depicted in Figure 20 (left) shows growth zoning parallel to the basal pinacoid and parallel to prism faces. In the centre of the crystal, a seed (s) of synthetic emerald is visible. The crystal was removed from the platinum net on which it grew, and residual wires (Pt) can be seen at the base of the sample. View perpendicular to the c-axis in transmitted fibre-optic light; photomicrograph by K. Schmetzer.

similar appearance (Figure 13, left). The basal faces were either rough (i.e. having remained unpolished after the last growth cycle) or polished. The polishing was likely undertaken to select samples either for further growth runs or for cutting. The faceted samples from the Technische Universität Bergakademie Freiberg, the Gübelin collection and the Berthold jewellery had all been cut with the c-axis perpendicular to the table facet and showed, in that direction of view, homogeneous colour with only small variations (Figure 22).

EDXRF chemical analyses obtained in Munich showed almost identical spectra in 18 of the 20 samples obtained from the Freiberg collection (Figure 15). One piece with a somewhat more intense green coloration gave a slightly higher Cr concentration, while one sample with a more yellowish green colour showed an increased Ni signal. Such consistency indicated that these Igemeralds were produced by means of a well-established growth process using a standard recipe for the composition of the flux and the ingredients of the nutrient. Compared to other synthetic emeralds without Ni, these faceted

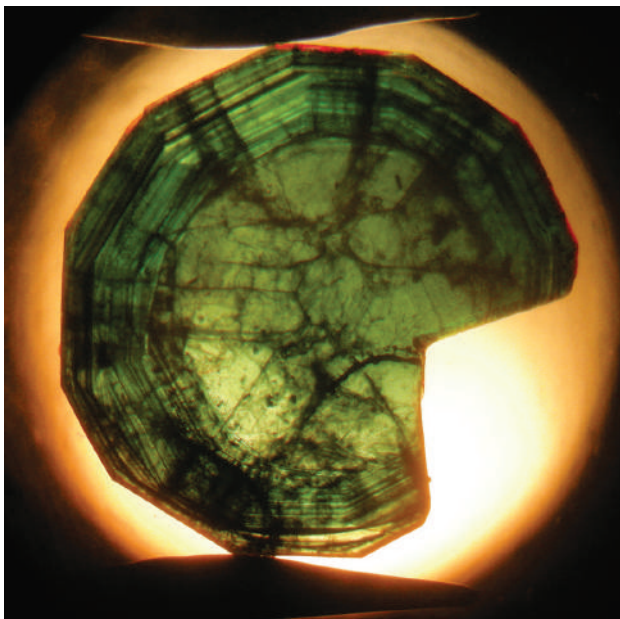


Figure 23: Growth zoning combined with colour zoning in a type 4 synthetic emerald crystal produced in Bitterfeld is seen parallel to first- and second-order prism faces. The diameter of the sample is approximately 14 mm. Immersion, view parallel to the c-axis in transmitted light; photomicrograph by K. Schmetzer.

Igmeralds were slightly more yellowish green and less bluish (Figure 22).

When viewed parallel to the c-axis, most rough and faceted type 4 samples showed primarily residual flux (see below), and only a few samples had growth structures parallel to the prism faces (Figure 23). The prismatic growth pattern clearly reflected the morphology of the rough samples, comprised of first- and second-order hexagonal prism faces (see Figure 20, right), but such prismatic growth zoning was seen only in one faceted sample (Figure 24). The results thereby

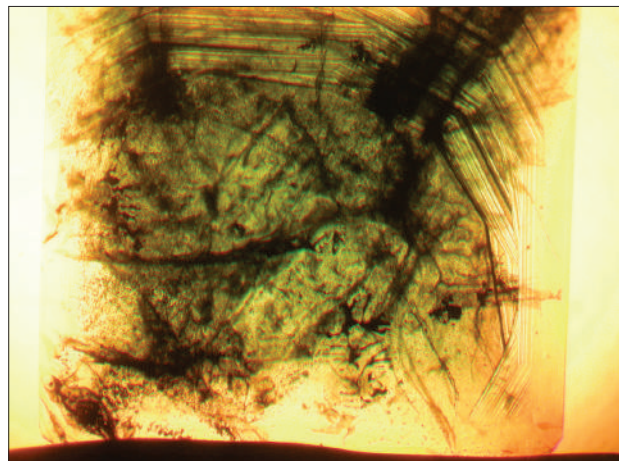


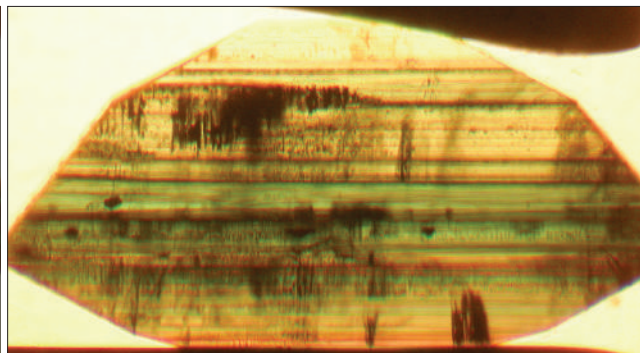
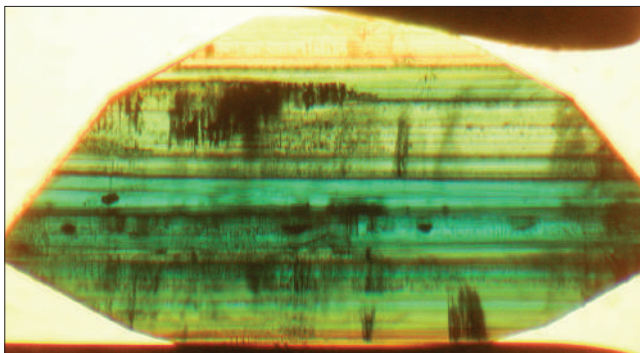
Figure 24: Growth zoning combined with colour zoning in a faceted type 4 synthetic emerald produced in Bitterfeld is seen parallel to first- and second-order prism faces. The sample was cut and polished between different growth cycles to remove impure areas. Immersion, view parallel to the c-axis in transmitted light, field of view 7.6 × 5.7 mm; photomicrograph by K. Schmetzer.

demonstrated that growth zones related to prism faces were mostly removed between the different growth cycles.

Viewed perpendicular to the c-axis, growth sectors parallel to the basal faces showed very intense growth and colour zoning with numerous layers. This was best seen in faceted samples in a view perpendicular to the table facet, since the preferred cutting style oriented the table at a right angle to the c-axis. The perpendicular view also revealed the distinct pleochroism of the samples, which was bluish green parallel to the c-axis and yellowish green perpendicular to the c-axis (Figure 25).

Most type 4 samples contained a few included synthetic emerald crystals that were oriented

Figure 25: Growth zoning combined with colour zoning in a type 4 synthetic emerald produced in Bitterfeld is seen parallel to the basal pinacoid. Pleochroism is observed in plane-polarized light parallel (left) and perpendicular (right) to the c-axis. The sample was cut and polished between different growth cycles to remove impure areas. Immersion, view perpendicular to the c-axis, field of view 3.6 × 2.7 mm; photomicrographs by K. Schmetzer.



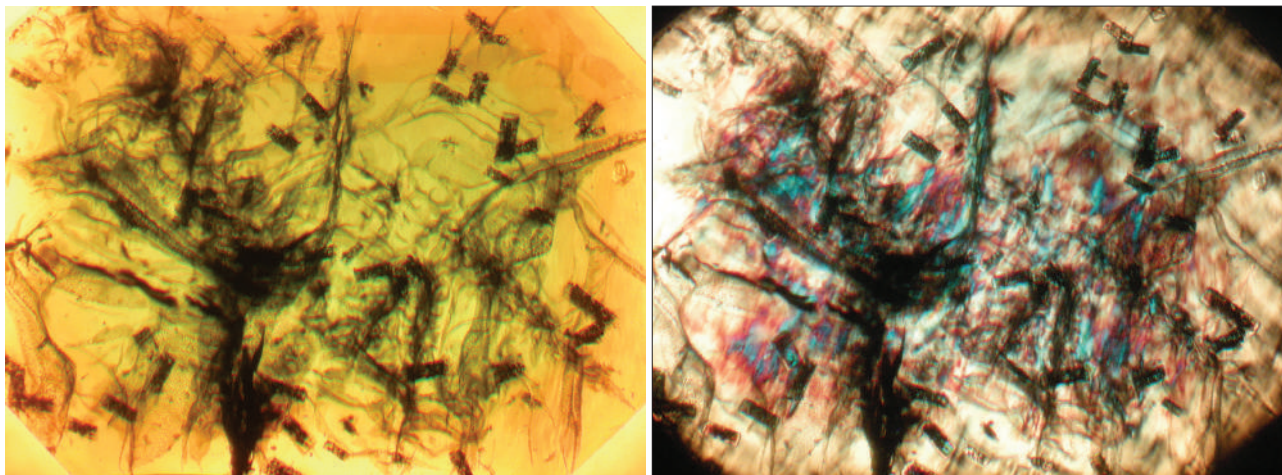


Figure 26: Numerous inclusions of tiny synthetic emerald crystals, grown by spontaneous nucleation, are present in this type 4 synthetic emerald grown in Bitterfeld (left); they are particularly evident under crossed polarizers (right). Immersion, view parallel to the *c*-axis, field of view 6.7 × 5.0 mm; photomicrographs by K. Schmetzer.

differently from the host. As noted above, such small prismatic crystals were formed by spontaneous nucleation. One sample in particular showed many of these tiny inclusions, which were best seen between crossed polarizers (Figure 26).

Small inclusions of birefringent phenakite crystals were occasionally seen. Such inclusions were identified by micro-Raman spectroscopy in a previous study (Schmetzer and Kiefert, 1998).

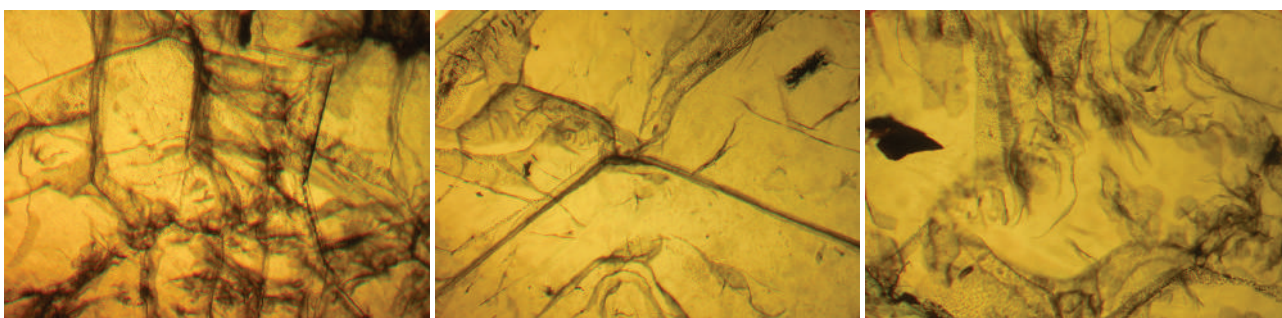
Residual flux was always present, mostly in the form of wispy veils, but occasionally as straight lines made up of numerous tiny particles (Figure 27). There were also instances where a cellular pattern of almost hexagonal structures could be seen (Figure 23). The different forms of residual flux showed net-like, interconnected structures or isolated particles of various shapes. Likewise frequent were phase boundaries between different components of the flux, as well as contraction bubbles (Figure 28). At higher magnification, the multiphase nature of the residual flux inclusions was clearly visible (Figure 29).

Discussion and Conclusions

The IG Farben internal documents, archived primarily in the Landesarchiv Sachsen-Anhalt, Abteilung Merseburg and at Kreismuseum Bitterfeld, disclosed various steps undertaken to develop emerald synthesis at the Bitterfeld facility. They also reflected the discrepancy between the intentions of IG Farben management, who hoped to create a process for cheap mass production, and the limitations of the synthesis technology ultimately realized.

Equally apparent was the divergence of opinion between factions within IG Farben. Among managers and scientists were many who wanted to commercialize production with a process protected by patent applications, while on the IG Farben board were a number of directors who decided that the synthetic emeralds should be used only for public relations activities. These various opinions arose because the process for synthesizing emerald by the flux technique applied at Bitterfeld was extremely

Figure 27: Various forms of residual flux are commonly seen in type 4 synthetic emeralds from Bitterfeld. Occasionally flux particles are concentrated along straight lines, forming a three-dimensional net-like or cellular pattern. Immersion, transmitted light, field of view 6.0 × 4.5 mm (left and centre) and 4.1 × 3.1 mm (right); photomicrographs by K. Schmetzer.



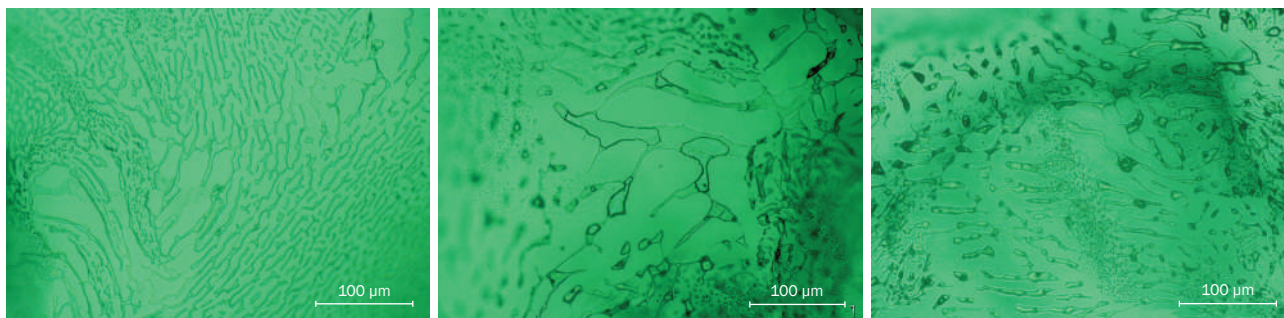


Figure 28: Residual flux in type 4 synthetic emeralds grown in Bitterfeld forms net-like patterns or isolated single dots. Transmitted light; photomicrographs by H. A. Gilg.

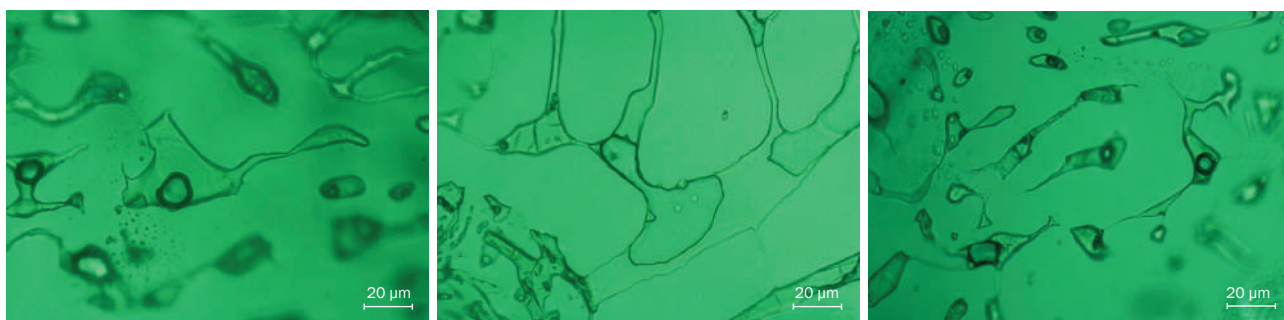


Figure 29: At higher magnification, residual flux inclusions in type 4 synthetic emeralds grown in Bitterfeld are seen as mostly multiphase inclusions consisting of different components of the flux and contraction bubbles. Transmitted light; photomicrographs by H. A. Gilg.

expensive, with lengthy production times (in the range of at least one year) required to grow crystals of facetable size. The resultant relatively high production cost and low monthly yield (~20 carats of faceted material) meant that the wholesale price to the trade would be substantial, yet the retail price for a synthetic material would need to be comparatively low. Traders had little incentive to place a product on the market with such minimal profitability.

Chemical analyses of samples grown by Wild around 1912 established that the crystals were produced in a Mo-bearing flux. That, in turn, indicated a growth method identical or similar to the technique applied by French scientists in the late 19th century. The synthetic emeralds grown by Hofmann in Berlin in the 1920s also were produced from a molybdate melt, and they bore many similarities with the small crystals obtained in Bitterfeld in the 1920s (see Figure 6).

The different types of synthetic emeralds (Table II) grown in Bitterfeld after the technological breakthrough in 1929 demonstrated the progressive development and improvement of seeding and production techniques. Colourless natural seeds used in early years were later replaced by tabular plates of synthetic emerald. Separation between the seeds and the silica

plates floating on top of the molybdate melt was first accomplished with a platinum net and then by a platinum baffle (see again Figure 8). With these changes in synthesis technology, the long prismatic habit of the synthetic emerald crystals (Figures 1, 7 and 20) changed to short prismatic or thick tabular (Figure 22). At the culmination, only single crystals were grown, eliminating both clusters of synthetic emeralds and attachment of the crystals to the platinum net.

Only the initial samples were grown with Cr as the sole colour-causing trace element; later samples always contained two transition metals, Cr and Ni. The chemistry of the latter thus parallels the data presented by Schmetzer and Kiefert (1998). However, it is worth mentioning that Espig added hexavalent chromium in the form of lithium chromate to the flux, and Cr needs to be trivalent to be incorporated into the beryl lattice and cause the desired green coloration of emerald. Thus, a change of the valence state of Cr in the complex flux system was necessary.

Chemical analysis also demonstrated use of yttrium oxide as a component of the nutrient in several synthetic emeralds (i.e. some from the collection of the Museum für Naturkunde in Berlin and one from the group examined by author KS

in the 1990s¹⁴). This addition of yttrium oxide finds historical corroboration both in Espig's 1946 list of ingredients and in his 1950s list of chemicals that would have to be purchased to re-start synthetic emerald production after World War II (see footnote 11).

Furthermore, the advantage to be gained by employing this additional ingredient as a colour-causing trace element was mentioned by Espig (1945). Nevertheless, a comparison of the samples obtained for this study that contained Y with those in which Y was not detected by EDXRF spectroscopy showed no colour difference. Therefore, the direct effect (if any) of Y on the colour of these synthetic emeralds is not clear.

Internal growth structures observed in the synthetic emeralds from different eras reflected the seeding technique applied and also showed—for faceted samples—the part of the crystal from which the synthetic gemstone was cut. In most faceted samples produced after the growth process was standardized in 1935, distinct growth and colour zoning was seen only parallel to the basal plane. Further growth planes parallel to the first- and second-order prism faces were present in just a small fraction of the samples examined.

Small prismatic synthetic emeralds were the most typical crystalline inclusion, consistent with previous descriptions (see, e.g., Eppler 1958a,b; Schmetzer and Kiefert, 1998). These inclusions were best seen between crossed polarizers. Birefringent phenakite crystals were another solid phase seen both in the present samples and in prior works.

In the current study, growth tubes—some with tiny birefringent crystals attached to their wider ends, so-called nail-head spicules—were found in only one sample with an irregularly shaped colourless seed.

Various forms of flux were present in all samples, frequently as multiphase inclusions containing contraction bubbles. Raman spectroscopy was used previously to identify these inclusions as components of the flux (e.g. polymolybdate and molybdenum trioxide; Schmetzer and Kiefert, 1998). Due to multiple devitrification processes

and chemical variability, residual flux in synthetic emerald can be complex and show numerous vitreous and crystalline constituents (Schmetzer et al., 1999).

IG Farben synthetic emeralds (Igemeralds) were the first synthetic emeralds to be produced in facetable sizes and released to the public. They became publicly known in 1935, and the history of their development, which spanned five decades of the 20th century during various political and economic conditions, is fascinating. At present, such synthetics are found as extreme rarities in a few private, public and university collections, as well as in reference and teaching collections of gemmological laboratories and associations. So, the possibility of encountering an Igemerald as an unknown sample for testing will be limited, but the description provided by this article—especially of the inclusions and chemical features—will help identify such samples.

References

- Anderson B.W., 1935. Igemerald—the German synthetic emerald. *The Gemmologist*, **4**(46), 295–300.
- Anonymous, 1935a. Synthetic beryl, with notes by Prof. Dr Karl Schlossmacher, B.W. Anderson and Georg O. Wild. *Gems & Gemology*, **1**(10), 281–286.
- Anonymous, 1935b. Synthetischer Smaragd. *Deutsche Goldschmiede-Zeitung*, **38**(6), 3–4.
- Bank H., 1965. Die Smaragdsynthese von Hermann Wild 1912. *Zeitschrift der Deutschen Gesellschaft für Edelsteinkunde*, No. 51, 43–47.
- Bauer M., 1909. Über künstliche Edelsteine. *Zeitschrift für Angewandte Chemie*, **22**(45), 2177–2181, <http://dx.doi.org/10.1002/ange.19090224502>.
- Bellatreccia F., Della Ventura G.D., Piccinini M. and Grubessi O., 2008. Single-crystal polarized-light FTIR study of an historical synthetic water-poor emerald. *Neues Jahrbuch für Mineralogie, Abhandlungen*, **185**(1), 11–16, <http://dx.doi.org/10.1127/0077-7757/2008/0115>.
- Berthold K.B., 1935. Über den synthetischen Smaragd (Igemerald) und seinen Wert. *Deutsche Goldschmiede-Zeitung*, **38**(25), 244–245.
- Brauns R., 1913. Schmucksteine. Künstliche Schmucksteine. In E. Korschelt, G.E. Linck, F. Oltmanns, K. Schaum, H.T. Simon, M. Verworn and E. Teichmann, Eds., *Handwörterbuch der Naturwissenschaften*, Verlag von Gustav Fischer, Achter Band, Jena, Germany, 963–970.
- Brauns R., 1936. Synthetischer Smaragd aus dem Jahre 1912. *Deutsche Goldschmiede-Zeitung*, **39**(19), 197–198.
- Cannawurf C., 1964. Die Frühgeschichte der Smaragdsynthese. *Zeitschrift der Deutschen*

¹⁴ A re-examination of the X-ray fluorescence diagrams for Igemerald recorded in the late 1990s by Schmetzer and Kiefert (1998) showed that one of the faceted synthetic emeralds (0.48 ct) from the collection of the late E. Gübelin displayed the characteristic Y line in the 15 keV range (see Figure 15).

- Gesellschaft für Edelsteinkunde*, No. 46, 7–11.
- Conradt O., 1959. Hermann Wild und seine Edelstein-Synthese. *Heimatkalender des Landkreises Birkenfeld*, **1959**, 93–97.
- Diehl R., 1977. Neues zum Thema “Synthetischer Smaragd”: Besuch bei Pierre Gilson. *Zeitschrift der Deutschen Gemmologischen Gesellschaft*, **26**(2), 61–75.
- Doelter C., 1909. Über die Einwirkung von Radium- und ultravioletten Strahlen auf die Mineralfarben. *Monatshefte für Chemie und verwandte Teile anderer Wissenschaften*, **30**(2), 179–229, <http://dx.doi.org/10.1007/BF01518117>.
- Doelter C., 1913. Neuere Darstellungen künstlicher Edelsteine. *Die Naturwissenschaften*, **1**(46), 1107–1110, <http://dx.doi.org/10.1007/bf01493156>.
- Doerner L., 1929. Edelsteine, künstliche. In F. Ullmann, Ed., *Encyklopädie der Technischen Chemie*, 2. Auflage, 4, Urban & Schwarzenberg, Berlin, Germany, 118–137.
- (Dreibrodt O., 1914.) Verfahren und Apparat zur Züchtung großer Kristalle durch Kristallisation in Bewegung aus Lösungen und Schmelzflüssen. German Patent DE 273 929, assigned to Elektrochemische Werke GmbH, 12 May.¹⁵
- Dreibrodt O., 1920. Method of and Apparatus for Forming Large Crystals. U.S. Patent 1353571 A, assigned to Elektrochemische Werke GmbH, 21 September.
- Dreibrodt O., Espig H. and Strauss D., 1923. Verfahren zur Herstellung grüner Korunde von epidotähnlicher Färbung. German Patent DE 385 374, assigned to Elektrochemische Werke GmbH, 23 November.
- Dreibrodt O., Espig H. and Strauss D., 1924. Verfahren zur Herstellung smaragdähnlich grüner Korunde. German Patent DE 390 794, assigned to Elektrochemische Werke GmbH, 23 February.
- Eppler W.F., 1935. Der synthetische Smaragd. *Deutsche Goldschmiede-Zeitung*, **38**(15), 144–146.
- Eppler W.F., 1936. Neue Untersuchungen an synthetischen Smaragden. *Deutsche Goldschmiede-Zeitung*, **39**(21), 215–217.
- Eppler W.F., 1958a. Synthetic emerald. *Journal of Gemmology*, **6**(8), 360–369, <http://dx.doi.org/10.15506/jog.1958.6.8.360>.
- Eppler W.F., 1958b. Synthetischer Smaragd. *Deutsche Goldschmiede-Zeitung*, **56**(4–7), 193–197, 249–251, 327–329, 381–385.
- Eppler W.F., 1961. Herbert Smith memorial lecture. *Journal of Gemmology*, **8**(3), 88–95, <http://dx.doi.org/10.15506/jog.1961.8.3.88>.
- Espig H., 1930. Die Smaragdsynthese. Internal report, Kreismuseum Bitterfeld, file SE 16, June, 21 pp.
- Espig H., 1935. Der synthetische Smaragd. *Zeitschrift für Kristallographie*, **92**, 387–391, <http://dx.doi.org/10.1524/zkri.1935.92.1.387>.
- Espig H., 1945. Die Herstellung des synthetischen Smaragds. Internal report, private property of K.-D. Heinrich, October, 5 pp.
- Espig H., 1946. Versuch einer Smaragdsynthese. Internal report, Kreismuseum Bitterfeld, file SE 10, February, 4 pp.
- Espig H., 1960. Die Synthese des Smaragds. *Chemische Technik*, **12**(6), 327–331.
- Espig H., 1961. Die Synthese des Smaragds. *Deutsche Goldschmiede-Zeitung*, **59**(10), 660–663.
- Espig H., 1962. Die Synthese des Smaragds und einiger anderer Minerale. *Berichte der Geologischen Gesellschaft der DDR*, **7**, 464–475.
- Fischer W., 1955. Smaragd-Synthese. In W. Foerst, Ed., *Ullmanns Encyklopädie der Technischen Chemie*, 3. Auflage, 6. Band, Urban & Schwarzenberg, Munich, Germany, 246–248.
- Flanigen E.M., Breck D.W., Mumbach N.R. and Taylor A.M., 1967. Characteristics of synthetic emeralds. *American Mineralogist*, **52**(5–6), 744–772.
- Hautefeuille P. and Perrey A., 1888. Sur la reproduction de la phénacite et de l'émeraude. *Comptes Rendus Hebdomadaires des Séances de l'Académie des Sciences*, **106**, 1800–1803.
- Hautefeuille P. and Perrey A., 1890. Sur les combinaisons silicatées de la glucine. *Annales de Chimie et de Physique*, **6**(20), 447–480.
- Henn U., 1995. Edelsteinkundliches Praktikum. *Gemmologie: Zeitschrift der Deutschen Gemmologischen Gesellschaft*, **44**(4), 3–112.
- Hunt W.F., 1921. Notes and news: An apparatus for growing large crystals. *American Mineralogist*, **6**(5), 90.
- Jaeger M. and Espig H., 1935. Der synthetische Smaragd. *Deutsche Goldschmiede-Zeitung*, **38**(35), 347–349.
- Metzger W., 2000. Ein Goldschmied auf der Suche nach dem »Großdeutschen Stil«. *Kritische Berichte*, **28**(3), 70–86.
- Michel H., 1914. *Die künstlichen Edelsteine*. Verlag von Wilhelm Diebener, Leipzig, Germany, 109 pp.
- Michel H., 1915. Künstliche Edelsteine. *Schriften des Vereins zur Verbreitung naturwissenschaftlicher Kenntnisse*, **55**, 73–112.
- Michel H., 1927. Neues von Edelsteinen. *Verein zur Verbreitung naturwissenschaftlicher Kenntnisse*, **67**, 30–58.
- Michel H. and Riedl G., 1925. Die Auswertung der Absorptions- und Lumineszenzerscheinungen der Edelsteine zu ihrer Unterscheidung. *Annalen des Naturhistorischen Museums in Wien*, **38**, 169–173.

¹⁵ Inventors during this time were not mentioned in German patent documents. However, a comparison with the U.S. patent, and with numerous internal letters, shows this was Dreibrodt's invention.

- Miethe A., 1908. Künstliche Edelsteine. *Deutsche Goldschmiede-Zeitung*, **11**(1), 12–14.
- Mitteilungen der Wiener Mineralogischen Gesellschaft, 1909. Review of a presentation of A. von Loehr entitled: Deutsche Edelsteingesellschaft. *Tschermaks mineralogische und petrographische Mitteilungen*, **28**(1–2), 168–169.
- Nassau K., 1976a. Synthetic emerald: The confusing history and the current technologies. *Lapidary Journal*, **30**(1,2), 196–202, 468–492.
- Nassau K., 1976b. Synthetic emerald: The confusing history and the current technologies. *Journal of Crystal Growth*, **35**, 211–222, [http://dx.doi.org/10.1016/0022-0248\(76\)90172-x](http://dx.doi.org/10.1016/0022-0248(76)90172-x).
- Recker K., 1973. Zur künstlichen Herstellung von Schmucksteinen. *Zeitschrift der Deutschen Gemmologischen Gesellschaft*, **22**(4), 145–178.
- Rühle C., 1952. Footnote about Igemerald. *Deutsche Goldschmiede-Zeitung*, **50**(11), 322.
- Schiebold E., 1935. Vergleichende Untersuchungen an natürlichen und synthetischen Smaragdskristallen. *Zeitschrift für Kristallographie*, **92**(1–6), 435–473, <http://dx.doi.org/10.1524/zkri.1935.92.1.435>.
- Schmetzer K., 2002. More than 100 years of emerald synthesis. In G. Giuliani, M. Jarnot, G. Neumeier, T. Ottaway, J. Sinkankas and G. Staebler, Eds., *Emeralds of the World*, extraLapis English No. 2, Lapis International LLC, East Hampton, Connecticut, USA, 84–92.
- Schmetzer K. and Kiefert L., 1998. The colour of Igemerald: I.G. Farbenindustrie flux-grown synthetic emerald. *Journal of Gemmology*, **26**(3), 145–155, <http://dx.doi.org/10.15506/jog.1998.26.3.145>.
- Schmetzer K., Kiefert L. and Bernhardt H.-J., 1999. Multicomponent inclusions in Nacken synthetic emeralds. *Journal of Gemmology*, **26**(8), 486–500, <http://dx.doi.org/10.15506/jog.1999.26.8.487>.
- Sinkankas J., 1981. *Emerald and Other Beryls*, Chilton Book Co., Radnor, Pennsylvania, USA, 665 pp.
- Vaupel E., 2015. Edelsteine aus der Fabrik. *Technikgeschichte*, **82**(4), 273–302, <http://dx.doi.org/10.5771/0040-117x-2015-4-273>.
- Webster R., 1952. The secrets of synthetic emerald. *The Gemmologist*, **21**(252), 117–121.
- Webster R., 1955. The emerald. *Journal of Gemmology*, **5**(4), 185–221, <http://dx.doi.org/10.15506/jog.1955.5.4.185>.
- Webster R., 1958. Synthesis of emerald. *The Gemmologist*, **27**(328), 203–206.
- Wisniak J., 2014. Four brilliant students of Henri Sainte-Claire Deville. 3. Paul Gabriel Hautefeuille. *Educación Química*, **25**(E1), 258–266, [http://dx.doi.org/http://dx.doi.org/10.1016/s0187-893x\(14\)70566-x](http://dx.doi.org/http://dx.doi.org/10.1016/s0187-893x(14)70566-x).

The Authors

Dr Karl Schmetzer

D-85238 Petershausen, Germany
Email: SchmetzerKarl@hotmail.com

Prof. Dr H. Albert Gilg

Lehrstuhl für Ingenieurgeologie, Technische Universität München, D-80333 Munich, Germany

Prof. Dr Elisabeth Vaupel

Forschungsinstitut für Wissenschafts- und Technikgeschichte, Deutsches Museum München, D-80538 Munich, Germany

Acknowledgements

The authors are grateful to the following individuals and institutions for kindly loaning samples and for providing information used in this study: S. Fordemann, Herford, Germany; Dr V. Hammer, Naturhistorisches Museum, Vienna, Austria; Prof. G. Heide and M. Hagen, Technische Universität Bergakademie, Freiberg, Germany; K.-D. Heinrich, Sandersdorf, Germany; Dr U. Henn, German Gemmological Association, Idar-Oberstein, Germany; D. Jerusalem, Idar-Oberstein; S. Pick, Kreismuseum Bitterfeld, Bitterfeld, Germany; M. Schatz, Landesarchiv Sachsen-Anhalt, Merseburg, Germany; Dr R.-T. Schmitt, Museum für Naturkunde, Berlin, Germany; Prof. E. Schlatter, Nottuln, Germany; Prof. H. Vollstädt, Seddiner See, Germany; C. Weise, Munich, Germany; and Dr A. Zacke, Bonn, Germany. X-ray fluorescence spectra of three synthetic emeralds from the Museum für Naturkunde were recorded by Dr L. Hecht, Berlin.

MAYER M & WATT



Download the Mayer and Watt
App for iOS/Droid.

We Deal in inspiration...Naturally.

US#: 606.564.3400 | www.mayerandwatt.com

A Diamond with a Transient 2804 cm⁻¹ Absorption Peak

Jianjun Li, Chengxing Fan, Shuxiang Chen and Guihua Li

The National Gold & Diamond Testing Center (NGDTC) in Shandong, China, recently encountered a colourless 0.08 ct diamond with strong greenish blue phosphorescence in the DiamondView. Such phosphorescence is often found in HPHT-grown synthetic diamonds from Russia and China. However, the sample proved to be a near-type-IIa natural diamond with weak A and B centres and a subtle type IIb component detectable in the infrared spectrum. The DiamondPLus indicated 'Pass', confirming it was an untreated natural diamond. Notably, while the diamond phosphoresced, the infrared spectrum displayed a transient ~2804 cm⁻¹ absorption peak associated with boron. This is the first evidence of charge transfer at boron acceptors being directly linked to phosphorescence in diamond.

The Journal of Gemmology, 35(3), 2016, pp. 248–252, <http://dx.doi.org/10.15506/JoG.2016.35.3.248>
© 2016 The Gemmological Association of Great Britain

Introduction

In recent years, synthetic diamonds grown by chemical vapour deposition (CVD) and high-pressure, high-temperature (HPHT) techniques have been more commonly encountered in gem testing laboratories. Especially in the last two years, a considerable number of melee-size (less than 0.20 ct) synthetic diamonds have entered the Chinese market, and most are HPHT synthetics from China and Russia. Nearly all show greenish blue phosphorescence that is similar in colour to Sleeping Beauty turquoise. Therefore, when a parcel of melee diamonds undergoes screening at NGDTC, the first step is to separate for further testing those specimens showing this phosphorescence.

Phosphorescence is rare in most natural diamonds, although it is frequently observed in

type IIb stones, as well as in some that do not show the type IIb-related absorption at ~2800 cm⁻¹ in their infrared spectra. For the latter diamonds, the boron concentration is below the level of detection, so they are nominally type IIa diamonds (see, e.g., Eaton-Magaña and Lu, 2011).

Recently during routine testing, the NGDTC laboratory encountered a natural diamond with strong greenish blue phosphorescence. Further analysis demonstrated that this unique diamond showed different infrared spectral features before and after the disappearance of its phosphorescence.

Methods

The 0.08 ct round brilliant diamond was tested and graded by standard gemmological methods. Testing also was performed on the DiamondSure, DiamondView and DiamondPLus verification

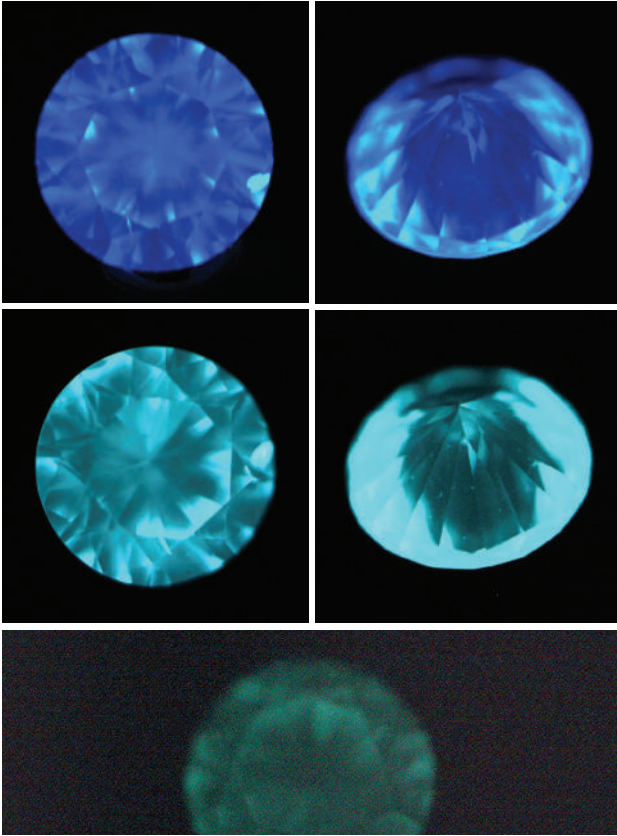


Figure 1: In the DiamondView, the 0.08 ct diamond displays vivid blue fluorescence (top) and strong slightly greenish blue phosphorescence (centre, as captured with the DiamondView's imaging system). When the hatch of the DiamondView was opened, greenish phosphorescence was visible to the naked eye (bottom). Images by Li Jianjun.

instruments manufactured by the International Institute of Diamond Grading & Research (IIDGR; De Beers Group of Companies). Ultra-violet-visible-near infrared (UV-Vis-NIR) spectroscopy was performed using a GEM-3000 instrument made by Biaoqi Scientific (China) Corp., and an integrating sphere was used to collect the internal reflectance spectra. (The incident light on the crown of a round brilliant diamond is internally reflected back through the crown by the pavilion facets, so the internal reflectance spectrum is a combination of reflection and transmission signals.) Fourier-transform infrared (FTIR) transmission spectra were collected using a Nicolet iS5 spectrometer with a Pike Technologies UpIR diffuse reflectance accessory, both during phosphorescence and after it disappeared. The spectra were scanned cumulatively four times while the diamond displayed phosphorescence and 32 times after the phosphorescence disappeared, and the resolution was set to 8 cm^{-1} .

Results

Standard Testing

The 0.08 ct diamond had a colour grade of F and clarity grade of SI₁ (due to a small brown feather). In addition, a small colourless transparent inclusion was visible at about 30×–40× magnification. The sample was inert to both long- and short-wave UV radiation.

Reactions to Verification Instruments

The DiamondSure indicated the sample was a type II diamond and referred it for further testing. The DiamondPlus showed 'Pass' when the sample was tested in liquid nitrogen.

In the DiamondView, the sample showed vivid blue fluorescence and strong phosphorescence in slightly greenish blue, but no strain pattern was visible (Figure 1). The phosphorescence lasted for a few seconds after the radiation source was turned off. Slightly greenish blue phosphorescence is often observed in synthetic diamonds in the DiamondView (D'Haenens-Johansson et al., 2015), so the sample was tested further to rule out a lab-grown origin.

UV-Vis-NIR Spectroscopy

The UV-Vis-NIR spectrum (Figure 2) displayed no significant absorption from 250 to 1000 nm, but it did show the strong 225 nm feature caused by the diamond energy bandgap at 5.47 eV.

Figure 2: The UV-Vis-NIR spectrum of the diamond shows strong absorption at 225 nm initiated by the diamond energy bandgap at 5.47 eV. The weak, broad absorption at 350 nm is likely an instrumental artefact.

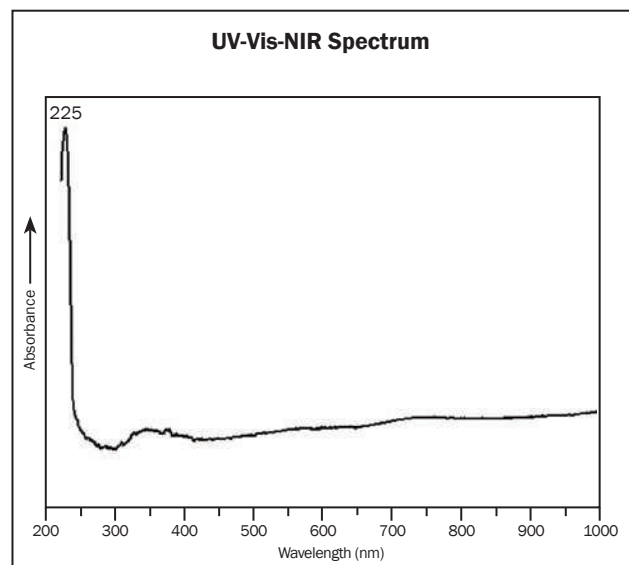
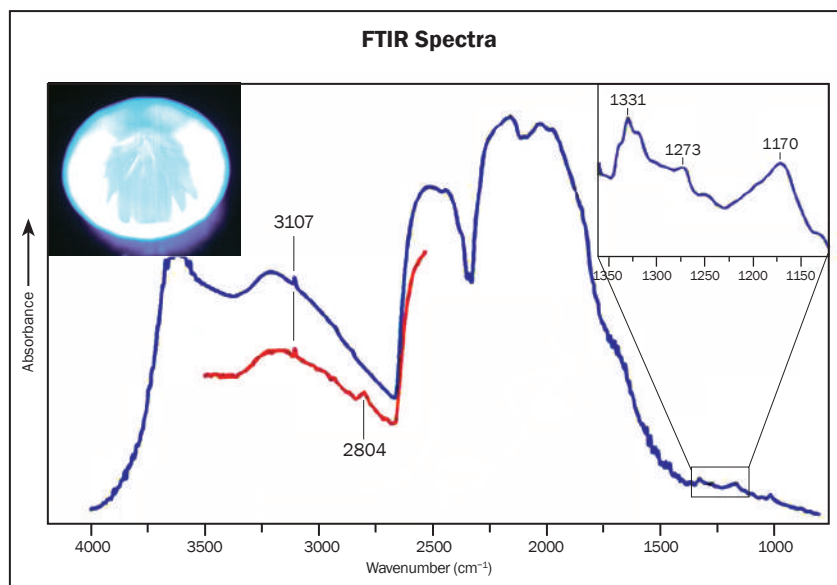


Figure 3: FTIR spectroscopy shows that the diamond is near type IIa with a 3107 cm^{-1} feature due to hydrogen; the weak bands at 1331 , 1273 and 1170 cm^{-1} (see inset) indicate the diamond also contains A and B centres and possibly N_s^+ (blue line). After the sample was excited using the DiamondView, it displayed strong greenish blue phosphorescence, and the resulting spectrum (red trace) shows an absorption peak at $\sim 2804\text{ cm}^{-1}$ related to neutral substitutional boron.



eV. A broad, weak absorption band centred at 350 nm may have been an instrumental artefact. There was no 270 nm absorption related to single nitrogen (Zaitsev, 2001). The absence of significant extrinsic absorption in the visible and ultraviolet regions suggested that the diamond is type IIa.

FTIR Spectroscopy

FTIR spectroscopy (Figure 3) confirmed that the sample was a near-type-IIa diamond. The spectra showed a sharp, weak band at 3107 cm^{-1} related to hydrogen (Woods and Collins, 1983; Field, 1992; Kiflawi et al., 1996; Goss et al., 2014). In the $1400\text{--}1100\text{ cm}^{-1}$ range (see Figure 3, inset), absorption bands were recorded at $1330/1331$, 1273 and 1170 cm^{-1} . These bands (and the 2804 cm^{-1} feature mentioned below) are usually reported as occurring at 1332 , 1282 , 1175 and 2803 cm^{-1} , respectively. As all these bands are very weak in this sample, the presence of noise might explain the apparent shift in the peak positions.

The absorption feature at 1273 cm^{-1} correlates to nearest-neighbour substitutional pairs of nitrogen (A centres), and the 1170 cm^{-1} band is attributed to nitrogen aggregates (B centres), that is, four nitrogen atoms symmetrically surrounding a vacancy. These spectral characteristics show that the diamond is natural in origin. The 1331 cm^{-1} peak is mostly related to B-centres (see, e.g., Breeding and Shigley, 2009) and/or might also indicate the diamond contains the positively charged state of the single substitutional

nitrogen centre (N_s^+). Therefore, the sample may be classified as near type IIa with a low IaAB component. Combined with the results of the DiamondPlus and the UV-Vis-NIR spectrum, the sample was confirmed as untreated natural diamond.

It is notable that while the diamond displayed phosphorescence, it showed a $\sim 2804\text{ cm}^{-1}$ absorption feature related to neutral substitutional boron (i.e. uncompensated boron: Collins and Williams, 1971; Fisher et al., 2009; Gaillou et al., 2012; D'Haenens-Johansson et al., 2014). To verify this phenomenon, we scanned the sample in the region $3500\text{--}2500\text{ cm}^{-1}$ after exciting it in the DiamondView until it displayed strong greenish blue phosphorescence. After the sample was removed from the DiamondView, the absorption spectrum was quickly measured using the diffuse reflectance accessory (Figure 3, red trace) while we could still see significant phosphorescence. According to the Omnic software, the scanning time was 3.95 seconds.

To obtain a higher signal-to-noise ratio, we attempted to accumulate eight scans of the phosphorescing diamond (Omnic software recorded a scanning time of 7.90 seconds), but we found that the $\sim 2804\text{ cm}^{-1}$ absorption feature had disappeared after about six or seven scans.

Repeated testing as described above (i.e. exciting the sample in the DiamondView and then collecting the FTIR spectrum by accumulating four to eight scans) confirmed that the $\sim 2804\text{ cm}^{-1}$ feature only lasted for a few seconds; as the phosphorescence disappeared, the absorption

band became extinct. Thus, the $\sim 2804\text{ cm}^{-1}$ feature was only recorded while the diamond phosphoresced (i.e. for about 4–8 seconds).

The current understanding of the phosphorescence process in diamond is in terms of a charge transfer between the boron acceptor and a deep donor (Watanabe et al., 1997), changing the charge state of boron from compensated to uncompensated and back again. There are other instances in which a short-lived charge-transfer effect has been observed in diamond, such as $\text{SiV}^{-/0}$ in highly silicon-doped CVD synthetic diamond (D'Haenens-Johansson et al., 2011). To our knowledge, however, this is the first record of a transient $\sim 2804\text{ cm}^{-1}$ absorption peak observable only during the process of phosphorescence. Compared with the 2803 cm^{-1} peak in the spectra of diamonds containing more boron, this is the most direct evidence of charge transfer at boron acceptors being immediately linked to phosphorescence in diamond.

Conclusions

A 0.08 ct round brilliant displaying greenish blue phosphorescence in the DiamondView was verified as a near-type-IIa natural untreated diamond of a mixed type that contained a low IaAB component and a IIB boron content near the detection limit of infrared spectroscopy. Infrared spectra recorded while the diamond phosphoresced displayed an absorption feature at $\sim 2804\text{ cm}^{-1}$ related to boron. This is the first instance of UV radiation inducing a characteristic IR absorption feature during phosphorescence in diamond. The specimen provides evidence that charge transfer (from negative to neutral) at boron acceptors is directly linked to phosphorescence in diamond.

References

- Breeding C.M. and Shigley J.E., 2009. The “type” classification system of diamonds and its importance in gemology. *Gems & Gemology*, **45**(2), 96–111, <http://dx.doi.org/10.5741/gems.45.2.96>.
- Collins A.T. and Williams A.W.S., 1971. The nature of the acceptor centre in semiconducting diamond. *Journal of Physics C: Solid State Physics*, **4**(13), 1789–1800, <http://dx.doi.org/10.1088/0022-3719/4/13/030>.
- D'Haenens-Johansson U.F.S., Edmonds A.M., Green B.L., Newton M.E., Davies G., Martineau P.M., Khan R.U.A. and Twitchen D.J., 2011. Optical properties of the neutral silicon split-vacancy center in diamond. *Physical Review B*, **84**(24), article 245208, 14 pp., <http://dx.doi.org/10.1103/PhysRevB.84.245208>.
- D'Haenens-Johansson U.F.S., Moe K.S., Johnson P., Wong S.Y., Lu R. and Wang W., 2014. Near-colorless HPHT synthetic diamonds from AOTC Group. *Gems & Gemology*, **50**(1), 30–45, <http://dx.doi.org/10.5741/gems.50.1.30>.
- D'Haenens-Johansson U.F.S., Katruscha A., Moe K.S., Johnson P. and Wang W., 2015. Large colorless HPHT-grown synthetic gem diamonds from New Diamond Technology, Russia. *Gems & Gemology*, **51**(3), 260–279, <http://dx.doi.org/10.5741/gems.51.3.260>.
- Eaton-Magaña S. and Lu R., 2011. Phosphorescence in type IIB diamonds. *Diamond and Related Materials*, **20**(7), 983–989, <http://dx.doi.org/10.1016/j.diamond.2011.05.007>.
- Field J.E., Ed. 1992. *The Properties of Natural and Synthetic Diamond*. Academic Press, San Diego, California, USA, 710 pp.
- Fisher D., Sibley S.J. and Kelly C.J., 2009. Brown colour in natural diamond and interaction between the brown related and other colour-inducing defects. *Journal of Physics: Condensed Matter*, **21**(36), 1–10, <http://dx.doi.org/10.1088/0953-8984/21/36/364213>.
- Gaillou E., Post J.E., Rost D. and Butler J.E., 2012. Boron in natural type IIB blue diamonds: Chemical and spectroscopic measurements. *American Mineralogist*, **97**(1), 1–18, <http://dx.doi.org/10.2138/am.2012.3925>.
- Goss J.P., Briddon P.R., Hill V., Jones R. and Rayson M.J., 2014. Identification of the structure of the 3107 cm^{-1} H-related defect in diamond. *Journal of Physics: Condensed Matter*, **26**(14), 1–6, <http://dx.doi.org/10.1088/0953-8984/26/14/145801>.
- Kiflawi I., Fisher D., Kanda H. and Sittas G., 1996. The creation of the 3107 cm^{-1} hydrogen absorption peak in synthetic diamond single crystals. *Diamond and Related Materials*, **5**(12), 1516–1518, [http://dx.doi.org/10.1016/s0925-9635\(96\)00568-7](http://dx.doi.org/10.1016/s0925-9635(96)00568-7).
- Watanabe K., Lawson S.C., Isoya J., Kanda H. and Sato Y., 1997. Phosphorescence in high-pressure synthetic diamond. *Diamond and Related Materials*, **6**(1), 99–106, [http://dx.doi.org/10.1016/s0925-9635\(96\)00764-9](http://dx.doi.org/10.1016/s0925-9635(96)00764-9).
- Woods G.S. and Collins A.T., 1983. Infrared absorption spectra of hydrogen complexes in type I diamonds. *Journal of Physics and Chemistry of Solids*, **44**(5), 471–475, [http://dx.doi.org/10.1016/0022-3697\(83\)90078-1](http://dx.doi.org/10.1016/0022-3697(83)90078-1).
- Zaitsev A.M., 2001. *Optical Properties of Diamond*. Springer, New York, USA, 502 pp., <http://dx.doi.org/10.1007/978-3-662-04548-0>.

The Authors

Jianjun Li

National Gold & Diamond Testing Center and Shandong Provincial Key Laboratory of Metrology and Measurement, Shandong Institute of Metrology, 28 Qianfoshandong Road, Lixia District, Jinan 250014, Shandong, China
Email: geoli@vip.sina.com

Chengxing Fan

National Jewellery Quality Supervision and Inspection Center of China, Fourth Floor South, West Building, Weiping Plaza, 2109 Cuizhu Road, Luohu District, Shenzhen 518020, Guangdong, China

Dr Shuxiang Chen

School of Material Science and Engineering, Qilu University of Technology, 3501 Daxue Road, Changqing District, Jinan 250353, Shandong, China

Dr Guihua Li

National Gold & Diamond Testing Center, 28 Qianfoshandong Road, Lixia District, Jinan 250014, Shandong, China

Acknowledgements

The authors thank three anonymous reviewers for their academic viewpoints. Jinda Song, CEO of Biaoqi Scientific (China) Corp., provided this interesting sample for identification.



TIM ROARK, INC.
FINE COLORED GEMSTONES

Offering Quality & Value Since 1974

ATLANTA, GA USA
info@trimportsatl.com 1.404.872.8937

ICA AGTA MJSA JBT SITA

JCK LAS VEGAS & AGTA TUCSON GEMFAIR

GemTalk is back!

Gem-A's popular online forum is back. Visit the new Gem-A website and login with your credentials. Once logged in you can start sharing knowledge and ideas, or simply introduce yourself.

Visit www.gem-a.com/forum/index

Conferences

Arizona Geological Society Presentations

On 3 May 2016, the Arizona Geological Society hosted two presentations in Tucson, Arizona, USA, that were of interest to gemmologists. **Dr Pete Modreski** of the U.S. Geological Survey in Denver, Colorado, USA, spoke on Colorado diamonds and gem-bearing pegmatites.

Colorado kimberlites are numerous, but only two have been commercially viable for diamond. First noted in the early 1900s as 'serpentine-olivine' intrusions, they were identified as diamond-bearing kimberlites in the 1960s by geologist Malcolm McCallum. While preparing thin sections of the rock, he noticed that the polishing wheel became gouged. Kelsey Lake became the best-known mine, operating between 1994 and 1997 as an open pit. Of particular note was a 28.3 ct rough diamond yielding a 5.39 ct yellow pear shape that reportedly sold for US\$100,000 in December 1996. The Sloan I and II kimberlites also were a source of gem-quality diamonds. Sloan I was mined as an open pit where the kimberlite broke the earth's surface, and Sloan II explored the pipe underground.

A processing mill was built on site utilizing heavy mineral separation, X-ray luminescence and a grease table to collect the diamonds. Diamond yield was 1/100 to 1/10 ct per tonne of ore.

Gem-bearing pegmatites are known for their large, well-formed crystals. In Modreski's home state of Colorado, the pegmatites of the Pikes Peak area commonly host amazonite, and this bluish green feldspar is sought primarily for mineral specimens. From adjacent areas in Colorado, aquamarine and topaz are mined for specimens and gem rough (e.g. Figure 1). Gem-quality tourmaline is rare in the state due to a lack of boron in the pegmatites. In general, from an economic standpoint, pegmatites rich in Li are important for commercial mining. Traditional scientific thought was that the large crystals in pegmatite dykes formed over many years or centuries. It is now believed that gem-bearing 'pockets' or cavities crystallize in a matter of days or weeks.

*Eric W. Fritz (EricFritz@gem-a.com)
Gem-A, Tucson, Arizona, USA*



Figure 1: Fine aquamarine and topaz crystals have been mined from pegmatites in Colorado, USA. The aquamarine cluster on the left is part of a larger matrix specimen with feldspar and smoky quartz from 'Diane's Pocket' at Mt Antero. The largest crystal is approximately 4 cm long, and the specimen (94 × 64 cm) is on display at the Denver Museum of Nature and Science. The topaz crystal on the right (approximately 6 cm wide) is from the 'Tribute Pocket' in the Pikes Peak area, and was collected by Rich Freterd and Jean Cowman. Photos by Pete Modreski.

35th International Geological Congress

This large quadrennial conference took place in Cape Town, South Africa, from 27 August to 4 September 2016, and attracted over 4,200 delegates from 115 countries. The programme included a session titled 'Gems: Bringing the World Together', and some additional gem-related presentations took place in other sessions. Gemmologically relevant talks and posters that were

seen by the author are summarized below. Several field excursions took place before and after the Congress, including one trip to various alluvial diamond deposits in South Africa (to be covered in a future issue of *The Journal*).

Considering the conference's location in South Africa, it is not surprising that diamonds were well re-



Figure 2: This thin slice of a Marange diamond (5.8 mm across) cut parallel to a cubic direction shows curved growth zones revealed by abundant graphite micro-inclusions in the cuboid sectors. Photo by Joshua Balduf/GIA.

presented in the programme. **Prof. Paolo Nimis** (University of Padova, Italy) described the pitfalls of using conventional two-phase thermobarometry of mineral inclusions to elucidate the pressure and temperature conditions of diamond formation, since the inclusions might not be in equilibrium with one another. He indicated that future developments in thermobarometric methods will allow scientists to refine their models of the vertical distribution of diamond formation in the sub-cratonic lithosphere. In another presentation, Nimis and co-authors documented for the first time hydrous silicic fluid films at the interface between solid inclusions and their gem-quality diamond hosts. These thin films were found around all types of mineral inclusions in both peridotitic and eclogitic diamonds, and suggest that they commonly form in the presence of H₂O-rich fluids. **Dr Alexander Proyer** (University of Botswana, Gaborone) proposed a mechanism for diamond formation in deep and relatively cool cratonic roots in which exsolution of Ti minerals (rutile or ilmenite) might create a localized reducing environment where oxidized carbon could undergo reduction and crystallize into diamond. **Dr Herwart Helmstaedt** (Queen's University, Kingston, Ontario, Canada) examined the interaction of diamond tectonic history and geotectonics during the formation of the earth's oldest diamonds in the Archean Eon. Peridotitic diamonds formed first (3.5–3.2 billion years ago) with the establishment of continental lithospheric roots, and subsequently eclogitic diamonds initially formed during the amalgamation and breakup of early continental nuclei (3.0–2.5 billion years ago).

Dr Katie Smart (University of the Witwatersrand, Wits, South Africa) and co-authors proposed that the oldest known diamonds—controversially inferred to have formed as early as 3.5 billion years ago, and recovered as a by-product of gold mining in the Witwatersrand Supergroup of South Africa—record an early Archean onset of plate tectonics.

Alluvial diamond deposits were the focus of various presentations. **Lyndon De Meillon** (Paleostone Mineral Consultants, Kimberley, South Africa) and his co-author described those along the Orange and Riet Rivers in the vicinity of Douglas, Northern Cape Province, South Africa. These areas are known for producing large high-value gem diamonds (generally US\$1,200–\$7,000 per carat) but have ultra-low grades. Strategies for the successful exploration of such deposits include detailed geological modelling and selective mining based on the geological controls of each specific occurrence. **Dr Mike C. J. de Wit** (University of Pretoria, South Africa, and Tsodilo Resources Ltd., Toronto, Ontario, Canada) reported recent research on alluvial diamond 'runs' in the Lichtenburg-Ventersdorp area of North West Province, South Africa. It is inferred that the diamonds originated from local sources and were redeposited in the alluvial runs by proximal eskers (glacial tunnels) that were active during the final stages of the Carboniferous-age Dwyka glaciation. The same deposits also were described by **Pieter Bosch** (Council for Geoscience, Pretoria, South Africa), who noted that the gravel runs are associated with karstic features in the dolomite basement rock, and that Dwyka glacial tillite sediments are closely associated with the diamondiferous gravels. **Dr Gabriele Schneider** (Namibian Uranium Institute, Swakopmund) chronicled the history of diamond mining in Namibia, from the April 1908 discovery of a diamond near Kolmanskop in the Namib Desert to modern marine operations exploiting offshore deposits using large and sophisticated mining vessels.

Other presentations focused on the properties and characteristics of diamonds. **Dr Karen Smit** (Gemological Institute of America, New York, New York, USA) and co-authors examined the preservation of unaggregated nitrogen (C centres) in yellow type Ib diamonds from the Zimmi alluvial deposit in Sierra Leone. Multiple lines of evidence suggest that after their formation in the root of the West African craton, the diamonds were rapidly exhumed to shallower depths by tectonic uplift following continental collision associated with the assembly of Gondwana. In another talk, Smit and co-authors described mixed-habit (octahedral and cuboid) diamonds from Marange in eastern Zimbabwe. The crystals contain abundant micro-inclusions of methane within the cuboid sectors, along with graphite micro-inclusions that reveal the curved growth zones in

transmitted light (e.g. Figure 2). Isotopic analyses suggest that diamond growth occurred under non-redox (reduction–oxidation reaction) conditions from cooling $\text{CH}_4\text{-CO}_2$ hydrous fluids. **Susan Foulkes** (Mintek, Randburg, South Africa) and her co-author studied nine diamond parcels from two different alluvial mining areas in the Central African Republic. LA-ICP-MS trace-element analysis and Fourier-transform infrared spectroscopy enabled them to tentatively separate the diamonds from the two localities, although more samples need to be analysed to make the database more robust. **Aparajita Bhattacharya** (Geological Survey of India, Kolkata) and co-authors examined diamonds from Panna belt in Madhya Pradesh, India. Morphological and Raman spectroscopic characteristics were consistent with an eclogitic affinity for some of the diamonds and a deep mantle origin for others.

Presentations related to coloured stones covered a wide range of gem materials. **Prof. Bruce Cairncross** (University of Johannesburg, South Africa) reviewed gems from the southern Africa subcontinent: amethyst, aquamarine, chrysoberyl (including alexandrite), diamond, emerald, hydrogrossular, jeremejevite, several quartz gem varieties, spessartine, tiger's-eye, topaz and tourmaline (e.g. Figure 3). **Stephen Harris** (University of New South Wales, Sydney, Australia) and co-authors studied an alluvial ruby-sapphire suite from the New England gem field, New South Wales, Australia. The unusual presence of rubies in this assemblage may be explained by magmatic interactions with Cr-bearing mafic-ultramafic rocks during corundum formation at depth, prior to transport of the xenocrysts to the earth's surface in alkali basalts. In another presentation, Harris and co-authors examined the origin of alluvial sapphires from the Orosmayo region, Sierra de Rinconada, Jujuy Province, north-west Argentina. The small transparent pebbles of colourless to blue sapphire contain a bimodal inclusion suite, suggesting that they formed through metasomatic exchange between a carbonatitic and an evolved felsic source. The sapphires were then transported to the surface as xenocrysts in lamprophyre dykes. **Kandy Wang** (University of New South Wales, Sydney, Australia) and co-authors reported on cabochon-quality rubies hosted by actinolite schist in the Paranesti region of north-eastern Greece. Oxygen isotope values of the rubies are extremely low ($\delta^{18}\text{O} \sim 1\%$), identical to seawater, suggesting a potential subduction zone genetic environment. **The author** (BML) described modern mining of primary and secondary gem deposits in Mogok, Myanmar (see Gem Notes in *The Journal*, **34**(5), 2015, 387–390). **Jullieta Lum** (University of Johannesburg, South Africa) and co-authors obtained chemical analyses of beryls of various colours (blue to green, yellow and colourless) from miarolitic cavities in the Erongo Mountains of Namibia. In general, the

samples had major- and trace-element contents similar to those of aquamarine from worldwide localities, with no distinctive locality-specific characteristics. **Dr Le Huong** (Vietnam National University Hanoi) and co-authors performed femtosecond LA-ICP-MS analysis of danburite from Tanzania (dark yellow), Mexico (colourless) and Vietnam (light yellow). Samples from the three localities could be separated by various trace elements (i.e. Be, Ti, Mn, Ni, As, Sr and Y), and the content of light rare-earth elements was greatest in the dark yellow danburite. **Dr Ian Graham** (University of New South Wales, Sydney, Australia) and co-authors studied deep green cabochon-quality viridine (Mn-andalusite) from Thassos Island in northern Greece. The viridine is associated with piemontite and other Mn-bearing silicates of the epidote group. **Sonwabile Rasmeni** (Mintek, Randburg, South Africa) and co-authors described the mining and beneficiation of gem materials in the Northern Cape Province of South Africa. The various resources include 'red aventurine' (quartzite with pink Mn- and Fe-rich muscovite) from Pella, rose quartz from Riemvasmaak and Kakamas, tiger's-eye from Prieska, and green fluorite from Riemvasmaak. **Dr João Reynolds Marques** (Gondwana – Exploration and Mining Consultants Ltd., Maputo, Mozambique) and co-authors examined the regional distribution of granitic pegmatites in the Zambézia Province of Mozambique. The most important pegmatites for gem production include LCT (lithium, cesium,

Figure 3: Southern Africa is an important source of various gem varieties, such as those shown here that were faceted by Massimo Leone. Top row: citrine from Zambia (11.06 and 16.88 ct). Next row: greenish blue tourmaline (8.72 ct), aquamarine (8.62 ct) and pink tourmaline (8.72 ct) from Mozambique. Next row: greenish yellow tourmaline (2.21 ct) and spessartine (3.74 ct) from Zambia, and greenish blue tourmaline (1.73 ct), purplish pink tourmaline (1.70 ct) and greyish green tourmaline (2.85 ct) from Mozambique. Bottom row: spessartine from Namibia (1.81 and 1.64 ct). Photo by Bruce Cairncross.



tantalum)-type dykes in the Alto Ligonha District for tourmaline, and NYF (niobium, yttrium, fluorine)-type bodies of the Nampula Complex for dark blue aquamarine. **Prof. Olugbenga Okunlola** (University of Ibadan, Nigeria) and co-authors mapped Precambrian rare-metal (Ta-Nb-Sn) granitic pegmatites in south-western Nigeria, some of which contain gem mineralization. They designated 10 pegmatite subfields, and geochemical data from muscovite suggests that those of Lema-Ndeji show the highest potential for economically significant rare-metal mineralization.

There were two talks related to instrumentation. **Dr Anton Du Plessis** (Stellenbosch University, South Africa) and co-authors reported applications of X-ray computed microtomography for faceted diamonds and coloured stones. The method can be used to visualize internal and external features of gemstones, and the full three-dimensional dataset is recordable to provide

a unique identifier for insurance purposes. **Nicolaas Steenkamp** (geological consultant, Pretoria, South Africa) and his co-author investigated the use of electric pulsed-power disaggregation using a Russian-made selfFrag instrument to break down massive pegmatite, potentially liberating gem-quality garnet and tourmaline. Pegmatite samples from the Limpopo Province of South Africa were submerged in water and subjected to high-voltage discharges, causing them to be fragmented along pre-existing fractures as well as mineral grain boundaries. Due to the fractured nature of the minerals in the pegmatite, the experiments produced ~30% grains measuring <1 mm (i.e. powder), while ~70% consisted of >1 mm pieces that were not completely liberated along the grain boundaries.

The next International Geological Congress will take place in March 2020 in Delhi, India.

Brendan M. Laurs

Letters

Digital Manipulation of Gem Photos—Author's Reply

In *The Journal of Gemmology* (Vol. 35, No. 2, 2016, p. 162), a letter by Grenville Millington addressed the caption of the lead figure that appeared in my article 'Oriented Inclusions in Cat's-eye, Star and Other Chrysoberyls' published in *The Journal* (Vol. 35, No. 1, 2016, pp. 28–54). In summary, Mr Millington concluded that any "manipulation" of digital photos should be indicated in the corresponding figure caption. I disagree with this statement.

When photos of gems are taken with modern digital cameras, certain types of stones (e.g. rubies or sapphires) frequently yield images that closely approximate the visual appearance of the gem to the human eye. This stands in stark contrast to the results of digital photography involving colour-change gemstones such as alexandrites or some garnets, even if the camera has been calibrated against a white standard for the actual lighting used. For such stones showing a different colour appearance in daylight and incandescent light, what is obtained in the digital photo most often does not match the visual impression of the sample. After many attempts, I have been fortunate on occasion to have the photo of a colour-change stone under one of the two relevant light sources appear close to what is actually seen with the eye, but rarely can this be achieved for both light sources. In most cases the results of such efforts, or at least some results, are highly disappointing.

Thus, I normally select the photo 'closest' in appearance to the actual gemstone and then adjust this digital

image to attain as nearly as possible the real impression of the stone, having the sample, the computer screen and different light sources available on my desk. For my alexandrite book (*Russian Alexandrites*, 2010), a pre-print of all photos representing colour and colour change of 'critical' samples was even prepared in a paper version, enabling the colour of the paper pre-print to be corrected against the real gem. Such a procedure is, however, as a practical matter infeasible for articles in gemmological journals, simply for cost reasons.

I had the chance to examine in Germany some years ago the cat's-eye alexandrite mentioned above and depicted in *The Journal* (Vol. 35, No. 1, 2016, p. 29). The photo of that stone in its jewellery setting taken by Erica and Harold Van Pelt reportedly was carefully adjusted in the USA by modern digital techniques to match the actual impression of the gem in daylight and incandescent light. I consider such colour adjustment to be not a "manipulation" but rather a normal part of modern digital photography or digital processing of existing photos, what I would call 'state of the art' in modern publication technology. Therefore, I do not think that it is necessary to mention such colour adjustment in figure captions. Rather, digital adjustment should be indicated only if the appearance of a sample in the photo has been shifted toward a colour ('beautified') which, for whatever reason, is not consistent with the true coloration and visual appearance of the gemstone.

*Dr Karl Schmetzer
Petershausen, Germany*

Gem-A Notices

ANNUAL GENERAL MEETING

The Annual General Meeting of the Gemmological Association of Great Britain was held on 9 September 2016 at the Goldsmiths' Centre, 42 Britton Street, London EC1M 5AD. Nigel Israel chaired the meeting and welcomed those present.

Hazlems Fenton were re-appointed auditors for the year.

The Council had nominated the international organics expert Maggie Campbell Pedersen for the office of President and the nomination was unanimously carried. The outgoing President, Harry Levy (who could not be present), was thanked for his support and commitment to Gem-A during his four years in office.

Kathryn Bonanno and Nigel Israel retired from the Council in rotation and being eligible offered themselves for re-election. Nominations also were received from Ronnie Bauer and Starla Turner. There were only two places vacant on the Council and following a poll vote Kathryn Bonanno and Nigel Israel were re-elected. Mary Burland retired in rotation and did not seek re-election.

The meeting was followed by a brief address from the new CEO Alan Hart who spoke of his Natural History Museum background, his long association with, and support for, Gem-A, and his initial thoughts on the Association's growth and development.



The newly elected President, Maggie Campbell Pedersen.

MEMBERSHIP

At a meeting of the Council held on 30 June 2016, the following were elected to membership. Also Diploma graduates of the examinations held in January 2016 (to be published in the **35**(4) 2016 issue of *The Journal*) were elected or transferred to Fellowship and/or Diamond Membership as appropriate.

Fellowship

Hou Fei-Feng, *Taipei, Taiwan, R.O. China*
 Khabrieva, Dilyara, *London*
 Li Meng, *Montreal, Quebec, Canada*
 Qin Yu Song, *Changyi, Jilin, P.R. China*
 Tan Yu, *Ningbo, Zhejiang, P.R. China*
 Xu Qian, *Huainan, Anhui, P.R. China*
 Zhang Rui, *Beijing, P.R. China*

Associate Membership

Fairclough, Philippa, *Swindon, Wiltshire*
 Gagnon, Luc, *Lasalle, Quebec, Canada*
 Nasim-Brittan, Natalie, *Canterbury, Kent*

Sapora, Raul, *Velletri, Rome, Italy*
 Vahman, Sarira, *Oxford, Oxfordshire*

At a meeting of the Council held on 9 September 2016, the following were elected to membership:

Fellowship

Woodmansterne, Chloë, *St Albans, Hertfordshire*

Associate Membership

Khourie, Kaylan, *Guateng, South Africa*
 Vasseur, Chantal, *Rixensart, Belgium*
 Durand, Jennifer, *Burton-on-Trent, Staffordshire*
 Pulese Aulehla, Herbert, *London*

GIFT TO THE ASSOCIATION

The Association is most grateful to the following for his gift for research and teaching purposes:

Valerio Zancanella of Cavalese, Trentino, Italy, for a faceted hyalite opal from Mexico weighing 0.16 ct.

EXTRAORDINARY GENERAL MEETING

On Thursday 30 June 2016 at Gem-A, 21 Ely Place, London EC1N 6TD, an Extraordinary General Meeting was held for the purpose of considering the following Special Resolution to amend the Articles of Association (changes and additions in *italics*):

Termination of Membership

4 Membership is terminated if:

- (3) any sum due from the member to the Charity is not paid in full within six months of it falling due, *except that the Council may by Bylaw(s) establish the period, not less than two months of it falling due, that a Member may be in subscription arrear before being deemed to have resigned from Membership.*

Notice of general meetings

7 (1) The minimum periods of notice required to hold a general meeting of the Charity are:

- *eighty-four clear days for the date of an Annual General Meeting*

Directors

20 *Unless determined otherwise by ordinary resolution:*

- (1) *The number of Elected or Co-opted Directors shall be not less than four [see Articles 26, 27 and 29(1)] and the number of Appointed Directors, who need not be members of the Charity, shall not be more than three [see Article 29(2)].*
- (2) *The total number of all Directors shall not exceed twelve.*

Retirement

24 At the first Annual General Meeting all the Council must retire from office unless by the close of the meeting the members have failed to elect sufficient Council to hold a quorate meeting of the Council. At each subsequent Annual General Meeting one-third of the *elected* Council or, if their number is not three or a multiple of three, the number nearest to one third must retire from office.

- (1) The *elected* Directors to retire by rotation shall be those who have been longest in office since their last *election*. If any Directors became or were appointed Directors on the same day, those to retire shall (unless they otherwise agree among themselves) be determined by lot.
- (2) *Elected Directors shall normally serve no more than three consecutive three-year terms, but may serve further terms upon recommendation of the Council.*
- (3) If a Director is required to retire at an Annual General Meeting by a provision of these articles, the retirement shall take effect upon the conclusion of the meeting.

The Election of Directors

26 The Charity may by ordinary resolution in any general meeting:

- *elect a person who is willing to act as a Director providing he is recommended by the Council, and*

27 No person other than a Director retiring by rotation may be *elected* a Director at any general meeting unless:

- (1) He is recommended for election by the Council;
- (2) If not recommended by the Council then at an Annual General Meeting only providing that: *Not less than forty-two clear days or more than seventy clear days before the date of the meeting, the Charity is given notice in writing that: A Fellow (FGA) and/or Diamond Member (DGA) who has been an FGA and/or DGA in good standing for a minimum of the two most recent whole subscription years has been nominated for election to the Council, by two nominators who both have been either Fellows and/or Diamond Members in good standing for a minimum of the most recent whole subscription year; or Associate Members in good standing for the two most recent whole subscription years.*

The written nomination must:

- (a) be signed by the *Nominators*;
- (b) state the *Nominators'* intention to propose the *election* of a person as a Director;
- (c) contain the details that, if the person were to be *elected*, the Charity would have to file at Companies House; and
- (d) be signed by the person who is to be proposed to show his willingness to be appointed.

28 All members who are entitled to receive notice of a general meeting must be given not less than seven *or more than twenty-eight clear days'* notice of any resolution to be put to the meeting to *elect* a Director other than a Director who is to retire by rotation.

29 (1) *The Council may co-opt a person who is a Member of the association to fill a casual vacancy or an extra Director who is willing to act as a Director, subject to the maximum number of Directors allowed. Co-opted members shall be appointed by Council and shall retire at the first General Meeting of the Association thereafter, but may offer themselves as candidates for election at that Annual General Meeting and shall not be taken into account in determining the Directors who are to retire by rotation.*

- (2) *In order that the Council may have an appropriate range of skills, it may, by resolution of two thirds of elected/co-opted Directors, appoint up to a further three Directors who need*

not be members of the Association. They shall serve a term up to the fourth Annual General Meeting following their appointment (or the third Annual General Meeting if appointed at an Annual General Meeting). They may serve further terms of three years at the request of the Council.

(3) *Appointed Directors may be removed by resolution of two thirds of elected/co-opted Directors.*

(4) *Nothing in these Rules shall require any person who is a Director at the date of adoption of these Rules to resign as a Trustee, or shall prevent such person offering themselves, if eligible, for re-election if retiring by rotation at an Annual General Meeting.*

30 *No election, co-option or appointment of Directors may cause the number of Directors to exceed the number fixed as the maximum number of Directors.*

Disqualification and removal of Directors

31 A Director shall cease to hold office if he:

- ceases to be a Director by virtue of any provision in the Act or is prohibited by law from being a director;
- is disqualified from acting as a Trustee by virtue of the Charities Acts;
- *ceases to be a member of the Charity unless an Appointed Director;*
- becomes incapable by reason of mental disorder, illness or injury of managing and administering his own affairs;
- resigns as a Director by notice to the Charity (but only if at least two *elected* Directors will remain in office when the notice of resignation is to take effect); or

- is absent without the permission of the Council from three consecutive meetings and the Council resolves that his office be vacated.

Proceedings of the Council

33 (1) *The Directors shall meet together for the despatch of business, adjourn, and otherwise regulate their meetings as they think fit, subject to the provision of the Articles. Such meetings may be held with one or more or all Directors participating by electronic communication if all the Directors so agree.*

34 (2) The quorum shall be *four elected or co-opted Directors*, or such larger number as may be decided from time to time by the Council.

President

52 On the nomination of the Council, the President shall be elected by the members of the Charity at a General Meeting. *The term of Office of the President shall run from the election at an Annual General Meeting until such President's re-election or a successor is elected at the second Annual General Meeting thereafter; if elected at a General Meeting not an Annual General Meeting, then until the third Annual General Meeting thereafter.* Subject to the discretion of the Council and the membership, a President would not normally be re-elected more than once. The President shall, ex officio, be entitled to attend meetings of the Council but shall not be entitled to vote unless he is also a member of the Council.

The motion was accepted with two abstentions.

A full version of the updated Memorandum and Articles of Association is available on Gem-A's website at www.gem-a.com/index.php/membership/resources/applications-articles/memorandum.

OBITUARY

Michael J. O'Donoghue FGA 1934–2016

The worldwide Gemmological community has been greatly saddened to hear of the passing of Michael O'Donoghue on 16 June 2016.

Michael did his National Service in the RAF, but, in spite of being offered a commission, he went to Selwyn College, Cambridge, graduating in 1959 with a degree in English Literature.

He became a librarian, working in Cambridge University Library, the National Library of Scotland and then in 1962, the British Museum Library. Initially he worked in the State Paper Room, but then moved to the Scientific and Technological Section where he became curator of Earth Sciences. He retired from the then renamed British Library ca. 1998. Being a curator

of a major earth science collection of printed material obviously stirred his interest in gem materials. He became an FGA in 1968, and began teaching the same year at Sir John Cass College.

I studied my gemmology preliminary in 1976–77, and while walking along Cass corridors often passed the open doors of two classrooms where the Gemmology Diploma was being studied. In one of the rooms there were always about 40 students, heads down continually taking notes by dictation. There were considerably fewer in the other room, but far from taking notes, they seemed to be having a lively vocal relationship with their lecturer: Michael, of course! When I selected my Diploma lecturer I had



no hesitation in choosing Michael, a decision I still have much to be thankful for. Michael had a happy knack of transferring his immense enthusiasm to his students. I remember well how impatient we all were for his classes to start, wondering each week what exciting gems and books he would bring to show us.

Michael was a truly inspirational teacher, and the considerable number of his past students that I have recently talked to about him have all stressed that. He continued teaching until ca. 2009, becoming the College's Head of Gemmology.

Knowing that, like him, I was a keen collector of historic gemmological literature, he persuaded me to give my first-ever lecture during a day event at the Library. I remember using covers and pages of books photocopied onto overhead projection transparencies; how times have changed! He visited me regularly to look at my latest purchases, but food and wine were equally important on those occasions.

Michael wrote or edited about 20 books on gemstones, and led gemmological trips to far-flung places. He was, in 1991, the first editor of *Gem & Jewellery News*, then the joint newsletter of Gem-A and The Society of Jewellery Historians that was later to become *Gems&Jewellery*. Michael also produced abstracts of gemmological journals and reviewed books for *The Journal of Gemmology* from 1972, and in 1997 was appointed an Assistant Editor, a post he held until he died. In addition, Michael was made a Vice President of Gem-A in 2009.

I would not like anyone to think, however, that Michael was a one-subject enthusiast. He had many other varied interests. He was an accomplished church organist, having started to learn when he was nine. He was also passionate about the railways (his father was a railway executive), and apparently visited at least 110 signal boxes. He was an exceptionally kind man, and for some time was a Samaritans' volunteer.

Michael leaves a wife, Annie, three children and five grandchildren. Michael's past students, Gem-A and, indeed, the whole world of gemmology, owe him a massive debt. He is sorely missed, but his gemmological legacy will continue into the far future.

Nigel Israel

Michael O'Donoghue's talents stretched far beyond gemmology, but it was as a gemmologist that I knew him. My background was not in the gem trade—I had a photographic studio specializing in jewellery, and was simply curious to know more about the gems. Thanks largely to Michael's inspirational and challenging method of teaching in my Diploma year, I became so engrossed in the subject that I considered switching careers. The evening study group, which was started by Michael (today called 'Gem Central' but to which we affectionately referred as 'The Playgroup'), clinched it for me. We brought our dogs along, we ate chocolate biscuits (both of which Michael enjoyed), and we worked hard for a couple of hours under his guidance. It brought gemmology to life and was fun. That weekly opportunity to study gemstones from his wonderful collection and to share views and experiences pointed me firmly in the direction which I then followed.

Michael did not encourage note-taking during class. He himself provided notes the following week on what we had studied, but in class he wanted his students to listen and give their full attention to what they were hearing. There was of course a certain amount of surreptitious note-taking, especially by some of the students for whom English was not their first language. Michael had a dry sense of humour, and he was fond of explaining things by use of analogy. Though I now forget what he was describing at the time, I well remember a rather bewildered foreign gentleman leaning over to me in class and whispering, 'How do you spell Kit Kat?'

Michael was never afraid of being challenged himself. He was delighted to be confronted with an unusual specimen or with new information. Often—to use an analogy myself—we would come into class a bit like puppies, full of enthusiasm and proudly wag-

ging our tails at some new-found knowledge, only to find that Michael already knew all about it, and could elaborate on it and teach us a lot more. He was always pleased when we showed initiative, and he made us feel good about our discoveries, encouraging us to go

out and investigate further. He wanted us to think for ourselves.

Personally, I owe Michael such a lot. He was very special, and he is greatly missed.

Maggie Campbell Pedersen

Ralph Ellis McRae Blacklock FGA (D.1967), Darlington, Co. Durham, died on 22 August 2016 following a short illness.

Born on 9 October 1946, Ralph started his career in 1965 in Birmingham with Bernard Lowe stone dealers sorting and selling gems. In 1966 he joined the family fine jewellery business, Blacklocks, in Sunderland. He was awarded his Gemmology Diploma in 1967, completing the course within one year.

Ralph worked with his father Ellis from 1966 until 1986. In that time the business grew with the opening of a second shop in Durham. In the early 1990s Ralph opened a third shop in Newcastle. In 2000 he sold the business and set up independently as a jewellery designer. From 2000 until 2016 he used his gemmological knowledge and design skills to create bespoke pieces, sourcing and identifying fine diamonds and gemstones to set within them, selling through a website. In 2009 he was joined by his son Christopher, who was the sixth generation to work in the family business, now entirely online.

By the time of his death, Ralph had designed multiple collections and fulfilled hundreds of bespoke orders.

Ralph was a founding director of the Company of Master Jewellers in 1981, served on the Board of the then National Association of Goldsmiths in 1997 and was a director of the Houlden Buying Group from 1998 to 2001.

Ralph leaves wife Roz, sons Chris and Mark, and three grandchildren.

Christopher Blacklock

Adi Inskeep (née Redman) FGA (D.1959 with Distinction), Oxford, died at home on 5 April 2016. Adi attended Witwatersrand University, Johannesburg, South Africa, from 1947, completing her BSc in Geology and Botany followed by BSc (Hons) in Economic Geology in 1952. At the age of 22 Adi was appointed a curator at the University's Geological Museum, where she constructed many new exciting exhibits, acquiring outstanding material and brought enthusiasm and life to what had previously become a dormant museum. Adi worked at the museum for 12 years, until 1965. She then pursued her interest in human artefacts.

Hugh Underhill

Individual Membership is changing...

Renew your Individual Membership before 1 January 2017 and pay just £110 — Individual Membership will be £135 for all renewals after this date.

Contact membership@gem-a.com for more information or to renew your Membership for 2017.

Learning Opportunities

CONFERENCES AND SEMINARS

CIBJO Congress 2016

26–28 October 2016
Yerevan, Armenia
www.cibjo.org/congress2016

The Munich Show

28–30 October 2016
Munich, Germany
www.mineralientage.de/en
Note: Includes a seminar programme.

MJSA ConFab

30 October 2016
New York, New York, USA
www.mjsa.org/eventsprograms/mjsa_confab

CGA Grad Gemmology Conference

29 October 2016
Vancouver, British Columbia, Canada
www.canadiangemmological.com

Fabergé Symposium – The Wonder of Fabergé

3–4 November 2016
Houston, Texas, USA
www.hmns.org/education/adults/faberge-symposium

Gem-A Conference

5–6 November 2016
London
www.gem-a.com/event/conference/conference-2016

The New Mexico Mineral Symposium

12–13 November 2016
Socorro, New Mexico, USA
<https://geoinfo.nmt.edu/museum/minsymp>

5th GIT International Gem and Jewelry Conference (GIT 2016)

14–15 November 2016
Pattaya, Thailand
www.git2016.com

3rd European Congress on Jewellery: The Jewel in Art and Art in Jewell

17–18 November 2016
Barcelona, Spain
www.museunacional.cat/en/jewel-art-and-art-jewellery

AGA Tucson Conference

1 February 2017
Tucson, Arizona, USA
<https://accreditedgemologists.org>

The 38th Annual Tucson Mineral Symposium: Mineral Treasures of the Midwest

11 February 2017
Tucson, Arizona, USA
www.friendsofmineralogy.org/symposia.html

Hasselt Diamond Workshop 2017 (SBDD XXII)

9–11 March 2017
Hasselt, Belgium
www.uhasselt.be/sbdd

Amberif International Fair of Amber, Jewellery and Gemstones

22–25 March 2017
Gdańsk, Poland
www.amberif.amberexpo.pl
Note: Includes a seminar programme.

American Gem Society International Conclave

5–8 April 2017
Hollywood, California, USA
www.americangemsociety.org/Content/uploads/Conclave2017RFP.pdf

14th Annual Sinkankas Symposium – Sapphire

8 April 2017
Carlsbad, California, USA
www.sinkankassymposium.net

The Santa Fe Symposium

21–24 May 2017
Albuquerque, New Mexico, USA
www.santafesymposium.org

Swiss Gemmological Society Conference and European Gemmological Symposium 2017

8–11 June 2017
Zermatt, Switzerland
www.gemmologie.ch

2017 Society of North American Goldsmiths (SNAG) Conference

24–27 May 2017
New Orleans, Louisiana, USA
www.snagmetalsmith.org/events/nexus-2017

11th International Conference on New Diamond and Nano Carbons

28 May–1 June 2017
Cairns, Australia
<http://ndnc2017.org>

Association for the Study of Jewelry and Related Arts (ASJRA) Annual Conference

9–10 June 2017

Compiled by Georgina Brown and Brendan Laurs

Boston, Massachusetts, USA
www.jewelryconference.com

PEG2017 – 8th International Symposium on Granitic Pegmatites

13–15 June 2017
 Kristiansand, Norway
www.nhm.uio.no/forskning/aktuelt/arrangementer/konferanser-seminarer/peg2017

11th International Kimberlite Conference

18–22 September 2017
 Gaborone, Botswana
www.11ikc.com
Note: Pre- and post-conference field trips will visit

diamond deposits in Botswana and neighbouring countries.

World of Gems Conference V

23–24 September 2017
 Rosemont, Illinois, USA
<http://gemguide.com/events/world-of-gems-conference>

35th International Gemmological Conference

11–15 October 2017
 Windhoek, Namibia
www.igc-gemmology.org/igc-2017-programme/4592655130
Note: Pre- and post-conference field trips will visit diamond and coloured stone deposits in Namibia.

EXHIBITIONS

Australia

Lustre: Pearling and Australia

Until 22 January 2017
 Immigration Museum, Melbourne, Victoria, Australia
<http://tinyurl.com/hcrhscq>

Europe

Heavenly Bodies—The Sun, Moon and Stars in Jewellery

Until 30 October 2016
 Schmuckmuseum, Pforzheim, Germany
www.schmuckmuseum.de/flash/SMP_en.html

Eggs-travagant—Ostereier aus Edelsteinen

Until 2 November 2016
 Edelsteinmuseum, Idar-Oberstein, Germany
www.edelsteinmuseum.de/ausstellungen-deutsches-edelsteinmuseum/sonderausstellungen.html

Enamoured

Until 18 November 2016
 The Goldsmiths' Centre, London
www.goldsmiths-centre.org/whats-on/exhibitions/enamoured

Eva's Beauty Case: Schmuck und Styling im Spiegel der Zeiten (Jewelry and Styling Through the Ages)

Until 22 January 2017
 LVR-LandesMuseum Bonn, Bonn, Germany
www.landesmuseum-bonn.lvr.de/de/ausstellungen/evas_bauty_case/evas_beauty_case.html

Elements: From Actinium to Zirconium

Until 26 February 2017
 Ulster Museum, Belfast, Northern Ireland
<http://nmni.com/um/What-s-on/Elements>

Warrior Treasures: Saxon Gold from the Staffordshire Hoard

Until 23 April 2017
 Bristol Museum & Art Gallery, Bristol
www.bristolmuseums.org.uk/bristol-museum-and-art-gallery/whats-on/warrior-treasures

Must-Haves—Jewellery Created by Greats of the Craft and Must-Sees—Jewellery in the Arts

21 May–10 September 2017
 Schmuckmuseum, Pforzheim, Germany
www.schmuckmuseum.de/flash/SMP_en.html

Authentically Inauthentic?—Jewellery from Pforzheim's Industrial Production

28 May–10 September 2017
 Municipal Museum, Pforzheim, Germany
www.schmuckmuseum.de/flash/SMP_en.html

Smycken: Jewellery. From Decorative to Practical

Ongoing
 Nordiska Museet, Stockholm, Sweden
www.nordiskamuseet.se/en/utstallningar/jewellery

North America

Fabergé from the Matilda Geddings Gray Foundation Collection

Until 27 November 2016
 The Metropolitan Museum of Art, New York, New York, USA
www.metmuseum.org/exhibitions/listings/2011/faberge

Glitterati: Portraits & Jewelry from Colonial Latin America

Until 27 November 2016
 Denver Art Museum, Denver, Colorado, USA
www.denverartmuseum.org/exhibitions/glitterati

Jewelry, from Pearls to Platinum to Plastic

Until 1 January 2017

Newark Museum, Newark, New Jersey, USA

www.newarkmuseum.org/jewelry

All That Sparkles...20th Century Artists' Jewelry

Until 8 January 2017

The Bechtler Museum of Modern Art, Charlotte, North Carolina, USA

<http://bechtler.org/Collection/All-that-sparkles>

Gold and the Gods: Jewels of Ancient Nubia

Until 8 January 2017

Museum of Fine Arts, Boston, Massachusetts, USA

www.mfa.org/exhibitions/gold-and-gods

Arts of Islamic Lands: Selections from The al-Sabah Collection, Kuwait

Until 29 January 2017

Museum of Fine Arts, Houston, Texas, USA

www.mfah.org/exhibitions/arts-islamic-lands-selections-al-sabah-collection

American Mineral Heritage: Harvard Collection

Until February 2017

Flandrau Science Center & Planetarium, Tucson, Arizona, USA

<http://flandrau.org/exhibits/harvard>

Beyond Bling: Jewelry from the Lois Boardman Collection

Until 5 February 2017

Los Angeles County Museum of Art, California, USA

www.lacma.org/art/exhibition/beyond-bling

Bijoux Parisiens: French Jewelry from the Petit Palais, Paris

11 February–14 May 2017

Taft Museum of Art, Cincinnati, Ohio, USA

www.taftmuseum.org/upcoming-exhibitions-draft

Spectacular! Gems and Jewelry from the Merriweather Post Collection

10 June 2017–14 January 2018

Hillwood Estate, Museum & Gardens, Washington DC, USA

www.hillwoodmuseum.org/Spectacular-Gems-and-Jewelry

Amber Secrets: Feathers from the Age of Dinosaurs

Ongoing

Houston Museum of Natural Science, Texas, USA

www.hmns.org/exhibits/special-exhibitions/amber-secrets-feathers-from-the-age-of-dinosaurs

City of Silver and Gold: From Tiffany to Cartier

Ongoing

Newark Museum, New Jersey, USA

www.newarkmuseum.org/SilverAndGold.html

Fabergé: From a Snowflake to an Iceberg

Ongoing

Houston Museum of Natural Science, Texas, USA

www.hmns.org/exhibits/special-exhibitions/faberge-a-brilliant-vision

Gemstone Carvings

Ongoing

Houston Museum of Natural Science, Texas, USA

www.hmns.org/exhibits/special-exhibitions/gemstone-carvings

Gilded New York

Ongoing

Museum of the City of New York, New York, USA

www.mcny.org/content/gilded-new-york

Mightier than the Sword: The Allure, Beauty and Enduring Power of Beads

Ongoing

Yale Peabody Museum of Natural History, New Haven, Connecticut, USA

<http://peabody.yale.edu/exhibits/mightier-sword-allure-beauty-and-enduring-power-beads>

OTHER EDUCATIONAL OPPORTUNITIES

Gem-A Workshops and Courses

Gem-A, London

www.gem-a.com/education/courses/workshops

Lectures with The Society of Jewellery Historians

Society of Antiquaries of London, Burlington House, London

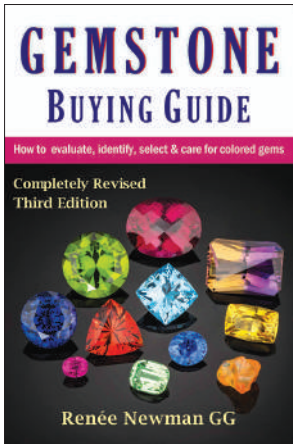
www.societyofjewelleryhistorians.ac.uk/current_lectures

- 25 October 2016
Robert Baines—Bogus or Real: Jewellery and the Capture of Human Drama

- 22 November 2016
Kieran McCarthy—Fabergé and London
- 24 January 2017
Noël Adams—Gold and Garnet Cloisonné Jewellery: Recent Discoveries and New Perspectives
- 28 February 2017
David Callaghan—(To be announced)
- 28 March 2017
Marjan Unger—My Jewellery Collection: Confessions of an Art Historian

New Media

Gemstone Buying Guide, 3rd Edn.



By Renée Newman, 2016.
International Jewelry
Publications, Los Angeles,
California, USA,
156 pages,
ISBN 978-0929975511.
US\$19.95 softcover.

This third edition is a completely revised version of the *Gemstone Buying Guide*, and it has been updated with well-rounded information that is organized into 12 chapters:

- Chapter 1 explains coloured gemstone pricing factors.
- Chapters 2–6 explain how to examine a stone according to the ‘4 Cs’ (cut, carat, colour and clarity).
- Chapter 7 is a short section on cat’s-eye and star stones.
- Chapters 8–9 cover various treatment processes and the identification features useful for dis-

tinguishing between natural and synthetic gemstones.

- Chapter 10 warns the reader about practices done with the intent to deceive the gemstone buyer.
- Chapter 11 provides 77 pages describing the history, characteristics and sources of the more important gem varieties on the market, organized alphabetically.
- Chapter 12 concludes with a short but nonetheless important section on how to care for your gems.

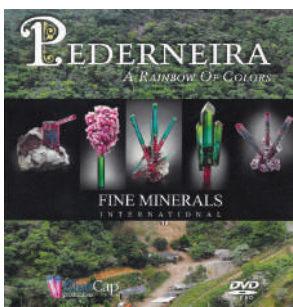
The final pages contain a tabulation of birthstones and anniversary stones, followed by a list of gem varieties in order of descending Mohs hardness.

The book includes several new gem varieties that were not covered in previous editions. It is also a ‘feast for the eye’, with 356 colour images by a variety of photographers. Newman once again included several of my photos, which I greatly appreciate. She has also conveyed captivating historical information on the gems that she profiles.

The book is an excellent tool for the novice, as well as for knowledgeable members of the gem and jewelry trade. I recommend Newman’s book to anybody buying or selling gemstones.

Mia Dixon
Palagems.com, Fallbrook, California, USA

Pederneira – A Rainbow of Colors (DVD)



By Fine Minerals International, 2014 (released 2016). Produced by Blue Cap Productions, Honolulu, Hawaii, 1 hour 28 minutes playing time, www.shop.bluecap-productions.com. US\$19.99.

In the world of tourmaline, few mines of the modern era have yielded more of the stunning beauty and variety of gem crystals than the Pederneira mine, located near São José da Safira, Minas Gerais, Brazil. This film was prepared to accompany an extensive article on this famous deposit that was published by *Mineralogical Record* (Vol. 46, No. 1, January–February 2015, 1–138). It takes the viewer on a journey from the 1940s

to 2014, from the transformation of coffee plantation to mine, and chronicles several incredibly productive eras, ending with an exploration programme to (hopefully) expand the mine in the future. The scene selection is divided into 21 topics, of which 14 are dedicated to individual gem ‘pockets’ (i.e. cavities in the pegmatite hosting tourmaline crystals).

The video is passionately narrated by various key players in Pederneira’s development, such as Daniel Trinchillo (mine co-owner and mineral dealer), José Menezes de Souza (mine partner, also known as ‘Ze’) and Dr Federico Pezzotta (pegmatite geologist). Each individual adds fascinating personal stories of his involvement, with a particularly memorable one by Ze who recounted the discovery of the Rocket Pocket in 2001: Ze received a call from the mine workers stating that they had broken into a new cavity showing gemmy tourmaline. He instructed them to stop work and wait for him to arrive the following morning. How-

ever, when he arrived he discovered, to his horror, that the miners conducted further blasting that ultimately caused considerable damage to the material; in Ze's words, "I almost cried." Although the colour and quality of the crystals were spectacular, only a very few matrix specimens could be salvaged. Since the same crystals still attached to their host matrix could have yielded "5 to 6 times" the selling price, Ze and the Pederneira team quickly learned an expensive lesson in gem and mineral mining. Fortunately, the team moved on from this misstep and subsequent pockets were handled more diligently.

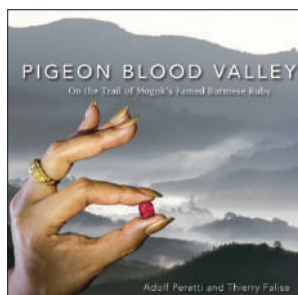
The narration is accompanied by video footage of amazing tourmalines as they are slowly rotated, including famous named specimens such as the 'Rocket' and the 'Big Blue' (the latter being a perfect 15-cm-diameter, 23-cm-tall blue-green tourmaline crystal perched upon

a 'soccer ball'-sized piece of white albite matrix). The film is full of such visual treats.

For those interested in the Pederneira locality, or tourmaline in general, this is a must-watch video. However, gemmologists will find little discussion of gem rough and faceted material, as they are not the subject of focus. Some of the narrators' English pronunciation is challenging to understand, but this actually adds to the authenticity of the story. The audio and video are both of excellent quality, and most of the video was filmed on location at Pederneira. The film truly captures the spectacular beauty of Pederneira tourmaline, and hopefully we will see similar video treatments of additional world-class gem and mineral localities in the future.

*Keith Mychaluk
Calgary, Alberta, Canada*

Pigeon Blood Valley—On the Trail of Mogok's Famed Burmese Ruby



By Adolf Peretti and
Thierry Falise, 2016.
GRS GemResearch
Swisslab AG, Lucerne,
Switzerland, 237 pages,
ISBN 978-952386774,
www.mogok.com. Fund-
raiser edition, US\$200.00
hardcover.

In the foreword of this attractive book, the authors explain that this is a personal journey through the history of this fascinating locality for vivid red rubies (commonly called *pigeon blood* red by gem traders). They divide the book into 12 chapters. The text is minimal (only 1–2 pages per chapter), but well written and concise. The authors prefer to let the photographs and captions tell much of their story.

The first four chapters focus on some of the famous old-time ruby dealers, as well as on Burmese kings and British colonization, before shifting to more modern history. The photos show the local people, places, mines and, of course, wonderful jewels. There are numerous spectacular full-page colour images supplied by auction houses Sotheby's and Christie's, as well as by a plethora of famous jewelers including Cartier, Graf, Van Cleef & Arpels, Harry Winston and Bulgari, to name a few. These photos show the reader exactly why Mogok is so famous for pigeon-blood rubies, with examples of modern and vintage necklaces, bracelets, rings, watches and earrings. The authors also include comprehensive historic maps, reproductions of original photos from the late 1800s, and antique letters and stamps from the famous collection of Santpal Sinchawla of Bangkok. These help the reader to better understand this amazing and complicated valley.

In Chapter 5 the authors introduce the reader to the 'Men Who Mine', covering many modern-day deposits and the miners who work them. Chapter 6, 'Till the Last Crumb', is a tribute to an old tradition of allowing village women and children to go through the mine tailings and keep whatever they find. Chapter 7, 'Ruby Royalty', covers some present-day local gem dealers, followed by 'Warlords and Smugglers' in Chapter 8. The latter characters are an age-old problem in Mogok, as well as in most gem-producing areas throughout history. Chapter 9 covers the 'Subcontinent Influence' of the many Indians and Nepalese who have become strong players in the Mogok gem business. Chapter 10, 'The Final Cut', describes how Mogok locals skilfully transform rough material into beautiful gems, often using techniques passed down from their grandfathers' time.

Chapter 11, 'The Soul of the City', shows how Mogok is focused completely on gemstones. The authors start with quotations from older books on Mogok that point out the fantasy and charm of this fabled place, and illustrate the chapter with photographs that confirm the beauty and mystique that visitors feel there. The final chapter, 'A Future between Gloom and Hope', tackles social and environmental issues in a realistic dialogue. The chapter ends with the author's statement that "only when the river is no longer red will Mogok be finished".

The last few pages focus on 'Specialist Doctor Wanted', as one of the overriding purposes of this book is to help the AIDS victims of the Mogok District.

For any gemmologist interested in classic Burmese gemstones, especially ruby, I recommend this book. The hundreds of photographs will give you a new understanding of the Mogok area, and you will gain an appreciation of just how rare and beautiful gemstones from this fabled valley are.

*William F. Larson
Palagems.com, Fallbrook, California, USA*

OTHER BOOK TITLES

General Reference***Collecting Rocks, Gems and Minerals: Identification, Values, Lapidary Uses, 3rd edn.***

By Patti Polk, 2016. Krause Publications, Fort Collins, Colorado, USA, 352 pages, ISBN 978-1440246159. US\$19.99 softcover.

Gem Identification Made Easy, 6th edn.

By Antoinette Matlins, 2016. Gemstone Press, Nashville, Tennessee, USA, 400 pages, ISBN 978-0997014556. US\$38.99 hardcover.

Gemstones: A Complete Color Reference for Precious and Semiprecious Stones of the World

By Karen Hurrell and Mary L. Johnson, 2016. Chartwell Books, New York, New York, USA, 320 pages, ISBN 978-0785834984. US\$14.99 softcover.

Jewellery and Objets d'Art***20th Century Jewelry & the Icons of Style***

By Stefano Papi and Alexandra Rhodes, 2016. Thames and Hudson, London, 224 pages, ISBN 978-0500519004. £28.00 hardcover.

The Art of Collecting Cartier: An Eye for Excellence

By Vivienne Becker and Nick Foulkes, 2016. Flammarion, Paris, France, 272 pages, ISBN 978-2080202680. €110.00 hardcover.

The Beverley Collection of Gems at Alnwick Castle

By Claudia Wagner, John Boardman and Diana Scarisbrick, 2016. Philip Wilson Publishers, London, 384 pages, ISBN 978-1781300442. £40.00 hardcover.

Evert Nijland: Mercurius & Psyche. Jewellery

By Ward Schrijver, 2016. Arnoldsche Art Publishers, Stuttgart, Germany, 316 pages, ISBN 978-3897904699. €34.80 hardcover.

Fine Jewelry Couture: Contemporary Heirlooms

By Olivier Dupon, 2016. Thames and Hudson, London, 256 pages, ISBN 978-0500518601. £39.95 hardcover.

Gemstone/Art: Renaissance to the Present Day

Ed. by Wilhelm Lindemann, 2016. Arnoldsche Art Publishers, Stuttgart, Germany, 352 pages, ISBN 978-3897904651. €49.80 hardcover.

Jeweler: Masters, Mavericks, and Visionaries of Modern Design

By Stellene Volandes and Carolina Herrera, 2016.

Rizzoli, New York, New York, USA, 256 pages, ISBN 978-0847848614. US\$85.00 hardcover.

Messika Joaillerie

By Vivienne Becker, 2016. Assouline Publishing, New York, New York, USA, 80 pages, ISBN 978-1614285274. US\$25.00 hardcover.

Open Space—Mind Maps: Positions in Contemporary Jewellery

Ed. by Ellen Maurer Zilioli, 2016. Arnoldsche Art Publishing, Stuttgart, Germany, 208 pages, ISBN 978-3897904637. €29.80 hardcover.

Precious Cufflinks: From Pablo Picasso to James Bond

By Walter Grasser, Franz Hemmerle and Alexander von Württemberg, 2016. Hirmer Publishing, Munich, Germany, 112 pages, ISBN 978-3777424231. €39.90 hardcover.

Precious Statements—John Donald: Designer · Jeweller

By John Donald and Russell Cassleton Elliott, 2016. McNidder & Grace, Carmarthen, Wales, 304 pages, ISBN 978-0857161284. £65.00 hardcover.

Stories in Stone: The Enchanted Gem Carvings of Vasily Konovalenko

By Stephen E. Nash, 2016. University Press of Colorado, Boulder, Colorado, USA, 304 pages, ISBN 978-1607325024. US\$39.95 softcover.

Untitled. Thomas Gentile. American Jeweler

Ed. by Angelika Nollert, 2016. Arnoldsche Art Publishers, Stuttgart, Germany, 208 pages, ISBN 978-3897904668. €39.80 hardcover.

Van Cleef & Arpels: The Art and Science of Gems

By Laurence Mouillefarine, 2016. Éditions Xavier Barral, Paris, France, 304 pages, ISBN 978-2365110983. €78.00 hardcover.

Wallace Chan: Dream Light Water

By Juliet Weir de La Rochefoucauld and Wallace Chan, 2016. Rizzoli, New York, New York, USA, 380 pages, ISBN 978-0847847549. US\$280.00 hardcover.

Organic Materials***Amber—Views, Opinions, Vol. 3***

By Barbara Kosmowska-Ceranowicz, Wiesław Gierłowski and Ewa Wagner-Wysiecka, 2016. Publ. by International Amber Association, PAS Museum of the Earth, MTG SA Gdańsk International Fair Co. and Gdańsk University of Technology (Faculty of Chemistry), Gdańsk–Warsaw, Poland, 204 pages., ISBN 978-8391289402. PLN35.00 softcover. [Note: Includes contributions from the 2010–2015 Amberif Seminars, excluding 2013.]

Literature of Interest

Coloured Stones

The challenges of cutting a large gem opal rough. T. Grussing, *Gems & Gemology*, **52**(2), 2016, 162–167, <http://dx.doi.org/10.5741/gems.52.2.162>.*

Classification géologique des gisements d'émeraude [Geological classification of emerald deposits]. G. Giuliani, Y. Branquet, A.E. Fallick, L.A. Groat and D. Marshall, *Revue de Gemmologie A.F.G.*, No. 196, 2016, 12–20.

Nano-structure of the cristobalite and tridymite stacking sequences in the common purple opal from the Gevrekseydi deposit, Seyitömer-Kütahya, Turkey. M. Hatipoğlu, Y. Kibici, G. Yanık, C. Özkul and Y. Yardımcı, *Oriental Journal of Chemistry*, **31**(1), 2015, 35–49, <http://dx.doi.org/10.13005/ojc/310104>.*

Texture, water content and formation mechanism of agate. M. Tao and H. Xu, *Acta Petrologica et Mineralogica*, **35**(2), 2016, 333–343 (in Chinese with English abstract).

Thoroughly ruby [Art Deco ruby ring]. G. Millington, *Gems&Jewellery*, **25**(4), 2016, 22–27.

Usambara effect in tourmaline: Optical spectroscopy and colourimetric studies. M.N. Taran and I.V. Naumenko, *Mineralogical Magazine*, **80**(5), 2016, 705–717, <http://dx.doi.org/10.1180/minmag.2016.080.016>.

Cultural Heritage

Fabergé cossack figures created from Russian gemstones. T. Adams and C.L. McCanless, *Gems & Gemology*, **52**(2), 2016, 132–143, <http://dx.doi.org/10.5741/gems.52.2.132>.*

A multidisciplinary study of a group of post-classical cameos from the National Museum in Krakow, Poland. P. Gołyźniak, L. Natkaniec-Nowak, M. Dumańska-Słowik and B. Naglik, *Archaeometry*, **58**(3), 2016, 413–426, <http://dx.doi.org/10.1111/arcms.12174>.

Diamonds

Diamond-bearing gravels along the lower Kwango River DRC. M.C.J. de Wit and E. Thorose, in M.J. de Wit, F. Guillocheau and M.C.J. de Wit, Eds., *Geology and Resource Potential of the Congo Basin*. Springer, Berlin, Germany, 2015, 341–360, http://dx.doi.org/10.1007/978-3-642-29482-2_16.

Diamonds: Gem set and match [history of diamond engagement rings]. J. Ogden, *Gems&Jewellery*, **25**(5), 2016, 33.

A method for quantitative evaluation of scintillation in round brilliant diamond. P. Liu, X. Yuan, N. Ang and S. Bin, *Journal of Gems & Gemmology*, **18**(3), 2016, 9–17 (in Chinese with English abstract).

Mining diamonds in the Canadian arctic: The Diavik mine. J.E. Shigley, R. Shor, P. Padua, C.M. Breeding, S.B. Shirey and D. Ashbury, *Gems & Gemology*, **52**(2), 2016, 104–131, <http://dx.doi.org/10.5741/gems.52.2.104>.*

Le monde des diamants roses et comment les identifier [The world of pink diamonds and how to identify them]. B. Deljanin, A. Peretti and M. Alessandri, *Revue de Gemmologie A.F.G.*, No. 196, 2016, 22–29.

Meet the heavyweights of international diamond mining. E. Laniado, *World Diamond Magazine*, No. 7, 2016, 74–76.

On land, underground and at sea: The many types of diamond mining. E. Laniado, *World Diamond Magazine*, No. 7, 2016, 80–82.

Overview of diamond resources in Africa. M. de Wit, Z. Bhebhe, J. Davidson, S.E. Haggerty, P. Hundt, J. Jacob, M. Lynn, T.R. Marshall, C. Skinner, K. Smithson, J. Stiefenhofer, M. Robert, A. Revitt, R. Spaggiari and J. Ward, *Episodes*, **39**(2), 2016, 198–237, <http://dx.doi.org/10.18814/epiugs/2016/v39i2/95776>.*

The state of the natural colored diamond market – Spring 2016. A. Bronstein, *The GemGuide*, **35**(4), 2016, 2–5.

Gem Localities

Almandine garnet from the Red Embers mine, Erving, Franklin County, Massachusetts. E.S. Greene, *Rocks & Minerals*, **91**(5), 2016, 453–458, <http://dx.doi.org/10.1080/00357529.2016.1205938>.

In Rainier's footsteps: Journey to the Chivor emerald mine. R. Weldon, J.G. Ortiz and T. Ottaway, *Gems & Gemology*, **52**(2), 2016, 168–187, <http://dx.doi.org/10.5741/gems.52.2.168>.*

L'aventure extraordinaire du Botswana [The extraordinary adventure of Botswana]. D. Girard, *Revue de Gemmologie A.F.G.*, No. 196, 2016, 5–11.

Muzo steps up Colombian emerald brand campaign. M. Feliciano, *JNA*, No. 383, 2016, 64–67.

* Article freely available for download, as of press time

Origin of sapphires from a lamprophyre dike at Yogo Gulch, Montana, USA: Clues from their melt inclusions. A.C. Palke, N.D. Renfro and R.B. Berg, *Lithos*, **260**, 2016, 339–344, <http://dx.doi.org/10.1016/j.lithos.2016.06.004>.

Instrumentation

Application of attenuated total reflectance infrared spectroscopy (ATR-FTIR) for amber identification and research. Y. Xing, *Spectroscopy and Spectral Analysis*, **36**(7), 2016, 2066–2070 (in Chinese with English abstract).

Characterization of pearls by X-ray phase contrast imaging with a grating interferometer. V. Revol, C. Hanser and M. Krzemnicki, *Case Studies in Nondestructive Testing and Evaluation*, **6**, 2016, 1–7, <http://dx.doi.org/10.1016/j.csnedt.2016.06.001>.*

Precious coral non-destructive characterization by Raman and XRF spectroscopy. M. Macchia, V. Resta, G. Quarta and L. Calcagnile, *X-Ray Spectrometry*, **45**(5), 2016, 281–287, <http://dx.doi.org/10.1002/xrs.2703>.

Review on the application of X-ray diffraction in gem identification, synthesis and crystal structure research. N. Zhang and C. Lin, *Rock and Mineral Analysis*, **35**(3), 2016, 217–228 (in Chinese with English abstract).

X-ray computed tomography for fast and non-destructive multiple pearl inspection. J. Rosc, V.M.F. Hammer and R. Brunner, *Case Studies in Nondestructive Testing and Evaluation*, **6**, 2016, 32–37, <http://dx.doi.org/10.1016/j.csnedt.2016.08.002>.*

Miscellaneous

The color of money. E. Blauer, *Rapaport Magazine*, **39**(2), 2016, 42–48. [Note: Discusses the impact of geographic origin reports and treatments on coloured stone prices.]

The education of a native son. E. Konigsberg, *Men's Journal*, **25**(8), 2016, 70–75 and 96, www.mensjournal.com/features/articles/the-murder-of-an-african-miner-and-his-sons-quest-for-revenge-w437780.* [Note: Describes the situation at the Bridges family's tsavorite mine in Kenya.]

The foundations constructivism and design to trends in the drafting of metal jewelry in Art Nouveau: Analytical study of Rene Lalique's jewelry as a new entrance for teaching metal works in the faculties of art education. N.A.G. Elsaid, *American Journal of Educational Research*, **3**(12), 2015, 1579–1591.

Framework for resource uncertainty prediction and data valuation: An application to diamond deposits. J.G. Manchuk, J. Stiefenhofer, M. Thurston and C.V. Deutsch, *CIM Journal*, **6**(3), 2015, 178–190, <http://dx.doi.org/10.15834/cimj.2015.19>.

Investing in diamonds. L. Renneboog, *Business and Economic Research*, **5**(1), 2015, 166–196, <http://dx.doi.org/10.5296/ber.v5i1.7518>.*

Tales from the Tower [British Crown Jewels]. A. Fellows, *Gems&Jewellery*, **25**(5), 2016, 14–15.

News Press

The diamond industry: In the rough. *The Economist*, 2 July 2016, www.economist.com/news/business/21701497-diamond-ever-its-allure-comes-and-goes-rough.*

Diamonds illuminate the origins of Earth's deepest oceans. R. Becker, *Smithsonian.com*, 21 June 2016, www.smithsonianmag.com/science-nature/diamonds-illuminate-origins-earths-deepest-oceans-180959480.*

First, find the world's biggest diamonds. Then don't break them. T. Biesheuvel and K. Crowley, *Bloomberg*, 5 July 2016, www.bloomberg.com/news/articles/2016-07-05/first-find-the-world-s-biggest-diamonds-then-don-t-break-them.*

Fisherman found giant 34kg pearl worth \$100million – but kept the two-foot long gem under his bed for TEN YEARS as a good luck charm. D. Boyle, *DailyMail.com*, 22 August 2016, www.dailymail.co.uk/news/article-3753300/Fisherman-giant-34kg-pearl-worth-100million-kept-bed-TEN-YEARS-good-luck-charm.html.*

How do you cut a massive, 404-carat diamond? J. Tarmy, *Bloomberg*, 6 July 2016, www.bloomberg.com/news/articles/2016-07-06/how-do-you-cut-a-massive-404-carat-diamond.*

Hunting for diamonds under Canada's frozen tundra. D. Bochove, *Bloomberg*, 11 July 2016, www.bloomberg.com/news/features/2016-07-11/hunting-for-diamonds-under-canada-s-frozen-tundra.*

New gold rush: Ivory hunters dig for woolly mammoths in Siberia. A. Chapple, *The Guardian.com*, 1 September 2016, www.theguardian.com/world/gallery/2016/sep/01/mining-woolly-mammoths-ivory-siberia-amos-chapple-in-pictures.*

Why buyers shunned the world's largest diamond. M. Hart, *Vanity Fair*, 5 August 2016, www.vanityfair.com/news/2016/08/why-buyers-shunned-the-worlds-largest-diamond.*

Organic Gems and Pearls

Advanced jet testing. S. Steele, *Gems&Jewellery*, **25**(5), 2016, 22–25.

Does the quality of cultured pearls from the black-lip pearl oyster, *Pinctada margaritifera*, improve after the second graft? P. Kishore and P.C. Southgate, *Aquaculture*, **446**, 2015, 97–102, <http://dx.doi.org/10.1016/j.aquaculture.2015.04.024>.

The effect of different culture methods on the quality of round pearls produced by the black-lip pearl oyster *Pinctada margaritifera* (Linnaeus, 1758). P. Kishore and P.C. Southgate, *Aquaculture*, **451**, 2016, 65–71, <http://dx.doi.org/10.1016/j.aquaculture.2015.08.031>.

Host and donor influence on pearls produced by the silver-lip pearl oyster, *Pinctada maxima*. C. McDougall, P. Moase and B.M. Degnan, *Aquaculture*, **450**, 2016, 313–320, <http://dx.doi.org/10.1016/j.aquaculture.2015.08.008>.

Paua. M.C. Pedersen, *Gems&Jewellery*, **25**(4), 2016, 10–12.

Is pearl colour produced from *Pinctada margaritifera* predictable through shell phenotypes and rearing environments selections? C.-L. Ky, L. Le Pabic, M.S. Koua, N. Molinari, S. Nakasai and D. Devaux, *Aquaculture Research*, December 2015, 17 pp., <http://dx.doi.org/10.1111/are.12947>.

Social Studies

The color of responsibility: Ethical issues and solutions in colored gemstones. J. Archuleta, *Gems & Gemology*, **52**(2), 2016, 144–160, <http://dx.doi.org/10.5741/gems.52.2.144>.*

Nostalgia for war and the paradox of peace in the Colombian emerald trade. B. Brazeal, *The Extractive Industries and Society*, **3**(2), 2016, 340–349, <http://dx.doi.org/10.1016/j.exis.2015.04.006>.

Synthetics and Simulants

B–C bond in diamond single crystal synthesized with h-BN additive at high pressure and high temperature. Y. Li, Z. Zhou, X. Guan, S. Li, Y. Wang, X. Jia and H. Ma, *Chinese Physics Letters*, **33**(2), 2016, article 028101, <http://dx.doi.org/10.1088/0256-307x/33/2/028101>.

Studying the effect of hydrogen on diamond growth by adding C₁₀H₁₀Fe under high pressures and high temperatures. C. Fang, X. Jia, S. Sun, B. Yan, Y. Li, N. Chen, Y. Li and H. Ma, *High Pressure Research*, **36**(1), 2016, 42–54, <http://dx.doi.org/10.1080/08957959.2015.1129405>.

The synthesis and application of high-quality large diamond single crystal. Y. Liu, *Superhard Material Engineering*, **28**(3), 2016, 41–44 (in Chinese with English abstract).

Technical note: Fake turquoises investigated by Raman microscopy. N.D.E. Bernardino, C.M.S. Izumi and D.L.A. de Faria, *Forensic Science International*, **262**, 2016, 196–200, <http://dx.doi.org/10.1016/j.forsciint.2016.03.041>.

Treatments

Analysis of UV-Vis spectrum on pink-purple spinel from Burma before and after heat treatment. Q. Ren, M. Chen, C. Wang and G. Wu, *Journal of Gems & Gemmology*, **18**(3), 2016, 24–30 (in Chinese with English abstract).

N and Cr ion implantation of natural ruby surfaces and their characterization. K.S. Rao, R.K. Sahoo, T. Dash, P. Magudapathy, B.K. Panigrahi, B.B. Nayak and B.K. Mishra, *Nuclear Instruments and Methods in Physics Research Section B: Beam Interactions with Materials and Atoms*, **373**, 2016, 70–75, <http://dx.doi.org/10.1016/j.nimb.2016.03.017>.

The soaking experiment of Zachery-treated turquoise and the untreated turquoise ore. J. Li, G. Li, C. Fan and X. Yang, *Superhard Material Engineering*, **28**(2), 2016, 57–61 (in Chinese with English abstract).

Compilations

G&G Micro-World. Iris agate with aurora-like appearance • Inclusions in Burmese amber • Chalcedony-quartz intergrowth • Orbicular chalcedony • Manufactured garnet inclusion in quartz • Spondylus pearl with iridescent flame structure • Metal sulfide in pyrope • Cr inclusions in industrial slag synthetic ruby • Triplite in topaz. *Gems & Gemology*, **52**(2), 2016, 198–205, www.gia.edu/gems-gemmology.*

Gem News International. Kämmererite from India • UV-Vis spectra of two *Pinctada* species shells • Ruby cabochons from Macedonia • Fluid inclusions in Russian sapphires • Tremolite and diopside bead • Coloured synthetic moissanite submitted as synthetic diamonds • Steam-dyed Baltic amber • Polymer-coated serpentine carving • Almandine in graphite schist • Australian opal beads with blue play-of-color • Honduran and Turkish opal • South African rhodochrosite crystals • Colombian quartz with trapiche-like patterns • Angela Conty jewellery collection • Robotic colored stone cutting machines. *Gems & Gemology*, **52**(2), 2016, 206–220, www.gia.edu/gems-gemmology.*

Lab Notes. Largest Canadian rough diamond, 187.66 ct • Type IIa diamond with red fluorescence • Black NPD synthetic diamond • Emerald with filled drill holes • Natural blister pearls with partial filling • Yellowish green spinel • Large blue and colourless HPHT-grown synthetic diamonds • Yellow synthetic diamond with Ni-related green fluorescence. *Gems & Gemology*, **52**(2), 2016, 188–197, www.gia.edu/gems-gemmology.*



Gem-A
INSTRUMENTS

20% Off



See better with the dark

The dark-field loupe is an essential piece of kit used the world over by gemmology professionals to help identify coloured gemstones and fracture-filled diamonds. The loupe allows the stone to be observed against a dark background with reflected illumination, enabling easier viewing of internal features and inclusions. Also an excellent tool for identifying treated gemstones, including diamonds, which could be fracture-filled to improve the stone's overall appearance.

Usual price £40 + VAT

Now only £32 + VAT*

To place an order contact instruments@gem-a.com

As recommended by Edward Boehm, RareSource:

"The dark-field loupe is the single most significant development in portable gemmological instruments for the serious gemmologist."

* Postage and packing fee applies. 20% VAT applies to UK and European countries, except companies with a valid VAT registration number. Offer ends 31 October 2016.

Creating gemmologists since 1908

Join us.



Gemmological Instruments Ltd is a company limited by guarantee and registered in England No. 838324. Registered office: 3rd Floor, 1-4 Argyll Street, London W1F 7LD VAT Reg. No.: 995 8813 45. Gemmological Instruments Ltd is a wholly owned subsidiary of The Gemmological Association of Great Britain (UK Registered Charity No. 1109555).



D

*esire never stops;
it increases even after satisfaction.*

— Sri Lanka proverb

Pala International

Palagems.com / Palaminerals.com

+1 800 854 1598 / +1 760 728 9121

Padparadscha Sapphire from Sri Lanka • 5.30 ct • 9.84 x 8.99 x 6.40 mm
Blooms from Pala International Grounds • Photo: Mia Dixon